

R-05-24

Thermal modelling

Preliminary site description Simpevarp subarea – version 1.2

Jan Sundberg, Pär-Erik Back
Anna Bengtsson, Märta Ländell
Geo Innova AB

August 2005

Svensk Kärnbränslehantering AB

Swedish Nuclear Fuel
and Waste Management Co
Box 5864
SE-102 40 Stockholm Sweden
Tel 08-459 84 00
+46 8 459 84 00
Fax 08-661 57 19
+46 8 661 57 19



ISSN 1402-3091

SKB Rapport R-05-24

Thermal modelling

Preliminary site description Simpevarp subarea – version 1.2

Jan Sundberg, Pär-Erik Back
Anna Bengtsson, Märta Ländell
Geo Innova AB

August 2005

This report concerns a study which was conducted for SKB. The conclusions and viewpoints presented in the report are those of the authors and do not necessarily coincide with those of the client.

A pdf version of this document can be downloaded from www.skb.se

Summary

This report presents the thermal site descriptive model for the Simpevarp subarea, version 1.2. The main objective of this report is to present the thermal modelling work where data has been identified, quality controlled, evaluated and summarised in order to make an upscaling to lithological domain level possible.

The thermal conductivity at possible canister scale has been modelled for four different lithological domains (RSMA01 (Ävrö granite), RSMB01 (Fine-grained dioritoid), RSMC01 (mixture of Ävrö granite and Quartz monzodiorite), and RSMD01 (Quartz monzodiorite)). A main modelling approach has been used to determine the mean value of the thermal conductivity. Three alternative/complementary approaches have been used to evaluate the spatial variability of the thermal conductivity at domain level. The thermal modelling approaches are based on the lithological model for the Simpevarp subarea, version 1.2 together with rock type models constituted from measured and calculated (from mineral composition) thermal conductivities. For one rock type, the Ävrö granite (501044), density loggings within the specific rock type has also been used in the domain modelling in order to consider the spatial variability within the Ävrö granite. This has been possible due to the presented relationship between density and thermal conductivity, valid for the Ävrö granite.

Results indicate that the mean of thermal conductivity is expected to exhibit only a small variation between the different domains, from 2.62 W/(m·K) to 2.80 W/(m·K). The standard deviation varies according to the scale considered and for the canister scale it is expected to range from 0.20 to 0.28 W/(m·K). Consequently, the lower confidence limit (95% confidence) for the canister scale is within the range 2.04–2.35 W/(m·K) for the different domains. The temperature dependence is rather small with a decrease in thermal conductivity of 1.1–3.4% per 100°C increase in temperature for the dominating rock types.

There are a number of important uncertainties associated with these results. One of the uncertainties considers the representative scale for the canister. Another important uncertainty is the methodological uncertainties associated with the upscaling of thermal conductivity from cm-scale to canister scale. In addition, the representativeness of rock samples is uncertain and it is not known how large the bias, introduced by judgmental sample selection is.

In general, the thermal conductivity is estimated to be higher in the Simpevarp site description model version 1.2 than in the Simpevarp site description model version 1.1 for all four lithological domains which have been considered. The difference is 5–23% depending on domain. However, the variability is estimated to be larger in the Simpevarp site descriptive model version 1.2, and substantially larger for all domains except RSMA01 (Ävrö granite).

Mean values of heat capacity ranges from 2.18 to 2.23 MJ/(m³·K) for the three dominating rock types. The standard deviation varies more, from 0.06 to 0.21 MJ/(m³·K), but the number of samples are relatively small. There is also a question of the representativeness of the samples. Modelling on domain level of the four lithological domains according to a Monte Carlo simulation gave mean values of the heat capacity ranging in a narrow interval from 2.23 to 2.25 MJ/(m³·K) and standard deviations ranging from 0.06 to 0.12 MJ/(m³·K). The heat capacity exhibits large temperature dependence, from 25% to 32% increase per 100°C temperature increase.

The coefficient of thermal expansion was determined to $6.0\text{--}8.0\text{E-}6$ m/(m·K) for the three dominating rock types.

In situ temperature has been measured in six boreholes. The temperature has been logged at different occasions in two of them. The mean of all temperature loggings is 14.4°C at 500 m depth, (one deviant borehole excluded). Temperature vs. depth is presented in both tables and figures for each borehole. There is a variation in temperature between the boreholes at a specified depth.

Different loggings in the same borehole give slightly different results, indicating that there is a potential error. Possible sources of uncertainty in the temperature logging results include the timing of the logging after drilling, water movements along the boreholes, calibration errors and measured inclination of the boreholes.

Sammanfattning

Föreliggande rapport presenterar den termiska platsbeskrivningsmodellen för Simpevarpsområdet version 1.2. Syftet med denna rapport är att presentera det termiska modelleringsarbetet där data har identifierats, kvalitetssäkrats, utvärderats och sammanfattats för att möjliggöra en uppskalning till litologisk domännivå.

Den termiska konduktiviteten i möjlig kapselskala har modellerats för fyra olika litologiska domäner (RSMA01 (Ävrö granit), RSMB01 (Finkornig dioritoid), RSMC01 (blandning av Ävrö granit och Kvartsmonzodiorit) och RSMD01 (Kvartsmonzodiorit)). Det huvudsakliga angreppssättet för den termiska modelleringen har använts för bestämning av den termiska konduktivitetens medelvärde. Tre alternativa/kompletterande angreppssätt har använts för att utvärdera den termiska konduktivitetens spatiala variation på domän nivå. Den termiska modelleringens olika angreppssätt baseras på den litologiska modellen för Simpevarpsområdet version 1.2 tillsammans med bergartsmodeller upprättade med utgångspunkt ifrån mätningar och beräkningar (utifrån mineralsammansättning) av den termiska konduktiviteten. För en bergart, Ävrö graniten (501044), så har densitetsloggningar uppmätta inom den specifika bergarten också använts i domänmodelleringen för att betrakta den spatiala variationen inom just Ävrö graniten. Detta har varit möjligt på grund av det presenterade sambandet mellan densitet och termisk konduktivitet gällande för Ävrö graniten.

Resultat indikerar att medelvärdet för den termiska konduktiviteten är förväntad att uppvisa endast en liten variation mellan de olika domänerna, från 2,62 W/(m·K) till 2,80 W/(m·K). Standardavvikelsen varierar beroende på vilken skala som bedöms och för kapselskalan så är den förväntad att variera från 0,20 till 0,28 W/(m·K). Följaktligen så förväntas den undre konfidensgränsen (95 % konfidens) för kapselskalan inom intervallet 2,04–2,35 W/(m·K) för de olika domäner. Temperaturberoendet är relativt litet med en minskning i termisk konduktivitet på 1,1–3,4 % per 100°C temperaturökning för de dominerande bergarterna.

Det finns ett antal viktiga osäkerheter associerade med dessa resultat. En av osäkerheterna tar hänsyn till den representativa skalan för kapseln. Ytterligare en viktig osäkerhet är de metodrelaterade osäkerheterna i samband med uppskalningen av den termiska konduktiviteten från cm- till kapselskala. Till detta skall även läggas osäkerheten i representativitet för bergartsproverna där det ännu inte är klargjort hur stor avvikelsen är på grund av metodiken för provernas urval.

Generellt sett så har den termiska konduktiviteten uppskattats vara högre för samtliga fyra bedömda litologiska domäner i den termiska platsbeskrivningsmodellen för Simpevarpsområdet version 1.2 än för den termiska platsbeskrivningsmodellen för Simpevarpsområdet version 1.1. Differensen är 5–23 % beroende av domän. Variationen uppskattas vara större i den termiska platsbeskrivningsmodellen för Simpevarpsområdet version 1.2 och då avsevärt större för samtliga domäner undantaget RSMA01 (Ävrö granit).

Medelvärdena för värmekapaciteten varierar inom ett small intervall från 2,18 till 2,23 MJ/(m³·K) för de tre dominerande bergarterna. Standardavvikelsen varierar dock mer, från 0,06 till 0,21 MJ/(m³·K), men antalet prov är relativt litet. Representativiteten för proven kan ifrågasättas. Modelleringen på domännivå för de fyra litologiska domänerna genomfördes enligt en Monte Carlo simulering och gav medelvärden för värmekapaciteten varierande mellan 2,23–2,25 MJ/(m³·K) samt standardavvikelser varierande mellan 0,06–0,12 MJ/(m³·K). Värmekapaciteten uppvisar stort temperaturberoende från 25–32 % ökning per 100°C temperaturökning.

Längdutvidgningskoefficienten bestämdes till $6,0-8,0 \cdot 10^{-6} \text{ m}/(\text{m} \cdot \text{K})$ för de tre dominerande bergarterna.

In situ temperaturer har uppmätts i sex borrhål. Temperaturer har loggats vid olika tillfällen i två av dem. Medelvärdet för samtliga temperaturloggningar är $14,4^\circ\text{C}$ vid 500 m djup, (ett avvikande borrhål exkluderat). Temperatur relativt djup presenteras både i tabellform samt i figurer för respektive borrhål. Det finns en variation i temperatur mellan de olika borrhålen för ett specifikt djup.

Olika temperaturloggningar i samma borrhål ger något skilda resultat vilket indikerar att det finns ett potentiellt fel. Möjliga källor till osäkerheter i temperaturloggningens resultat innefattar tiden för loggning relativt borrhålsaktiviteten, vattenrörelser längs borrhålet, kalibreringsfel och uppmätt lutning av borrhålet.

Contents

1	Introduction	9
2	Objective and scope	11
3	State of knowledge at previous model version	13
4	Evaluation of primary data	15
4.1	Summary of used data	15
4.2	Geological introduction	16
4.3	Thermal conductivity from measurements	17
4.3.1	Method	17
4.3.2	Result	18
4.3.3	Temperature dependence	19
4.4	Thermal conductivity from mineral composition	21
4.4.1	Method	21
4.4.2	Result	23
4.4.3	Comparison with measurements on comparable samples	24
4.4.4	Comparison with measurements on all samples	28
4.5	Thermal conductivity from density	29
4.5.1	Method	29
4.5.2	Result	30
4.5.3	Comparison with measurements and calculations	36
4.6	Modelling of thermal conductivity (rock type level)	36
4.6.1	Method	36
4.6.2	Ävrö granite (501044)	38
4.6.3	Quartz monzodiorite (501036)	40
4.6.4	Fine-grained dioritoid (501030)	42
4.6.5	Other rock types (505102, 501033, 501058 and 511058)	44
4.6.6	All investigated rock types	44
4.7	Spatial variability	45
4.7.1	Spatial variability in thermal conductivity from measurements	45
4.7.2	Spatial variability in thermal conductivity from density loggings	47
4.7.3	Spatial variability of rock types	50
4.8	Anisotropy	50
4.9	Heat capacity from determinations	50
4.9.1	Method	50
4.9.2	Result	50
4.9.3	Temperature dependence	51
4.9.4	Modelling of heat capacity (rock type level)	53
4.10	Coefficient of thermal expansion	54
4.11	In situ temperature	54
4.11.1	Method	54
4.11.2	Result	62
4.11.3	Modelling from temperature loggings	65
5	Thermal modelling of lithological domains	67
5.1	Modelling assumptions and input from other disciplines	67
5.1.1	Geological model	67
5.1.2	Borehole data	68

5.2	Conceptual model	68
5.3	Modelling approach for domain properties	70
5.3.1	Introduction	70
5.3.2	Approach 1: Main approach	71
5.3.3	Approach 2: Extrapolation – spatial variation in all rock types	75
5.3.4	Approach 3: Reduction of small scale variability	75
5.3.5	Approach 4: Addition of “between rock type” and “within rock type” variance	75
5.3.6	Modelling approach: Heat capacity	76
5.4	Domain modelling results	76
5.4.1	Approach 1: Main approach	76
5.4.2	Approach 2: Extrapolation – spatial variation in all rock types	86
5.4.3	Approach 3: Reduction of small scale variability	86
5.4.4	Approach 4: Addition of “between rock type” and “within rock type” variance	87
5.4.5	Heat capacity	89
5.5	Evaluation – Thermal conductivity	89
5.6	Concluding domain modelling results	91
5.6.1	Thermal conductivity	91
5.6.2	Heat capacity	92
5.6.3	Coefficient of thermal expansion	92
5.6.4	In situ temperature	92
6	Evaluation of uncertainties	93
6.1	Thermal conductivity	93
6.1.1	Data level	93
6.1.2	Rock type level	95
6.1.3	Domain level	96
6.2	Heat capacity	98
6.3	In situ temperature	98
6.4	Thermal expansion	98
	References	99
	Appendix A Probability plots of thermal conductivity per rock type	101
	Appendix B Probability plots of domain modelling results	103
	Appendix C Spatial variation of rock types – indicator variograms	105

1 Introduction

The Swedish Nuclear Fuel and Waste Management Co (SKB) is responsible for the handling and final disposal of the nuclear waste produced in Sweden. Site investigations have started during 2002. The site investigations are carried out in different stages and shall provide the knowledge required to evaluate the suitability of investigated sites for a deep repository.

The interpretation of the measured data is made in terms of a site descriptive model covering geology, rock mechanics, thermal properties, hydrogeology, hydrogeochemistry, transport properties of the rock and surface ecosystems. The site descriptive model is the foundation for the understanding of investigated data and a base for planning of the repository design and for studies of constructability, environmental impact and safety assessment. A strategy for the thermal modelling is presented in Sundberg, 2003a.

This report presents the thermal site descriptive model for the Simpevarp subarea, version 1.2. Parallel to this modelling, a study on uncertainties, scale factors and modelling methodology is ongoing for the prototype repository at the Äspö HRL /Sundberg et al. 2005/. The experiences from this parallel study are not fully implemented in the present modelling report.

2 Objective and scope

The purpose of this document is to present the thermal modelling work and result for the Simpevarp site descriptive model version 1.2. Primary data originate from the work in connection to Simpevarp site descriptive model version 1.2, previous work at Äspö HRL and the Simpevarp site descriptive model version 1.1, which has partly been re-evaluated. Data has been identified, quality controlled, evaluated and summarised in order to make the upscaling possible to domain level.

The thermal model of the bedrock describes thermal properties on lithological domain level which is of importance since the thermal properties of the rock mass affects the possible distance, both between canisters and deposition tunnels, and therefore puts requirements on the necessary repository volume. Of main interest is the thermal conductivity since it directly influences the design of a repository. Measurements of thermal properties are performed in cm scale but values are requested in the canister scale and therefore the spatial variability is required to be considered. Due to this, the thermal modelling includes elements of upscaling of thermal properties which is further described in /Sundberg et al. 2005/. The work has been performed according to a strategy presented in /Sundberg, 2003a/.

3 State of knowledge at previous model version

The only thermal conductivities available in Simpevarp site descriptive model version 1.1 were values estimated from mineral composition, no laboratory measurements were available. The upscaling from calculated values at cm scale to domain scale (1·1·1 m) was performed based on the assumption that the averaging and variance reduction of small scale variations when going from cm scale to domain scale is equitable to the variance contribution resulting from the fact that a domain consists of several different rock types. Therefore the cm scale was assumed to be representative also for the domain scale. Thermal conductivity properties were reported separately for each lithological domain and seemed to be fairly low, 2.2–2.7 W/(m·K). No distinction was made between different domains for specific heat capacity and thermal expansion coefficient. The specific heat was given the range 2.0–2.3 MJ/(m³·K) and the thermal expansion coefficient the range 6.0–8.0 ·10⁻⁶ mm/(mm·°C). The in situ temperature of the Simpevarp subarea was determined to be 15.5–16°C at a depth of 600 m.

In the Simpevarp site descriptive model version 1.1 the thermal properties for the regional scale were assumed to coincide with those of the local scale model.

The main uncertainties of the thermal model in Simpevarp site descriptive model version 1.1 concerned:

- Modelling from mineral composition.
- Thermal properties on domain level.
- Upscaling from core samples to rock domains.

4 Evaluation of primary data

The evaluation of primary data includes measurements of thermal conductivity, heat capacity, temperature dependence of thermal transport properties, coefficient of thermal expansion and in situ temperatures. It also includes calculations of thermal conductivity from mineral composition and establishment of rock type distributions (PDF) of thermal conductivity. The spatial variation in thermal conductivity is also investigated by using density loggings.

4.1 Summary of used data

Table 4-1 summarises the available data on thermal properties used in the evaluation. A translation key to names on rock types is available in Table 4-2.

Table 4-1. Summary of data used in the evaluation of primary data.

Data specification	Ref.	Rock type	Number of samples/ measurements	Borehole (depth)	
Cored borehole data					
Laboratory thermal test on cores from Simpevarp and old boreholes at Äspö HRL	R-03-10	501044	37	KAV01 (508–509 m), KA2599G01 (4–127 m), Äspö prototype repository tunnel (section 3,539–3,587 m)	
	IPR-99-17				
	R-02-27			KSH01A (399–415 m, 480–496 m), KSH02 (311–323 m, 791–795 m, 609–610 m)	
	P-04-53	501030	26		
P-04-54					
	P-04-55			KSH01A (299–306 m, 703–713 m)	
	/Sundberg et al. 2005/	501036	10		
Modal analyses	P-04-53	501044	21	KLX01, KLX02, KSH01A, KAV01	
	P-04-54	501030	18		
	P-04-55			KLX02, KSH01A, KSH02	
	/Wahlgren, 2004/	501036	8		
	Sicada 04-114 date 04-05-25			KLX02, KSH01A, KSH01B	
Density logging	Results	Interpret.			
	P-04-232	P-04-77	501044	13,037	KAV01 (2–743 m) KLX02 (202–1,001 m) KSH01A (101–999 m)
	P-03-111	P-04-214			
	P-03-16	P-04-28			
Temperature and gradient logging	Results	Interpret.			
	P-03-16	P-04-28			KSH01A
	P-03-16	P-04-28			KSH02
	P-04-50	Sicada 04-07-05			KSH03A
	P-04-232	P-04-77			KAV01
	–	Sicada 04-07-05			KLX01
	P-03-111	Sicada 04-07-05			KLX02
Boremap logging	Dominating rock type Sicada 04-161 date 04-07-12				KAV01, KSH01A, KSH02, KLX02
	Subordinate rock type Sicada 04-161 date 04-09-07				
Laboratory test of thermal expansion	P-04-59	501044	5	KAV01 (505–509 m)	
	P-04-60	501030	17	KSH01A (399–412 m, 480–493 m), KSH02 (312–327 m)	
	P-04-61				
			501036	10	KSH01A (298–303 m, 701–714 m)
Surface based data					
Modal analyses	P-04-102	501044	18		
		501030	13		
		501036	3		

4.2 Geological introduction

The bedrock area, for which the thermal site descriptive model version 1.2 has been conducted, is predominated by three rock types, namely:

- Ävrö granite.
- Fine-grained dioritoid.
- Quartz monzodiorite.

Besides the three dominating rock types several subordinate rock types occur within the bedrock area for the thermal model. For illustration of the geological rock type classification of the bedrock, see Figure 4-1

Further on in this report all rock types will mainly be identified and described by the rock type code. Therefore, a translation table is introduced between rock types and rock names in Table 4-2.

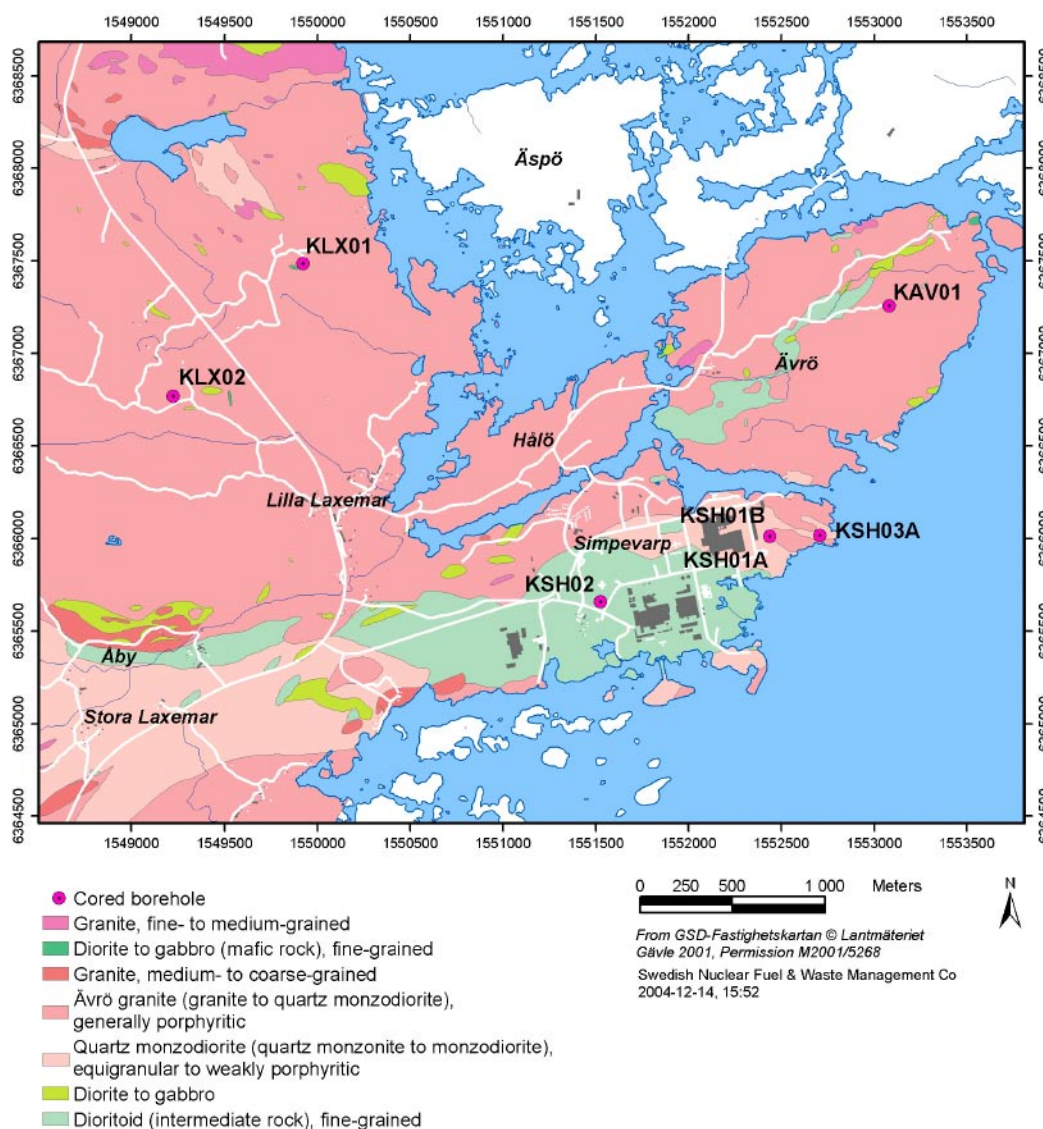


Figure 4-1. Location of boreholes used in this report within the Simpevarp and Laxemar subarea overlaid the bedrock classification.

Table 4-2. Translation table between rock types and rock names.

Rock type	Rock name
501044	Ävrö granite
501036	Quartz monzodiorite
501030	Fine-grained dioritoid
505102	Fine-grained diorite-gabbro
501033	Diorite/Gabbro
511058	Fine-grained granite
501058	Granite
501061	Pegmatite

Data from different boreholes, within the Simpevarp and Laxemar subarea, have been used and are evaluated in this report. Figure 4-1 illustrates the location of the boreholes.

Thermal properties of four main lithological rock domains within the Simpevarp subarea will be calculated and suggested within this report; domain RSMA01, RSMB01, RSMC01, and RSMD01. Classifying rock volumes in different domains is a way of handling and simplifying large rock volumes with, relatively seen, the same properties, from a lithological point of view. The dominating rock type in domain RSMA01 is Ävrö granite, in domain RSMB01 the Fine-grained dioritoid and in RSMD01 the Quartz monzodiorite. Domain RSMC01 consists of a mixture between Quartz monzodiorite and Ävrö granite. For a more detailed description of the rock type composition in the different lithological domains, see Table 5-1 and the geological domain modelling /SKB, 2005/.

4.3 Thermal conductivity from measurements

4.3.1 Method

Laboratory measurements of the properties thermal conductivity and thermal diffusivity have been performed with the Transient Plane Source method (TPS) /Gustafsson, 1991; Sundberg, 2003a/. The measurements are made on a defined rock volume (approximately 10 cm³) determined by the size of the sensor. The radius for the sensor is 6.403 mm. The TPS method can be used for measurements of thermal diffusivity and thermal conductivity of both fluids and solids, from cryogenic temperatures to approximately 250°C (if the sensor insulation is made of kapton). Measurements of thermal properties using the TPS method have been used before by SKB /Sundberg and Gabrielsson, 1999; Sundberg, 2002; Sundberg et al. 2005/ and also within the thermal programme of the site investigations.

Prior to the measurements, the rock samples from the drill core are cut in two halves, each with a thickness of approximately 25 mm. The two intersection surfaces need to be relatively smooth in order to limit the contact resistance between the probe and the sample surface.

The principle of the TPS instrument is to place a circular probe consisting of a Ni-spiral covered by an insulating material (usually kapton, at high temperatures mica is used) between the two sample pieces. The sensor generates a heat pulse while simultaneously the heating of the specimen is recorded. The heat pulse is selected to achieve a heat increase of about 1K at the sample surfaces facing the sensor. The output power and the duration of the pulse are dependent on sample size, material properties and sensor diameter. The thermal properties can be evaluated by using the fact that the resistance for the thin Ni-spiral at any time is a function of its initial resistance, the temperature increase and the temperature coefficient for the resistivity of Nickel. The measured temperatures is stored in the software and by comparing these values to a theoretical solution based on assumptions regarding a plane sensor and an infinite sample in perfect contact with the sensor surface, the thermal diffusivity and thermal conductivity can be determined. The volumetric heat capacity can thereafter be calculated.

According to the manufacturer the accuracy of the thermal conductivity measurements is $\pm 2\%$, thermal diffusivity $\pm 5\%$ and specific heat $\pm 7\%$ /HotDisk, 2004/. This is accomplished if the sample size, sensor diameter, output of power and total time of the temperature measurement is properly selected together with letting the sample reach temperature equilibrium before beginning the measuring process.

Measurements on samples from the Simpevarp area have been conducted by SP, Swedish National Testing and Research Institute.

4.3.2 Result

In Table 4-3 the results from all performed laboratory measurements of thermal conductivity are summarised. The variability in the results is possibly overestimated due to the small scale of the measurements. Observe that samples from rock type Ävrö granite (501044) are gathered from both the Simpevarp subarea /Adl-Zarrabi, 2004a,b,c/ and the Äspö HRL /Sundberg and Gabrielsson, 1999; Sundberg, 2002; Sundberg et al. 2005/. The diagram on the right hand side in Figure 4-2 illustrates how samples in borehole KA2599G01 within the rock type Ävrö granite (501044) are grouped. Other samples within Ävrö granite are gathered in the prototype tunnel (9 samples) and within a 1 m long interval of borehole KAV01 (secup 508.25–509.20 m). Samples from rock type Fine-grained dioritoid (501030) and Quartz monzodiorite (501036) all comes from the Simpevarp subarea /Adl-Zarrabi, 2004a,b,c/. Some of the samples are spatially located close to each other with approximately 2–5 samples in each group which is illustrated in Figure 4-2 (left diagram).

Table 4-3. Measured thermal conductivity (W/(m·K)) of samples using the TPS method. Samples are from boreholes KAV01, KSH01A, and KSH02 (Simpevarp subarea) together with borehole KA2599G01 (Äspö HRL) and boreholes from the prototype repository tunnel (Äspö HRL).

Rock name	Rock type	Sample location	Mean	St. dev	Number of samples
Fine-grained dioritoid	501030	Borehole KSH01A and KSH02	2.79	0.16	26
Quartz monzodiorite	501036	Borehole KSH01A	2.83	0.07	10
Ävrö granite	501044	Borehole KAV01, KA2599G01, Äspö HRL prototype tunnel	2.73	0.35	37

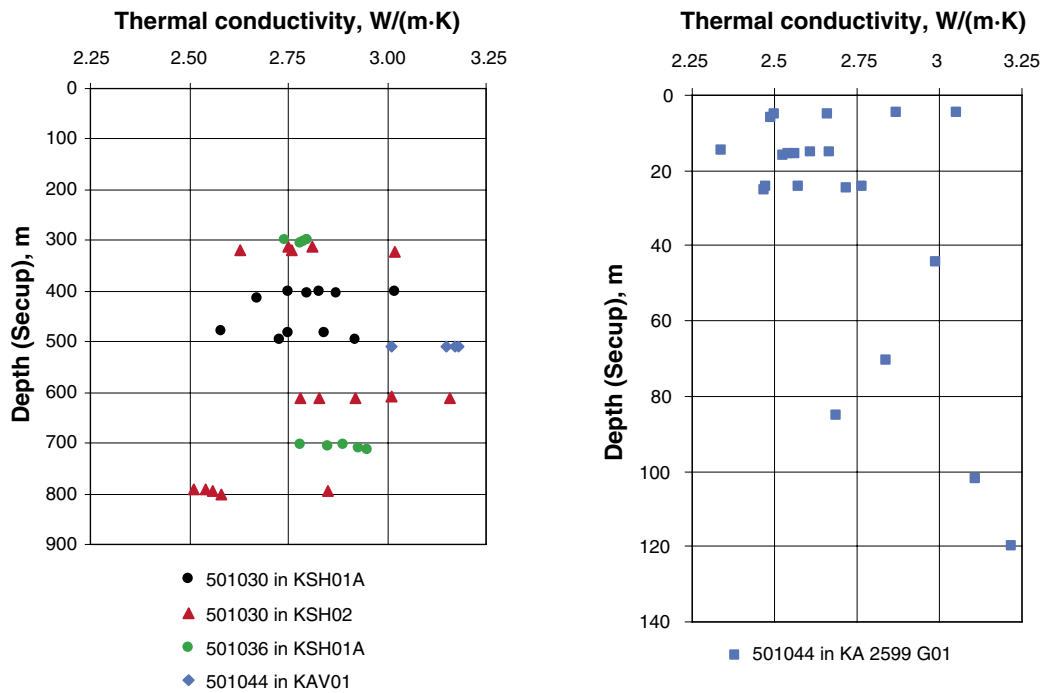


Figure 4-2. Sample location in boreholes measured with the TPS method divided on rock type and borehole. Y-axis in diagrams represents secup of samples. KA2599G01 is situated at Äspö HRL.

4.3.3 Temperature dependence

The temperature dependence of the thermal conductivity has been investigated by laboratory measurements, for the two rock types Fine-grained dioritoid (501030) and Quartz monzodiorite (501036), at three different temperatures (20, 50 and 80°C) /Adl-Zarrabi, 2004a,b/. Eleven samples from rock type Fine-grained dioritoid (501030) and five from Quartz monzodiorite (501036) have been measured. For rock type Ävrö granite (501044), the thermal conductivity has been measured on four samples at four different temperatures (25, 40, 60 and 80°C) /Sundberg, 2002/. Figure 4-3 to Figure 4-5 illustrates the measuring results for each sample while Table 4-4 summarises the temperature dependence of the thermal conductivity for the three separate rock types. However, the number of samples is few for most rock type and the small measured temperature dependence should therefore only be seen as an indication.

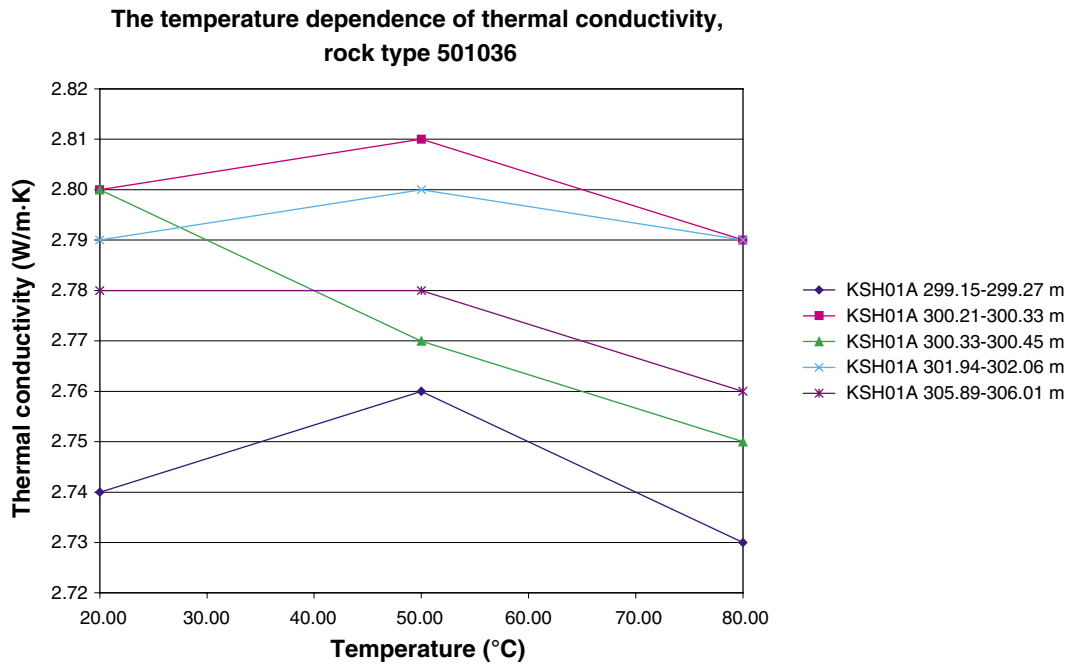


Figure 4-3. Temperature dependence of thermal conductivity, rock type Fine-grained dioritoid (501030).

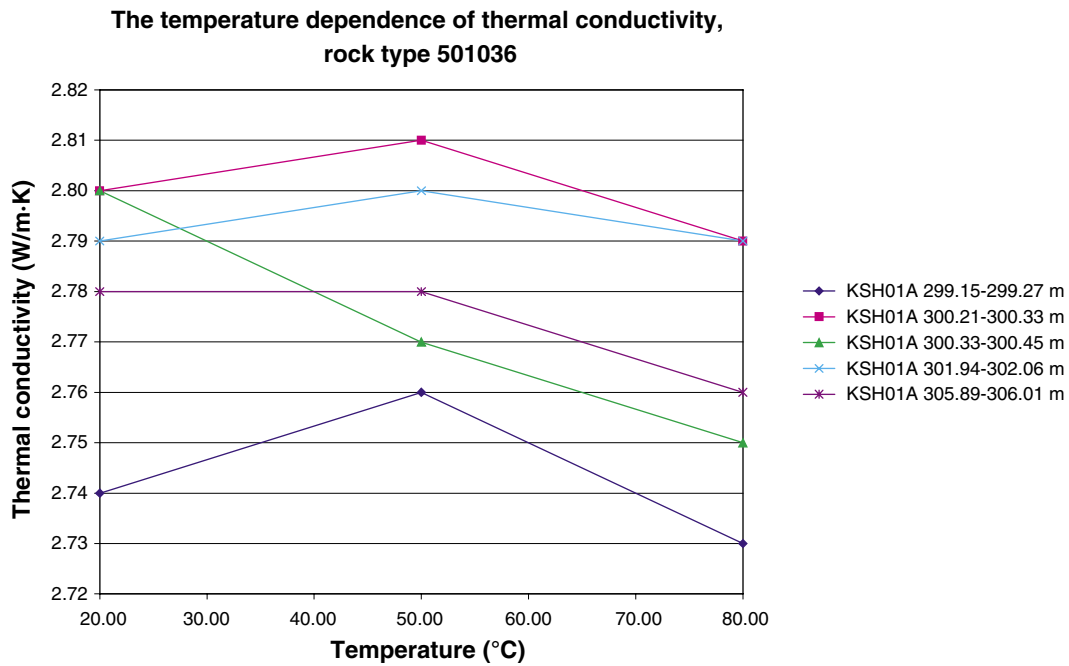


Figure 4-4. Temperature dependence of thermal conductivity, rock type Quartz monzodiorite (501036).

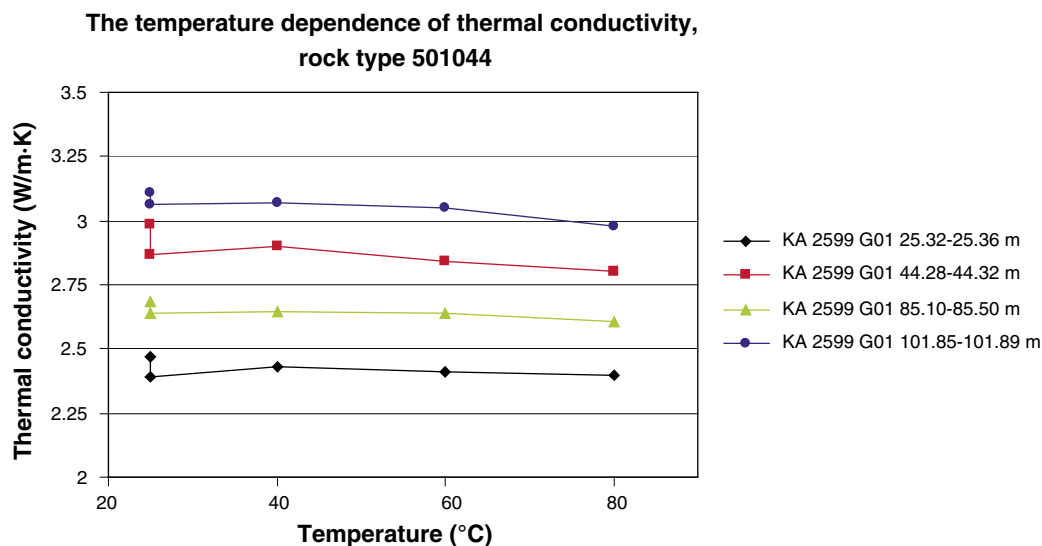


Figure 4-5. Temperature dependence of thermal conductivity, rock type Ävrö granite (501044).

Table 4-4. Measured temperature dependence of thermal conductivity (per 100°C temperature increase) on samples with different rock types from boreholes KSH01A, KSH02 (Simpevarp subarea) and KA2599G01 (Äspö HRL). Mean value of temperature dependence calculated with linear regression.

Rock name	Rock type	Sample location	Mean	St. dev	Number of samples
Fine-grained dioritoid	501030	boreholes KSH01A and KSH02	-3.4%	1.6%	11
Quartz monzodiorite	501036	borehole KSH01A	-1.1%	1.1%	5
Ävrö granite	501044	borehole KA2599G01	-2.3%	3.7%	4

4.4 Thermal conductivity from mineral composition

4.4.1 Method

Thermal conductivity of rock samples can be calculated with the SCA method (Self Consistent Approximation) using mineral compositions from modal analyses and reference values of the thermal conductivity of different minerals /Sundberg, 1988, 2003a/. The calculations are performed in mm scale and values have earlier been showed to be in good agreement with measured values /Sundberg, 1988, 2002/.

The following data was used for calculations with the SCA method:

- Modal analyses from the Sicada database performed in conjunction to Simpevarp site descriptive model version 1.1, reclassified rock types (62 samples) /Wahlgren, 2004/.
- Modal analyses in conjunction with measurements of thermal properties on samples from boreholes KAV01, KSH01A and KSH02 (6 samples) /Wahlgren, 2004/.
- Modal analyses on samples from boreholes KLX01 and KLX02 (39 samples).

Samples were excluded if the sum of minerals from the modal analyse had a large divergence from 100% (3 samples). For samples with a small divergence the volume fraction of the present minerals were corrected to reach 100% sum of minerals. This was done by splitting the lacking or extra percent on the present minerals by a weighting factor dependent on the minerals original volume fraction. This had to be done for 39 out of 107 samples.

Reference values of thermal conductivity for different minerals have been taken from /Horai, 1971; Horai and Baldrige, 1972/. In Table 4-5 the thermal conductivities of minerals used here, in site descriptive model version 1.2, are presented. The thermal conductivity of plagioclase, olivine and pyroxene depends on the chemical composition and may therefore vary within a certain interval. Because of this, these minerals are marked with red in Table 4-5. For minerals marked in yellow no reference values of the thermal conductivity have been found and an estimated value of 3.00 W/m·K have been used.

Table 4-5. Summary of used thermal conductivities (W/(m·K)) of minerals /Horai, 1971; Horai and Baldrige, 1972/.

Mineral	Simpevarp 1.2
Allanite	3.00
Amphibole	3.39
Apatite	1.38
Biotite	2.02
Calcite	3.59
Chlorite	5.15
Clinopyroxene	3.20
Epidote	2.83
Fluorite	9.51
Hornblend	2.81
K-feldspar	2.29
Muscovite	2.32
Olivine	4.57
Opaque	3.00
Orthopyroxene	3.20
Plagioclase	1.70
Prehnite	3.58
Pumpellyite	3.00
Pyroxene	3.20
Quartz	7.69
Titanite	2.34
Zircon	4.54
Zoisite	2.15

Yellow: data missing, estimated values.

Red: unknown chemical composition of the mineral.

The thermal conductivity of the plagioclase mineral is dependent on the anorthite content. This has been taken under consideration when calculating the thermal conductivity of rock samples. In Figure 4-6 the relationship is presented with a polynomial regression line. For the Simpevarp subarea the anorthite content of dominating rock types has been assumed as

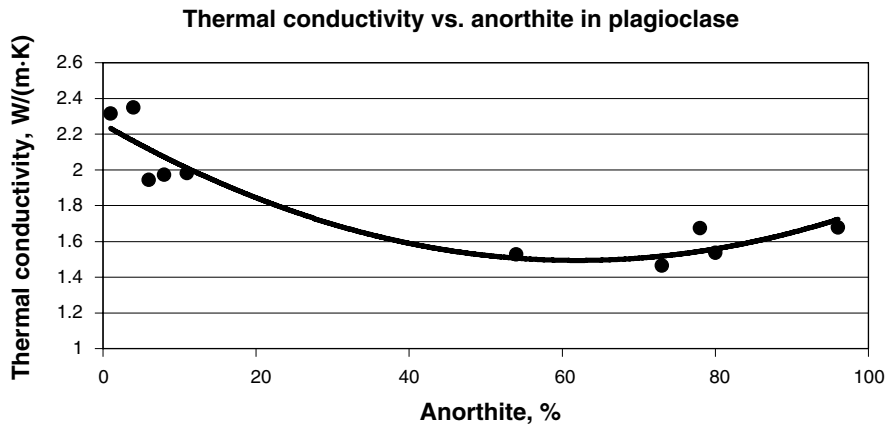


Figure 4-6. Thermal conductivity for plagioclase versus anorthite content. Polynomial regression with equation $y = 0.0002x^2 - 0.0246x + 2.2563$ and $R^2 = 0.8845$.

30% /Wahlgren, 2004/. When this anorthite content is applied to the regression ($y = 0.0002x^2 - 0.0246x + 2.2563$) the thermal conductivity of plagioclase within the Simpevarp subarea is set to 1.70 W/(m·K).

4.4.2 Result

The results of the SCA calculations, for samples from the Simpevarp subarea, are presented in Table 4-6 subdivided according to rock type. Samples from the Simpevarp subarea show a certain degree of alteration which results in an increase in the thermal conductivity. The variability at the SCA scale is probably overestimated compared with the canister scale.

Table 4-6. Thermal conductivity (W/(m·K)) of samples from different rock types, calculated from the mineralogical compositions (SCA method).

Rock name	Rock type	Mean	St. dev	Number of samples
Fine-grained dioritoid	501030	2.43	0.33	31
Quartz monzodiorite	501036	2.46	0.27	11
Ävrö granite	501044	2.72	0.33	39
Fine-grained diorite-gabbro	505102	2.57	0.23	10
Diorite/Gabbro	501033	2.46	0.21	6
Fine-grained granite	511058	3.26	0.35	8
Granite	501058	2.59	0.65	2

Thermal conductivities calculated with the SCA method in the site descriptive model version 1.1 gave both lower mean values and standard deviations (except the standard deviation of the Quartz monzodiorite (501036) which was smaller in version 1.1) compared to the calculations in this site descriptive model version 1.2. The thermal conductivities were between 0.05–0.19 W/(m·K) lower in the previous model version. The increase might depend on the fact that the thermal conductivities of minerals have been chosen slightly different and that the number of samples have increased and better represents the rock mass. This is also indicated with the increased standard deviation.

4.4.3 Comparison with measurements on comparable samples

For several of the sample groups with measured thermal conductivity (TPS), sampling for determination of mineral composition in each end of the group has also been carried out. This has been performed within the thermal program with the objective to correlate measurements of thermal properties to properties calculated from mineral composition, produced within the geological programme. The thermal conductivity has been calculated with the SCA method and a comparison with the TPS measurements is presented in Table 4-12. The comparison is not always performed for the identical sample although closely located.

Altogether 16 samples for modal analyses were taken in connection to samples for TPS measurements. When the first modal analyse (A) of these samples was used for SCA calculations, the results indicated the modal analyses to be incorrect. For 6 of the same samples a new modal analyse (B) was conducted which have been used as data in this report (rock type Fine-grained dioritoid (501030) and Quartz monzodiorite (501036)). The mineral compositions of these 6 samples, calculated by the two different laboratories, are presented in Table 4-7. A comparison of calculated thermal conductivities based on the two different modal analyses is presented in Table 4-8.

Table 4-7. Mineral composition of samples taken in connection to TPS measurements /Adl-Zarrabi, 2004a,; Wahlgren, 2004/. Comparison of results from different laboratories. First calculation (A) and second calculation (B) where the second calculation (the text in bold) has been used as data in this report.

Borehole Secup	KSH01A 301.94		KSH01A 401.63		KSH01A 482.9		KSH02 310.93		KSH02 610.12		KSH02 794.43	
	(A)	(B)	(A)	(B)	(A)	(B)	(A)	(B)	(A)	(B)	(A)	(B)
Rock type	501036		501030		501030		501030		501030		501030	
Version	(A)	(B)	(A)	(B)	(A)	(B)	(A)	(B)	(A)	(B)	(A)	(B)
Quartz	14	15.0	17	9.6	46	10.8	21	7.0	20	17.4	22	8.2
K-feldspar	35	18.0	22	12.2	14	12.2	25	22.6	38	18.6	16	14.2
Plagioclase	23	43.4 ¹	31	43.4 ¹	5	35.8 ¹	26	40.8 ²	21	47.0 ¹	15	44.6 ¹
Biotite	0	11.2 ⁴	4	15.4 ⁴	28	29.0	5	13.6	11	11.6 ³	18	17.0 ³
Muscovite												
Chlorite		X		X				X		X		X
Epidote				3.0		3.0		0.2				X
Titanite				0.8		0.2		X		X		X
Calcite	0		0.4	X	0.4	0.2		X		X		0.2
Hornblend		3.2		12.4		1.4		0.6		X		1.4
Opaque	2	1.8	0.4	1.8	3	2.6	1	2.4	2	1.4	3	3.4
Apatite		X		X		0.2		0.2		X		X
Zircon		X		X		X		X		0.2		X
Prehnite		X		X						0.2		X
Clinopyroxene		6.4		1.0		4.6		12.6		3.6		9.4
Chlorite	13		11		0		7		2		0	
Amphibole	7		3		0		0		0		15	
Zoisite	2		10		5		14		3		5	
Sericite	5		2		0		0		0		6	
Turmalin ?						X						
Orthopyroxene												1.6

Borehole Secup	KSH01A 301.94		KSH01A 401.63		KSH01A 482.9		KSH02 310.93		KSH02 610.12		KSH02 794.43	
Iddingsite												X
Dark brown mineral		1.0		0.4								
Bars of unidentified mineral										X		
Assessory mineral							1		3		0	
Sum	101	100	100.8	100	101.4	100	100	100	100	100	100	100
SCA calculation (W/(m-K))	2.83	2.78	2.82	2.64	3.90	2.45	3.09	2.47	3.19	2.73	3.10	2.51
X observed mineral												
¹ partly sericitised												
² sericitised												
³ partly chloritised												
⁴ chloritised												

Table 4-8. Comparison of SCA calculations based on the first (A) and second (B) calculation of mineral composition for the same samples.

Borehole secup	KSH01A 301.94	KSH01A 401.63	KSH01A 482.9	KSH02 310.93	KSH02 610.12	KSH02 794.43
Rock type	501036	501030	501030	501030	501030	501030
First calculation A	2.83	2.82	3.90	3.09	3.19	3.10
Second calculation B	2.78	2.64	2.45	2.47	2.73	2.51
Diff. (first-second)/second	1.8%	6.8%	59.2%	25.1%	16.8%	23.5%

Protocols from the second point counting contained information concerning alteration of minerals (plagioclase to sericite and biotite to chlorite). This information has been taken under consideration and together with /Wahlgren, 2004/ it has been assumed that for samples containing partly altered plagioclase, 25% of the plagioclase has been calculated as muscovite. If the plagioclase mineral has been classified as sericitised, 50% of the plagioclase has been calculated as muscovite. The same way of thinking has been applied for biotite transformed to chlorite. The percent of transformation for which the calculations are based on are only estimations which mean that there is an uncertainty in the mineral composition. How the transformation of minerals affects the SCA calculation for the 6 samples is illustrated in Table 4-9. Information about alteration has not been available for the rest of the modal analyses and therefore the degree of alteration has not been considered for the other modal analyses.

Within the Simpevarp subarea, the degree of sericitisation for the plagioclase mineral is hard to say since it depends on where the sample is taken. If the sample is taken in, what is estimated as, unaltered rock the sericitisation is probably relatively small. On the other hand, if the sample is taken where a secondary transformation may be suspected the alteration of course has a larger extension. Therefore the degree of sericitisation depends on the degree of transformation in the rock mass and the later is hard to estimate due to lack of good information. Generally it can be said that a certain degree of sericitisation appears in most cases.

Table 4-9. Effect on thermal conductivity (W/(m·K)) from sericitisation (S) and chloritisation (C) for 6 samples taken in connection to TPS measurements.

Borehole	Secup	Rock type	S+C taken into account	S not taken into account	Contribution from S taken into account	S+C not taken into account	Contribution from C taken into account
KSH01A	301.94	501036	2.780	2.692	0.088	2.537	0.155
KSH01A	401.63	501030	2.638	2.554	0.084	2.356	0.199
KSH01A	482.90	501030	2.451	2.386	0.066	2.386	0
KSH02	310.93	501030	2.467	2.320	0.147	2.320	0
KSH02	610.12	501030	2.725	2.632	0.094	2.552	0.080
KSH02	794.43	501030	2.511	2.429	0.083	2.323	0.106
Mean value					0.093		0.135

In Table 4-11 and Table 4-12, thermal conductivity values calculated using the SCA method are compared with measured values of the same sample (not always the identical sample although closely located). Only 6 samples are possible to compare regarding measured and calculated thermal conductivity for rock type Fine-grained dioritoid (501030) and Quartz monzodiorite (501036). To be able to compare values for the Ävrö granite (501044), altogether 18 measurements from Äspö HRL have been used. The rock types of these samples have been reclassified from Äspö to Simpevarp nomenclature /Wahlgren, 2004/. Due to reclassification the results differ slightly compared to earlier preliminary results. In Table 4-12 and Table 4-11 the comparison of TPS and SCA data for analyse (A) and (B) is presented and Table 4-10 specifies the samples included in the comparisons. Table 4-12 indicates a potential bias in the SCA calculations for some rock types (deviations between measurements and calculations).

Table 4-10. Specification of samples included in the comparison of thermal conductivity (W/(m·K)) calculated from mineral composition (SCA) and measured with TPS method.

Borehole/ sample ID	Secup (m)	Rock type	SCA	TPS	Diff. (SCA-TPS)/TPS (%)
KA2599G01	5.9	501044	2.35	2.49	-5.6
KA2599G01	14.63	501044	2.35	2.34	0.4
KA2599G01	25.32	501044	2.35	2.47	-4.9
KA2599G01	44.28	501044	3.01	2.99	0.7
KA2599G01	70.6	501044	2.35	2.84	-17.3
KA2599G01	85.1	501044	2.35	2.69	-12.6
KA2599G01	101.85	501044	3.38	3.11	8.7
KA2599G01	120.05	501044	3.01	3.22	-6.5
KA2599G01	126.35	501044	3.01	3.55	-15.2
KA 3539-1	1.00	501044	2.24	2.42	-7.4
KA 3545	0.83	501044	3.20	2.72	17.7
KA 3551	0.95	501044	3.20	2.76	15.9
KA 3563	0.88	501044	2.24	2.39	-6.3
KA 3569	0.87	501044	2.24	2.42	-7.4
KA 3575	1.03	501044	2.24	2.44	-8.2
KA 3581	1.10	501044	2.24	2.50	-10.4
KA 3587	0.97	501044	2.24	2.33	-3.9

Borehole/ sample ID	Secup (m)	Rock type	SCA	TPS	Diff. (SCA- TPS)/TPS (%)
KA 3593-1	1.42	501044	2.24	2.55	-12.2
KSH01A ¹	401.63	501030	2.64	3.02	-12.7
KSH01A ¹	482.90	501030	2.45	2.84	-13.7
KSH02 ¹	310.93	501030	2.47	2.75	-10.3
KSH02 ¹	610.12	501030	2.73	2.78	-2.0
KSH02 ¹	794.43	501030	2.51	2.85	-11.9
KSH01A ¹	301.94	501036	2.78	2.79	-0.4
KSH01A*	401.63	501030	2.82	3.02	-6.6
KSH01A*	482.90	501030	3.90	2.84	37.3
KSH02*	310.93	501030	3.09	2.75	12.4
KSH02*	610.12	501030	3.19	2.78	14.8
KSH02*	794.43	501030	3.10	2.85	8.8
KSH01A*	301.94	501036	2.83	2.79	1.43

¹ The degree of sericitisation and chloritisation has been considered.

* Based on the first (A) calculation of mineral composition. Observe only used in this section and not further in this report.

Table 4-11. Comparison of thermal conductivity for samples with different rock types calculated from mineralogical compositions (A) with the SCA method and measured with the TPS method. Observe that this comparison only is used in this section and not further in this report.

Method	Fine-grained dioritoid 501030, 5 samples Mean λ , (W/(m·K))	Quartz monzodiorite 501036, 1 sample Mean λ , (W/(m·K))
Calculated (SCA)	3.22	2.83
Measured (TPS)	2.85	2.79
Diff. (SCA-TPS)/TPS	13.3%	1.43%

Table 4-12. Comparison of thermal conductivity for samples with different rock types calculated from mineralogical compositions (B) with the SCA method and measured with the TPS method.

Method	Fine-grained dioritoid 5 samples Mean λ , (W/(m·K))	Quartz monzodiorite 1 sample Mean λ , (W/(m·K))	Ävrö granite 18 samples Mean λ , (W/(m·K))
Calculated (SCA)	2.56	2.78	2.57
Measured (TPS)	2.85	2.79	2.68
Diff. (SCA-TPS)/TPS	-10.1%	-0.4%	-4.1%

Statistical tests were performed to compare the mean and variance for measured (TPS) and calculated (SCA) values of thermal conductivity. Tests were performed on samples coming from the same locations (not always the identical sample although closely located) for rock type Fine-grained dioritoid (501030) and Ävrö granite (501044), see Table 4-10.

For Ävrö granite no significant differences in the mean and the variance were noted (5% significance level). For Fine-grained dioritoid the difference in mean between TPS and SCA data was significant but a significant difference in variance could not be detected. The paired t-test was applied to test for difference in the mean between TPS and SCA data.

4.4.4 Comparison with measurements on all samples

Similar tests, as in the chapter above, were also performed on all TPS data and SCA data coming from the Äspö and Simpevarp subarea for rock type Fine-grained dioritoid (501030), Quartz monzodiorite (501036), and Ävrö granite (501044), see Table 4-3 and Table 4-6. The tests indicate that there is a significant difference in both the mean and the variance for rock type Fine-grained dioritoid (501030) and Quartz monzodiorite (501036). This is illustrated in Figure 4-7 for rock type Fine-grained dioritoid where the two-sample t-test was applied to test for difference in the mean. The lower box plot in the figure illustrates the sample distribution where the middle line of the box corresponds to the median, the start and end of the box the first and third quartile, the horizontal lines from the box are upper and lower whisker. Values beyond the whiskers are defined as outliers, and are marked by stars.

For the Fine-grained dioritoid and the Quartz monzodiorite the mean value of SCA calculations is smaller than the mean value of TPS measurements meaning the SCA method is underestimating the thermal conductivity. The variance of TPS measurements is smaller than the variance of SCA calculations meaning the values are distributed within a smaller interval. The situation is different for rock type Ävrö granite (501044), where both mean and variance for TPS and SCA data are almost identical, i.e. no significant difference could be detected. TPS-data are supposed to be more reliable than SCA-data.

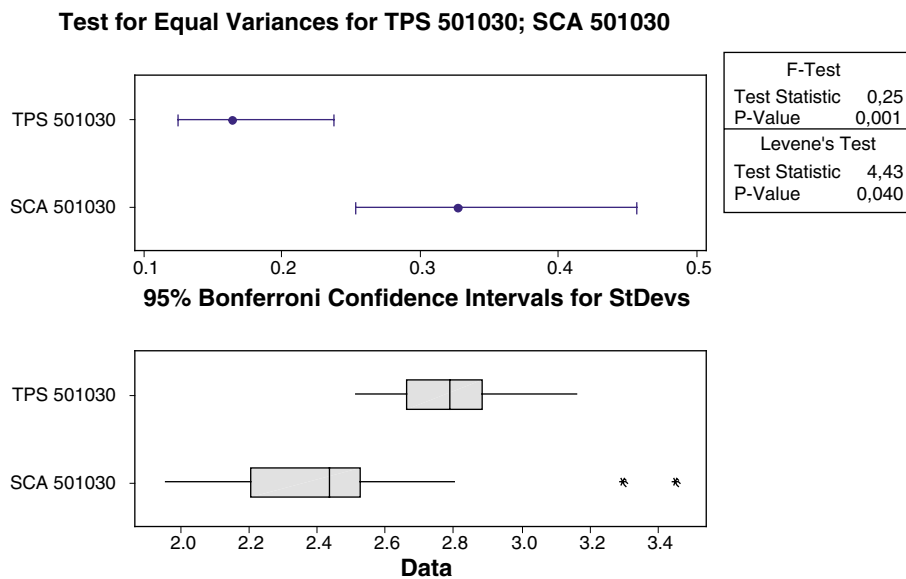


Figure 4-7. Result of test for equal variances between all TPS measurements and SCA calculations of thermal conductivity for rock type Fine-grained dioritoid (501030) (F-test and Levene's test). There is a significant difference in variance, as indicated by the low p-values.

4.5 Thermal conductivity from density

4.5.1 Method

In /Sundberg, 2003b/ an equation of the relationship between density and thermal conductivity for Ävrö granite (501044) was found and presented, see Figure 4-8 and Equation 4-1. The equation was derived based on 20 samples from Äspö HRL (the prototype repository and borehole KA2599G01) including Äspö diorite, Ävrö granite and Fine-grained granite (one xenolith sample was excluded) according to Äspö nomenclature.

The relationship between density and thermal conductivity according to /Sundberg, 2003b/ is:

$$y = 27.265x^2 - 156.67x + 227.18 \quad R^2 = 0.88 \quad \text{Equation 4-1}$$

The relationship has been further developed using new laboratory measurements on thermal properties and classifications of the samples according to Simpevarp nomenclature. The improved relationship is presented in /Sundberg et al. 2005/ but also below in Equation 4-2 and Figure 4-8. The relationship includes old measurements which have been reclassified as Ävrö granite and new measurements which have been carried out both within the Simpevarp site investigation program (5 samples within the Ävrö granite (501044) in KAV01) and in /Sundberg et al. 2005/ (14 samples in rock type Ävrö granite (501044), one sample excluded due to appearance of Granite) although no measurements from Laxemar have been included.

Relationship between density and thermal conductivity, Ävrö granite (501044), in this study.

$$y = -7.1668x + 22.326 \quad R^2 = 0.74 \quad \text{Equation 4-2}$$

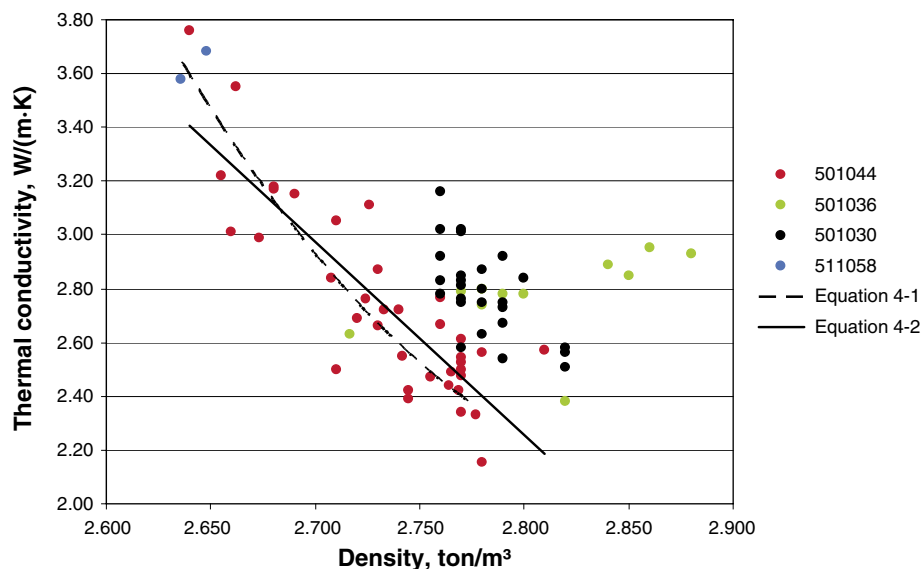


Figure 4-8. Relationships between density and thermal conductivity. Equation 4-1 is the relationship from /Sundberg, 2003b/ derived by polynomial regression and Equation 4-2 is the improved relationship based on a linear regression which is used in this study. The validity of both relationships is limited to rock type Ävrö granite (501044) and data from the other rock types are not used in the regression.

The model (relationship between density and thermal conductivity) has been evaluated statistically by calculating both the confidence and prediction interval. The confidence interval marked in Figure 4-9 with a red dashed line indicates the uncertainty of the model. The interval can be interpreted as the area the model will fall within with 95% probability. The prediction interval marked in Figure 4-9 with a green dashed line shows the uncertainty in predicting thermal conductivity from a density measurement. The interval can be interpreted as the area a prediction of the thermal conductivity will fall with 95% probability. As Figure 4-9 indicates, the prediction interval is much wider than the confidence interval, implying the model fitted to data is less uncertain than a prediction of thermal conductivity from density measurement.

4.5.2 Result

The relationship between density and thermal conductivity derived in previous Section 4.5.1 has been applied to density loggings of boreholes KAV01 and KSH01A. The density loggings of KAV01 and KSH01A used for this purpose are illustrated in Figure 4-10 and Figure 4-11. For the same boreholes the thermal conductivities are illustrated in Figure 4-12 and Figure 4-13. The rock type distribution (dominating rock type > 1 m) is connected to the illustration of the density loggings by different colour codes (similar to Boremap illustrations) and a legend.

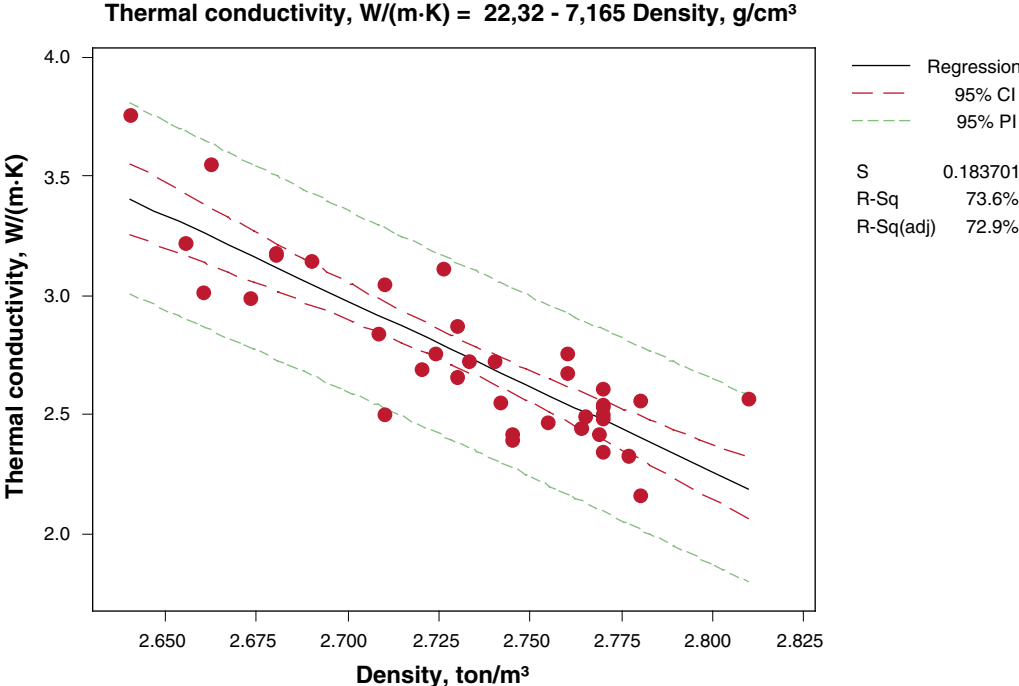


Figure 4-9. Statistical analysis of the relationship between density and thermal conductivity for rock type Ävrö granite (501044). The red lines indicate the confidence interval and the green lines the prediction interval.

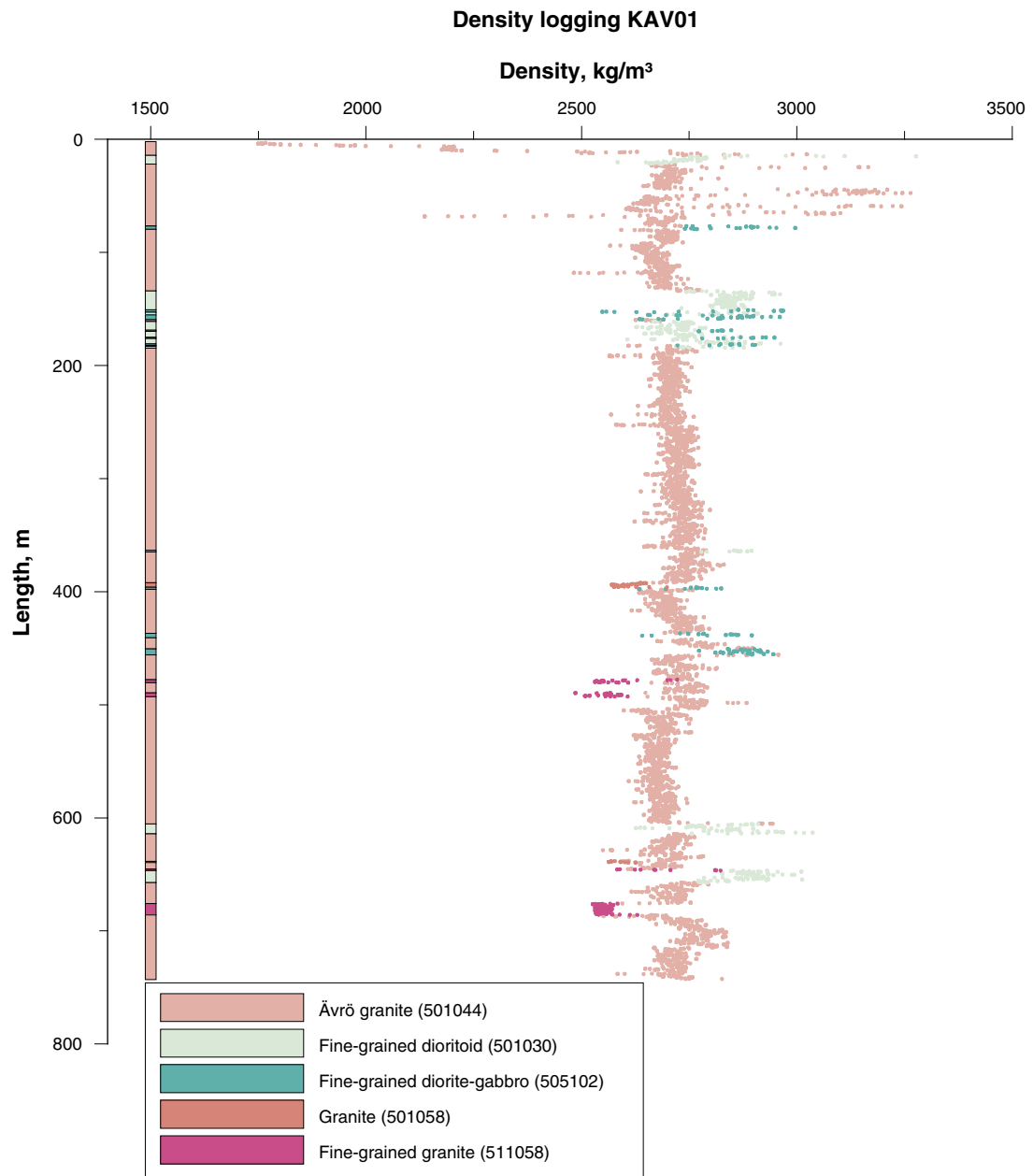


Figure 4-10. Density logging of KAV01 with rock types marked in different colours.

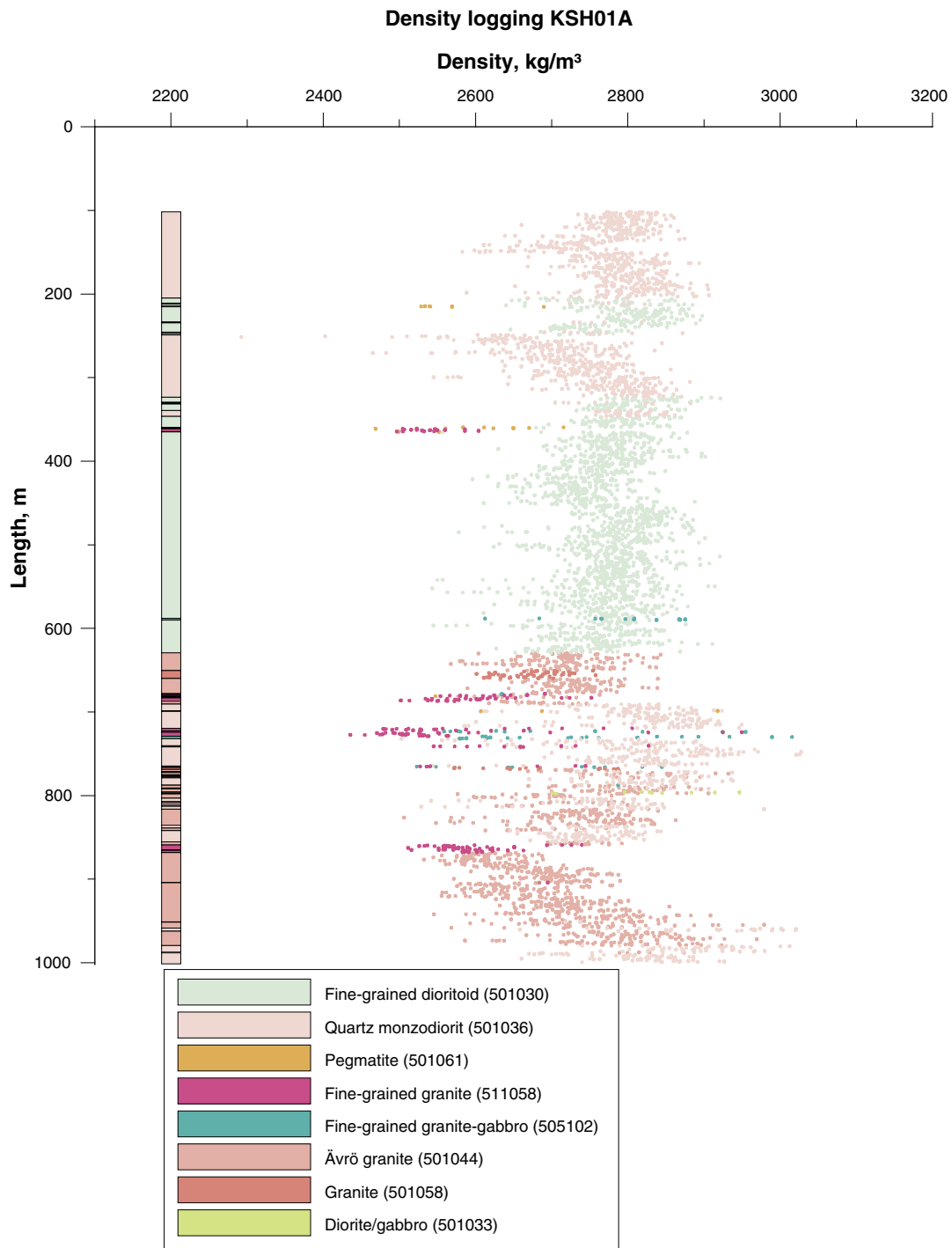


Figure 4-11. Density logging of KSH01A with rock types marked in different colours.

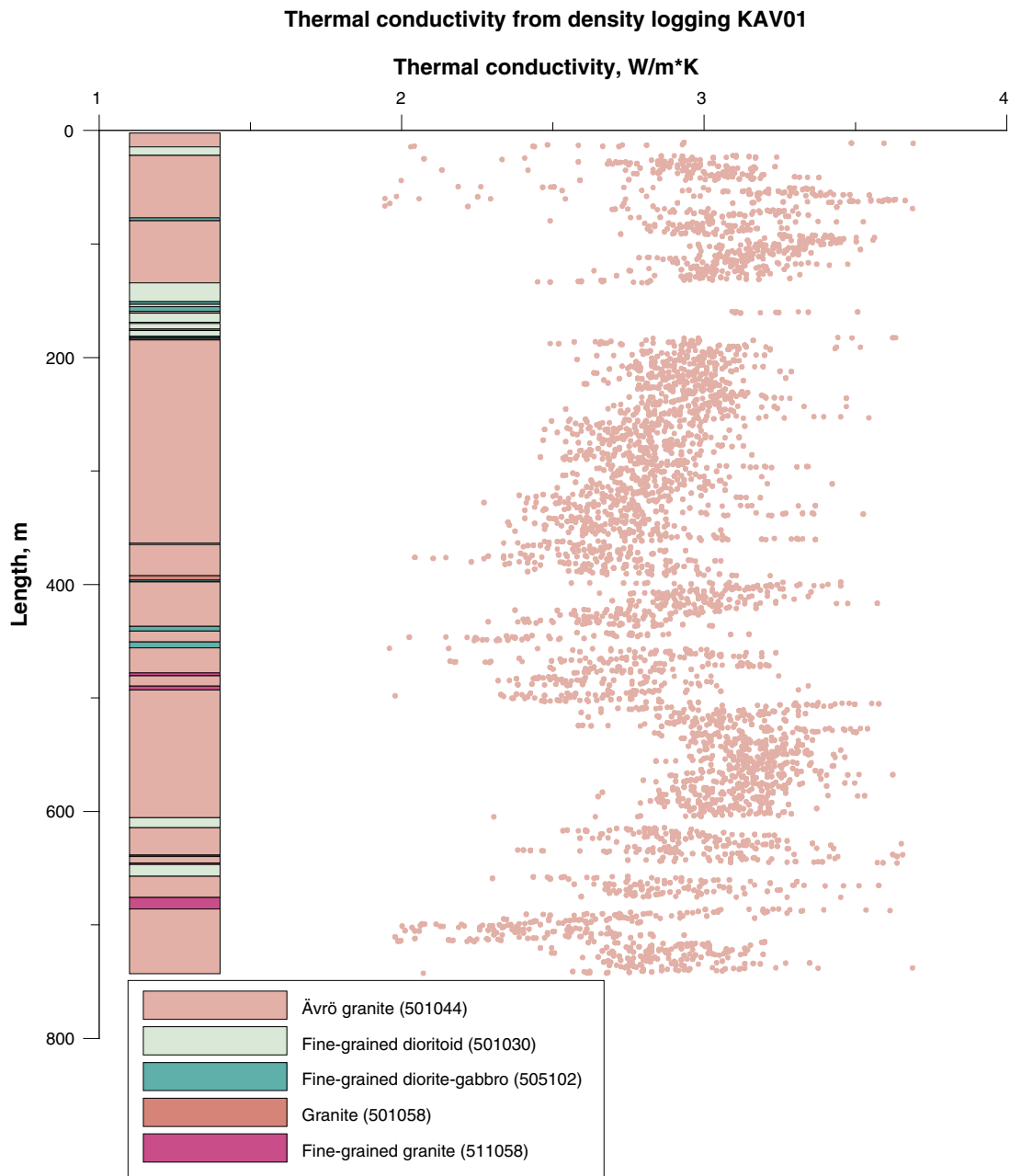


Figure 4-12. Thermal conductivity of Ävrö granite (501044) in KAV01 estimated from density logging alongside a generalised geological borehole log.

Thermal conductivity from density logging KSH01A

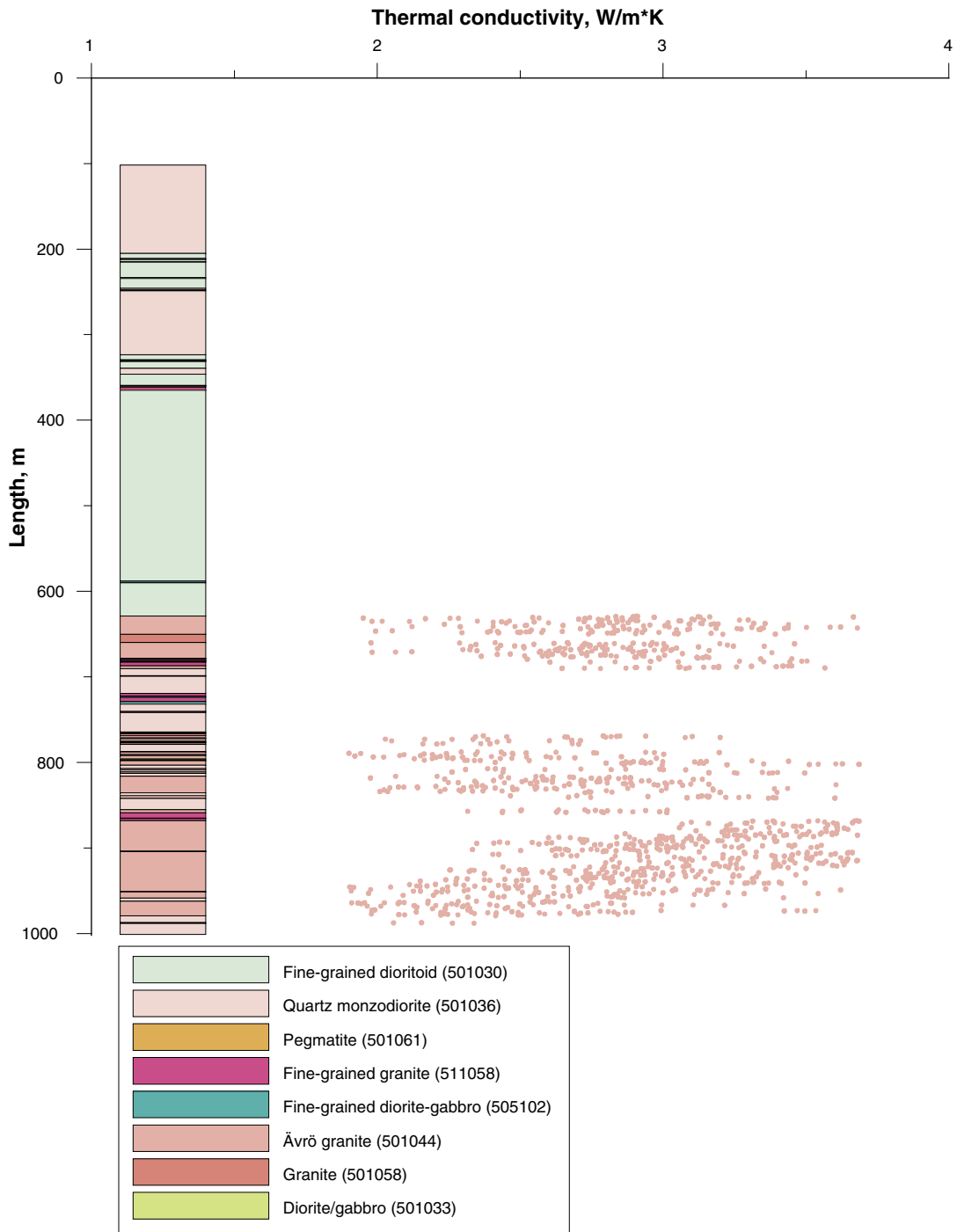


Figure 4-13. Thermal conductivity of Ävrö granite (501044) in KSH01A estimated from density logging alongside a generalised geological borehole log.

The background data to the density logging of KAV01 has been re-sampled, filtered and correlated to measured core samples along the borehole /Mattsson and Thunehed, 2004b/, see Table 4-13. The re-sampling is done to make sure that all logging methods have values for the same common depth co-ordinate with exactly 0.1 m point distance. A filter has been applied to the log to reduce the effects from high-frequency measurement noise. For data from borehole KAV01, KLX01, KLX02 and KSH03B a 3 point average filter has been used, while for KSH01A, KSH01B, KSH02 and KSH03A a 3 point median filter was used. The correlation to measured core samples has been done by fitting a regression line to a crossplot of density logging data versus density data from core samples. For KAV01 two regressions has been done, linear fit and fit through origin, where data correlated to the fit through origin is called re_density_corr and the data correlated to the linear fit is called new_re_density_corr in Sicada. For KAV01 data called new_re_density_corr and re_density_corr has been additionally filtered to reduce high frequent noise /Mattsson and Thunehed, 2004b/. In this report new_re_density_corr data has been used.

The background data of KSH01A has also been resampled, filtered and correlated to measured samples /Mattsson and Thunehed, 2004a/, see Table 4-13. Filtering and resampling of the density logging has been done in /Mattsson and Thunehed, 2004a/ while correlation to measured samples has been done in this report. The density logging from Sicada database called re_density has been correlated to measured samples in this report with the equation:

$$\text{Logging data} = 1.003 \cdot \text{sample data} \quad \text{/Mattsson and Thunehed, 2004a/}$$

This takes into account the correction between logging data and density measurement on samples. Additional filtering has not been performed for this borehole.

When the relationship between density and thermal conductivity is applied to density loggings of KAV01 and KSH01A the distribution of thermal conductivity within the boreholes can be illustrated, see Figure 4-12 and Figure 4-13. It is assumed that the developed relationship is valid within the density interval 2,600–2,850 kg/m³, which corresponds to the thermal conductivity interval 1.90–3.69 W/(m·K) that is slightly outside the data interval. When this is taken under consideration 280 density measurements along KAV01 has been excluded, resulting in 5,970 density measurements still valid. For KSH01A a total of 229 density measurements were excluded and 1,794 measurements were retained.

Table 4-13. Stepwise work on original density loggings of KAV01 and KSH01A.

Sicada name	Correction	Correction performed by
KAV01		
Re_density	Re-sampled and filtered	/Mattsson and Thunehed, 2004b/
Re_density_corr	Correlation to samples (fit through origin) and filtered	/Mattsson and Thunehed, 2004b/
New_re_density_corr	Correlation to samples (linear regression)	/Mattsson 2004c/
KSH01A		
Re_density	Re-sampled and filtered	/Mattsson and Thunehed 2004a/
Re_density_corr	Correlation to samples	See text

4.5.3 Comparison with measurements and calculations

In order to evaluate how well the model in Equation 4-2 (cf Figure 4-8) reflects the actual thermal conductivity in the borehole, a comparison of measured samples (TPS) and estimated values from density logging was performed. A comparison of measured densities on samples and the corresponding interval of the borehole have also been performed.

Five samples from KAV01 in Ävrö granite, all taken over a 1 m long section (secup 508.25 to seclow 509.26), was measured with the TPS method and density determined. For the same section of the borehole the thermal conductivity and density was calculated from the density logging and by Equation 4-2. The results of the comparisons are presented in Table 4-14 and Table 4-15.

Table 4-14. Comparison of thermal conductivity (W/(m·K)) measured with the TPS method on 5 samples from KAV01 in Ävrö granite vs. calculated thermal conductivity from density logging of the same borehole interval.

Method	Mean	St. dev	Min	Max	Number of samples
Thermal conductivity from density logging	2.80	0.049	2.71	2.88	12
TPS measurement on sample	3.25	0.29	3.01	3.76	5
Diff. (Density logging–TPS)/TPS	–14.0%				

Table 4-15. Comparison of density (kg/m³) measured on 5 samples from KAV01 in Ävrö granite and measured with density logging of the same borehole interval.

Method	Mean	St. dev	Min	Max	Number of samples
Density from density logging	2,725	6.8	2,714	2,736	12
Density measurements on samples	2,670	20.0	2,640	2,690	5
Diff. (Density logging–sample)/sample	2.0%				

The difference in mean for the density values calculated with the two separate methods, illustrated in Table 4-15, results a difference in thermal conductivity of 0.39 W/(m·K).

The two comparisons indicate a fairly large uncertainty in the method but it is noted that the comparison is based on a small number of samples, only reflecting a small interval of the borehole.

4.6 Modelling of thermal conductivity (rock type level)

4.6.1 Method

There are different data sets of thermal conductivity for the dominating rock types. The most reliable data comes from TPS measurements but these samples are probably not representative of the rock type due to limited number of samples and the sample selection. Therefore, also SCA calculations from the mineral distribution have to be included in the rock type model since they have a larger spatial distribution in the rock mass.

Rock type models (Probability Density Functions, PDF's) of thermal conductivity have been produced by adding the data from TPS measurements and SCA calculations from mineral composition. The SCA calculations of rock type Fine-grained dioritoid (501030) and Ävrö granite (501044) have been corrected in order to eliminate or reduce the effect of a potential bias in the SCA calculations according to Table 4-12. For the two rock types, a correction with a factor of 1.10 and 1.04 respectively is carried out due to the differences between the methods.

The rock type models are used to model thermal properties for lithological domains, see Section 5. Density loggings have not been used for the rock type models, but are applied in the domain modelling in order to include spatial variability. All rock types are assumed to be characterised by normal (gaussian) PDF's. Probability plots, assuming normal distribution of thermal conductivities, are illustrated in Figure 4-14 and lognormal distributions in Appendix A. There is a tendency for the PDF models to overestimate the number of low thermal conductivity values and to underestimate the number of high values.

Statistical tests were performed on differences in the mean and variance of TPS measurements between different rock types. Significant differences in both the mean and variance could be observed between rock type Fine-grained dioritoid (501030) and Ävrö granite (501044), as well as between Quartz monzodiorite (501036) and Ävrö granite (501044). The differences were not that obvious between Fine-grained diorite (501030) and Quartz monzodiorite (501036).

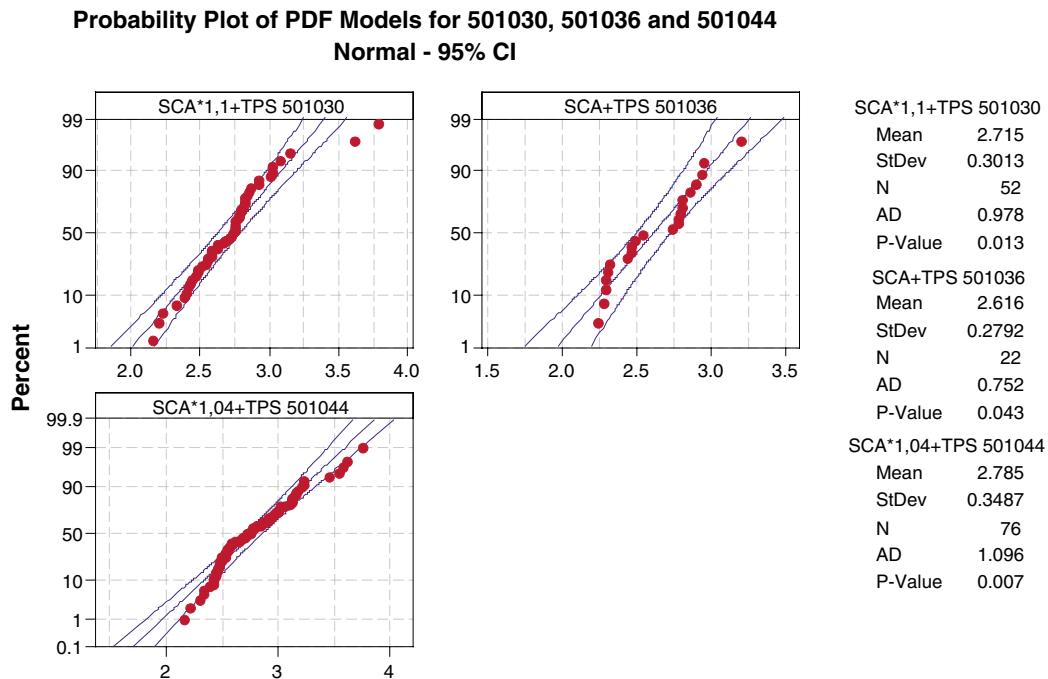


Figure 4-14. Probability plots (normal distributions) of thermal conductivity separated on rock types. For rock type Fine-grained dioritoid (501030) and Ävrö granite (501044) the SCA calculations have been corrected with a factor of 1.10 respectively 1.04.

4.6.2 Ävrö granite (501044)

For rock type Ävrö granite there are three sources to thermal conductivity data, SCA calculations from mineral compositions (modal analyse), TPS measurements and density loggings using the relationship presented in Section 4.5. Data from the three methods are summarised in Table 4-16. Distribution models (PDF's) based on data from the different methods are presented in Figure 4-15 and model properties of all rock types are presented in Table 4-20. In Figure 4-16 and Figure 4-17 empirical cumulative distribution functions with fitted models (normal distributions) of rock type Ävrö granite (501044) are presented.

SCA calculations used in the comparison with TPS measurements have been excluded since both methods supply a thermal conductivity value of the same sample (18 SCA data excluded). Thermal conductivity from density loggings has been calculated for data from borehole KSH01A, KAV01 and KLX02. Probability plots of data from the three methods indicate that data are neither lognormally nor normally distributed, except for SCA data (Appendix A). However, for the purpose of the domain modelling it is sufficient to use a normal distribution as rock type model. This is because calculated values from density loggings are used for almost all sections of Ävrö granite in the modelling. The rock type model is only utilised to fill the data gaps in logging data, see Figure 5-4.

Except for the three methods, a rock type model of the thermal conductivity of rock type Ävrö granite (501044), used in minor extent in the lithological domain modelling, has been supposed as a composition of both TPS measurements and SCA calculations, see Table 4-16. The SCA calculations have in this case been corrected with a factor 1.04 which in previous Section 4.4.3 has been shown as the difference between the two methods. A normal distribution is applied for TPS measurements and corrected SCA data, although probability plots indicate that lognormal distribution could be used, see Appendix A. As indicated by Figure 4-17 there is large difference in the mean between the PDF model and data calculated from density loggings.

For Ävrö granite, the standard deviation of thermal conductivity from density logging is partly a consequence of the restricted interval for the density vs. thermal conductivity relationship. The different mean values may indicate potential bias in density data. It is also possible that the density data represent a rock mass with higher thermal conductivity.

Table 4-16. Three different distributions of thermal conductivity (W/(m·K)) for rock type Ävrö granite (501044), based on different methods together with the rock type model.

	TPS measurements	Calculations from mineral composition	Calculations from density loggings	Rock type model
Mean	2.73	2.72	2.96	2.79
St. dev	0.35	0.33	0.36 ¹⁾	0.35
Number of samples	37	39	13,037	
Comment	Including samples from Äspö HRL.	Comparable samples indicates correction 4%.		TPS measurements and calculations from mineral composition combined.

¹⁾ The variance is a consequence of the restricted validity interval for the density vs. thermal conductivity relationship.

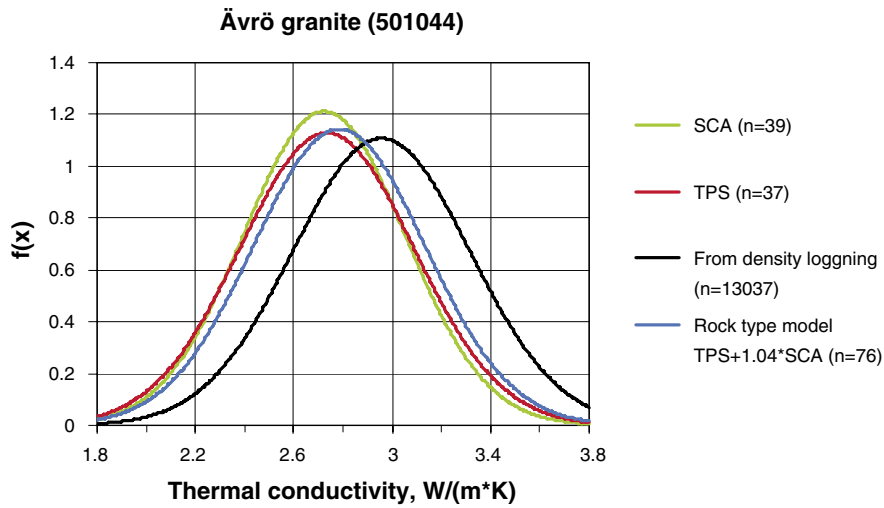


Figure 4-15. PDF's for calculated values (SCA), measured values (TPS), density logging for rock type Ävrö granite (501044), and a summarising rock type model where SCA values are corrected with a factor of 1.04. Data from the density loggings result in a higher mean value than TPS and SCA data.

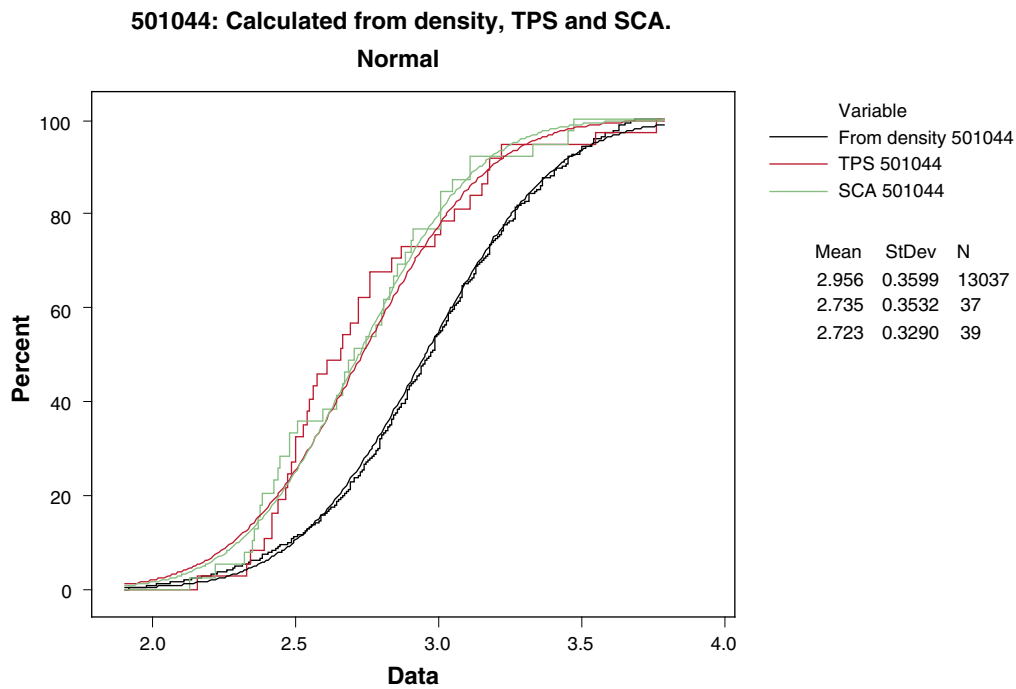


Figure 4-16. Cumulative histogram of Ävrö granite (501044) with data from three sources, calculated from density loggings, TPS measurements and SCA calculations from mineral composition.

501044: Calculated from density and model SCA*1,04+TPS.

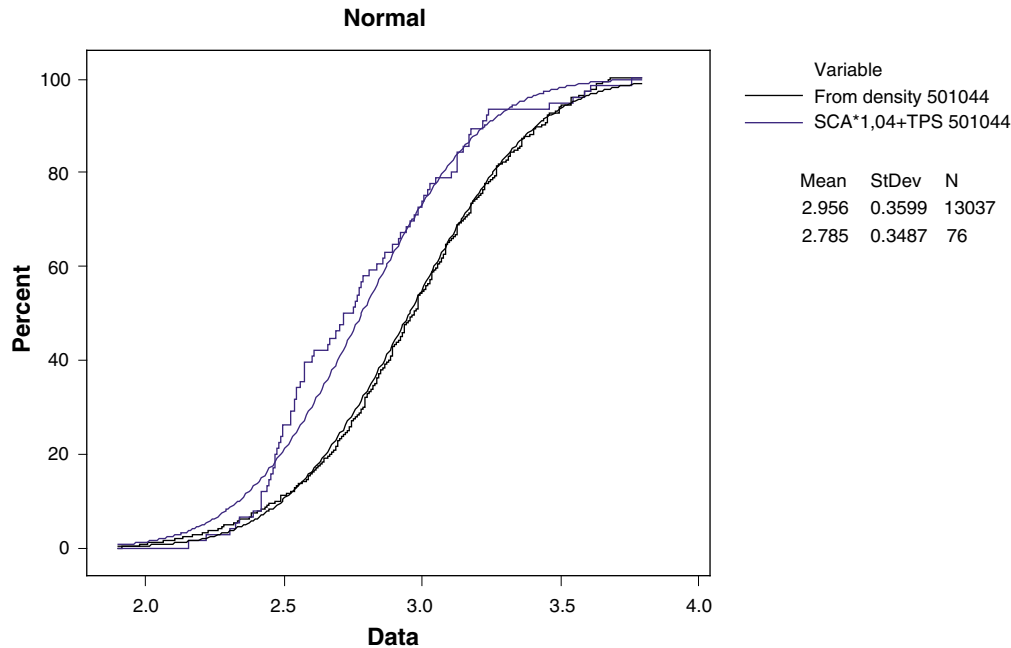


Figure 4-17. Cumulative histogram of Ävrö granite (501044) with thermal conductivity calculated from density loggings and the rock type model with corrected SCA and TPS data.

4.6.3 Quartz monzodiorite (501036)

For rock type Quartz monzodiorite (501036) there are two sources to thermal conductivity data, SCA calculations based on mineral composition and TPS measurements. Results from Äspö HRL are included. Data from the two methods are summarised in Table 4-17. Distribution models (PDF's) based on data from the different methods are presented in Figure 4-18 and model properties of all rock types are presented in Table 4-20. As can be seen in the distribution functions in Figure 4-18 the two methods results in different mean values and variances. Figure 4-19 presents empirical cumulative distribution functions with fitted models (normal distributions) of rock type Quartz monzodiorite (501036).

SCA calculations used in the comparison with TPS measurements have been excluded since both methods give a thermal conductivity of the same sample (1 sample excluded). Data from the TPS method has in probability plots shown to be normal distributed rather than lognormal distributed but data from the SCA method has shown not to be either lognormal or normal distributed, see Appendix A. This is dependent on an outlier. Although, data has been set as normal distributed.

Except from the two methods a rock type model of the thermal conductivity for rock type Quartz monzodiorite (501036), used in the lithological domain modelling, has been supposed as a composition of both TPS measurements and SCA calculations, see Table 4-17. The SCA calculations have in this case not been corrected due to insufficient data. The rock type model of TPS measurements and SCA calculations have, by probability plots, shown to be normal distributed rather than lognormal distributed, see Appendix A.

Table 4-17. Two different distributions of thermal conductivity (W/(m·K)) for rock type Quartz monzodiorite (501036), based on different methods together with the rock type model.

	TPS measurements	Calculations from mineral composition	Calculations from density loggings	Rock type model
Mean	2.83	2.44	–	2.62
St. dev	0.07	0.26	–	0.28
Number of samples	10	12	–	
Comment	Data from 2·1 m interval.	Comparable sample (only one!) indicate no correction.		TPS measurements and calculations from mineral composition combined.

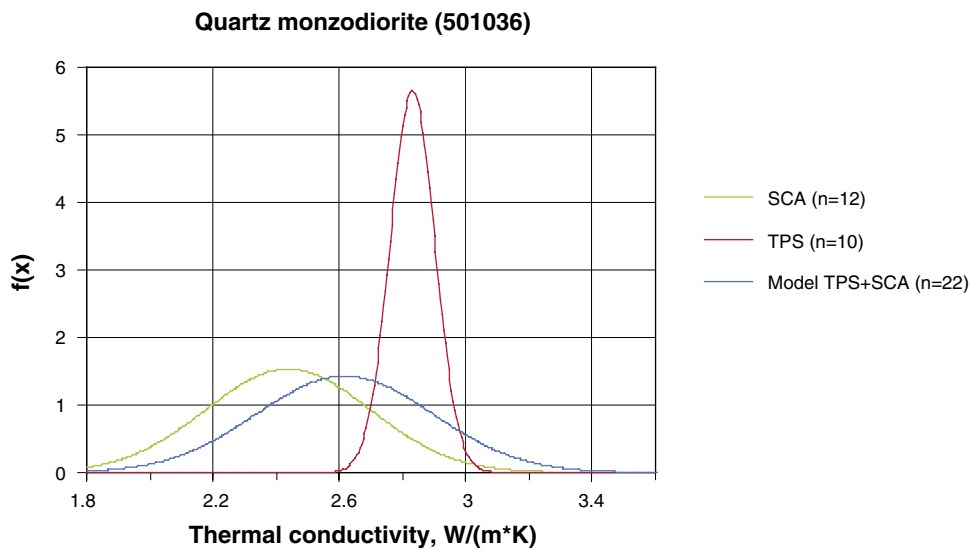


Figure 4-18. PDF's for calculated values (SCA) and measured values (TPS) based on rock type Quartz monzodiorite (501036). Data based on SCA has not been corrected in the summarising rock type model due to lack of data.

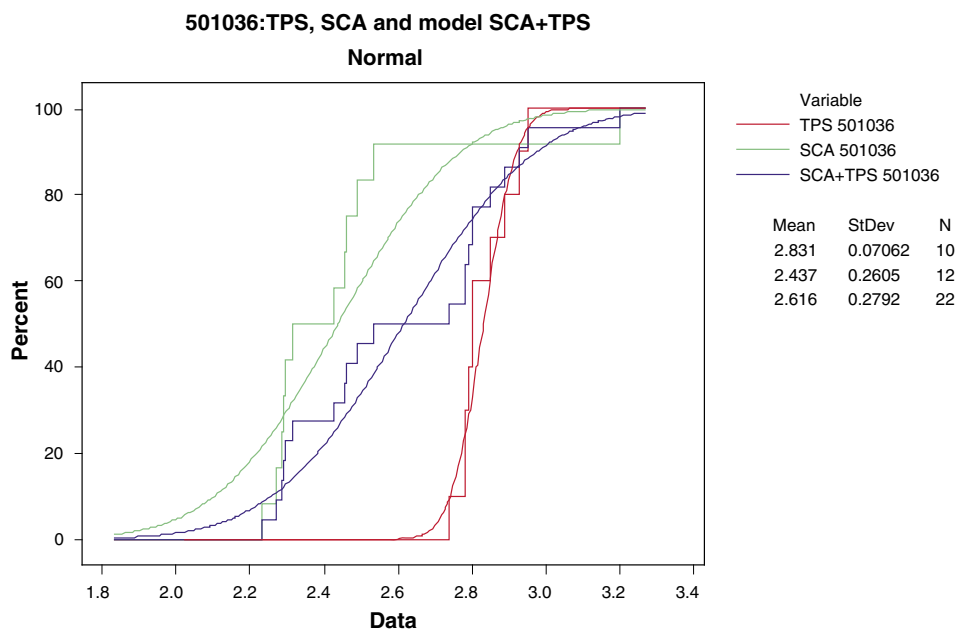


Figure 4-19. Cumulative histogram of Quartz monzodiorite (501036) with data from two different methods and a rock type model where TPS and SCA data has been summarised.

4.6.4 Fine-grained dioritoid (501030)

For rock type Fine-grained dioritoid (501030) there are two sources to thermal conductivity data, SCA calculations and TPS measurements. Data from the two methods are summarised in Table 4-18. Models based on data from the different methods are presented in Figure 4-20 and model properties of all rock types are presented in Table 4-20. As can be seen in the distribution functions in Figure 4-20 the two methods results in different mean values and variances. Table 4-19 shows that there is a difference in the distributions of SCA data depending on whether the samples are gathered in boreholes or as surface samples. Figure 4-21 presents empirical cumulative distribution functions with fitted models (normal distributions) of rock type Fine-grained dioritoid (501030).

SCA calculations used in the comparison with TPS measurements have been excluded since both methods give a thermal conductivity of the same sample (5 samples excluded). Data from the two methods has in probability plots shown to be lognormal distributed rather than normal distributed, see Appendix A. Although, data has been set as normal distributed since the probability plots show the distribution still good to use.

Except from the two methods a rock type model of the thermal conductivity for the Fine-grained dioritoid, used in the lithological domain modelling, has been supposed as a composition of both TPS measurements and SCA calculations. The SCA calculations has in this case been corrected with a factor 1.10 which in previous Section 4.4.3 has been shown as the difference between the two methods for this particular rock type. The model of TPS measurements and corrected SCA calculations has also, by probability plots, shown to be lognormal distributed rather than normal distributed but is still set to normal distributed, see Appendix A.

Table 4-18. Two different distributions of thermal conductivity (W/(m·K)) for rock type Fine-grained dioritoid (501030) based on different methods together with the rock type model.

	TPS measurements	Calculations from mineral composition	Calculations from density loggings	Rock type model
Mean	2.79	2.40	–	2.72
St. dev	0.16	0.35	–	0.30
Number of samples	26	26	–	
Comment		Comparable sample indicate correction +10%		TPS measurements and calculations from mineral composition combined.

Table 4-19. Distributions of thermal conductivity data (W/(m·K)) from different methods for Fine-grained dioritoid (501030) subdivided into borehole data and surface samples.

	SCA calculations Surface samples	Borehole samples	TPS measurements Borehole samples
Mean	2.28	2.53	2.79
St. dev	0.24	0.40	0.16
Number of samples	13	13	26

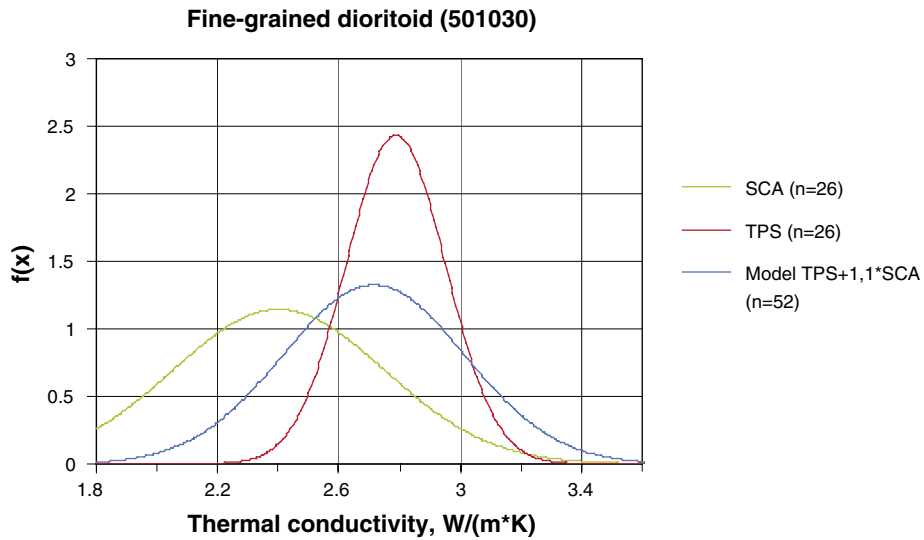


Figure 4-20. PDF's for calculated values (SCA) and measured values (TPS) based on rock type Fine-grained dioritoid (501030). Data based on SCA are corrected with a factor 1.10 in the summarised rock type model.

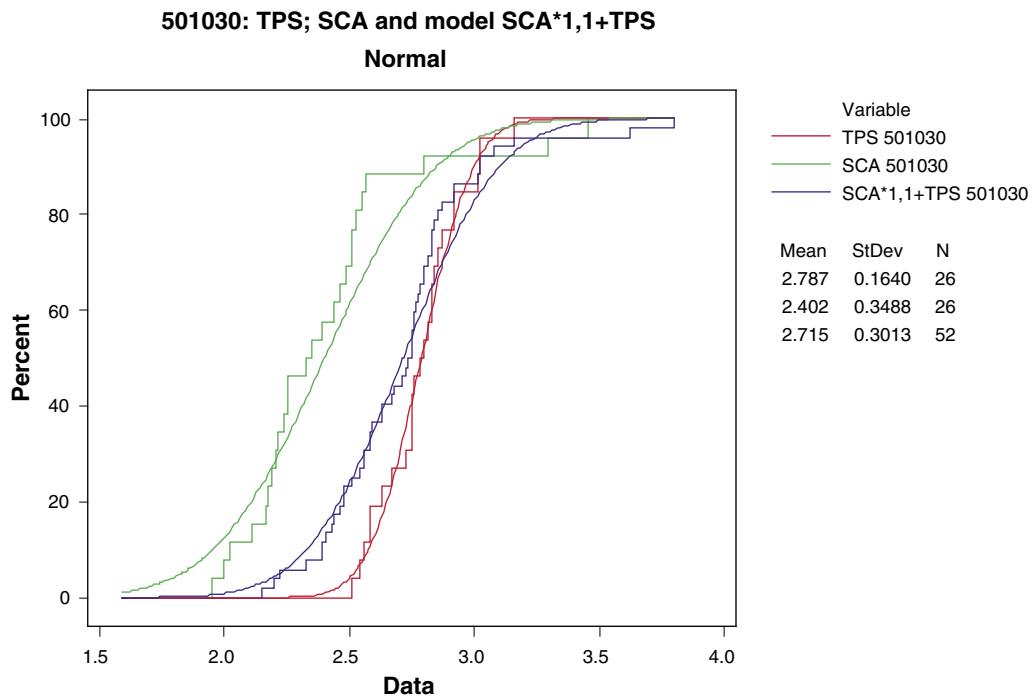


Figure 4-21. Cumulative histogram of Fine-grained dioritoid (501030) with data from two different methods and a rock type model where TPS and SCA data has been summarised.

4.6.5 Other rock types (505102, 501033, 501058 and 511058)

For other rock types except the Ävrö granite (501044), Quartz monzodiorite (501036), and Fine-grained dioritoid (501030), the extent of data is rather limited and in most cases only SCA calculations were available when modelling the different rock types. In Figure 4-22 empirical cumulative distribution functions of Fine-grained diorite-gabbro (505102), Diorite/Gabbro (501033), Granite (501058) and Fine-grained granite (511058) is presented together with fitted models (normal distributions). For granite (501058), the calculated thermal conductivity seems to be lower than expected for ordinary granite. Model properties of all rock types are presented in Table 4-20.

4.6.6 All investigated rock types

In Table 4-20 the model properties for the different investigated rock types are summarized. Thermal conductivity calculated by the SCA method is available for all seven of these rock types. TPS measurements are available for four rock types, while thermal conductivity could be calculated from density only for Ävrö granite (501044).

Empirical CDF of SCA 505102; SCA 501033; SCA 501058; SCA+TPS 511058

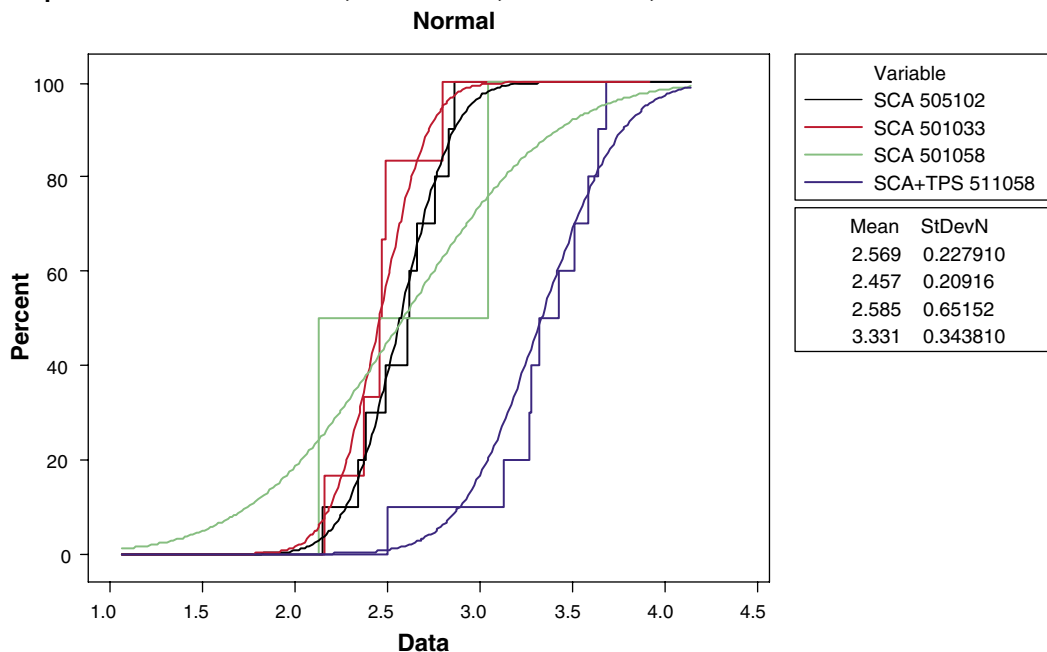


Figure 4-22. Cumulative histogram of Fine-grained diorite-gabbro (505102), Diorite/Gabbro (501033), Granite (501058) and Fine-grained granite (511058). For the Fine-grained granite (511058) data are from two different methods and a rock type model of summarised TPS and SCA data is illustrated. For the other three rock types (505102, 501033 and 501058), only SCA data was available.

Table 4-20. Model properties of thermal conductivity (W/(m·K)) from different methods and combinations divided by rock type. All rock type models are based on normal (Gaussian) distributions (PDF's).

Rock name (rock type)	Samples	Mean	St. dev	Number of samples	Comment
Ävrö granite (501044)	Therm. cond. from density logging	2.96	0.36	13,037	The st. dev of therm. cond. from density logging is partly a consequence of the restricted interval for the density vs. thermal conductivity relationship. Different mean values may indicate potential bias in density data.
	TPS	2.74	0.35	37	
	SCA	2.72	0.33	39	
	Rock type model: 1.04*SCA+TPS	2.79	0.35	76	
Quartz monzodiorite (501036)	TPS	2.83	0.07	10	
	SCA	2.44	0.26	12	
Fine-grained dioritoid (501030)	Rock type model: SCA+TPS	2.62	0.28	22	
	TPS	2.79	0.16	26	
Fine-grained granite (511058)	SCA	2.40	0.35	26	
	Rock type model: 1.1*SCA+TPS	2.72	0.30	52	
Fine-grained diorite-gabbro (505102)	TPS	3.63	0.07	2	
	SCA	3.26	0.35	8	
Diorite/Gabbro (501033)	Rock type model: SCA+TPS	3.33	0.34	10	
	Rock type model: SCA	2.57	0.23	10	
Granite (501058)	Rock type model: SCA	2.46	0.21	6	
	Rock type model: SCA	2.59	0.65	2	

4.7 Spatial variability

4.7.1 Spatial variability in thermal conductivity from measurements

In the Ävrö granite (501044), samples in groups of five over a distance of approximately 1 m have been taken for TPS measurements. Data for these four groups are presented in Table 4-21 and illustrated in Figure 4-23. Three of the groups are from the Äspö HRL in borehole KA2599G01 and one group is from the Simpevarp subarea in borehole KAV01. In one of the sample groups from the Äspö HRL, one sample has been excluded due to reclassification of the rock type. This sample was reclassified as Ävrö granite mixed with red granite and elements of fine-grained mafic rock type and is therefore no longer classified as Ävrö granite (501044).

Upscaling from TPS scale (cm) was performed by calculation of the geometric mean for each group, representing thermal conductivity at the group scale (1 m support). The values representing the 1 m scale are illustrated with the red box in Figure 4-23, 4 values in total. The mean at the 1 m scale was estimated to 2.77 W/(m·K) and the standard deviation to 0.24 W/(m·K), see Table 4-21. This standard deviation is estimated as the square root of the mean variance for the four groups of data. It illustrates the small-scale (< 1 m) variability in TPS data. The relatively high standard deviation at the 1 m scale is mainly due to high thermal conductivity values in the samples from KAV01, illustrating long distance changes in thermal conductivity for the Ävrö granite (501044).

Table 4-21. Estimation of thermal conductivity (W/(m·K)) at the 1 m scale from TPS measurements in the cm scale in Ävrö granite (501044). Samples in groups of five from boreholes KA2599G01 (Äspö HRL) and KAV01 (Simpevarp subarea). One measurement in the interval 24.02–24.72 (KA2599G01) was excluded because of ambiguous rock type.

Samples (secup–seclow)	Geometric mean	St. dev	Number of samples
KA2599G01 (4.33–5.23)	2.63	0.35	5
KA2599G01 (15.10–16.00)	2.58	0.06	5
KA2599G01 (24.02–24.72)	2.63	0.13	4
KAV01 (508.25–509.26)	3.24	0.29	5
Result for 1 m scale:	Arithmetic mean of 4 values: 2.77		
	St. dev of 4 values: 0.24 (representing small-scale variability, < 1 m)		

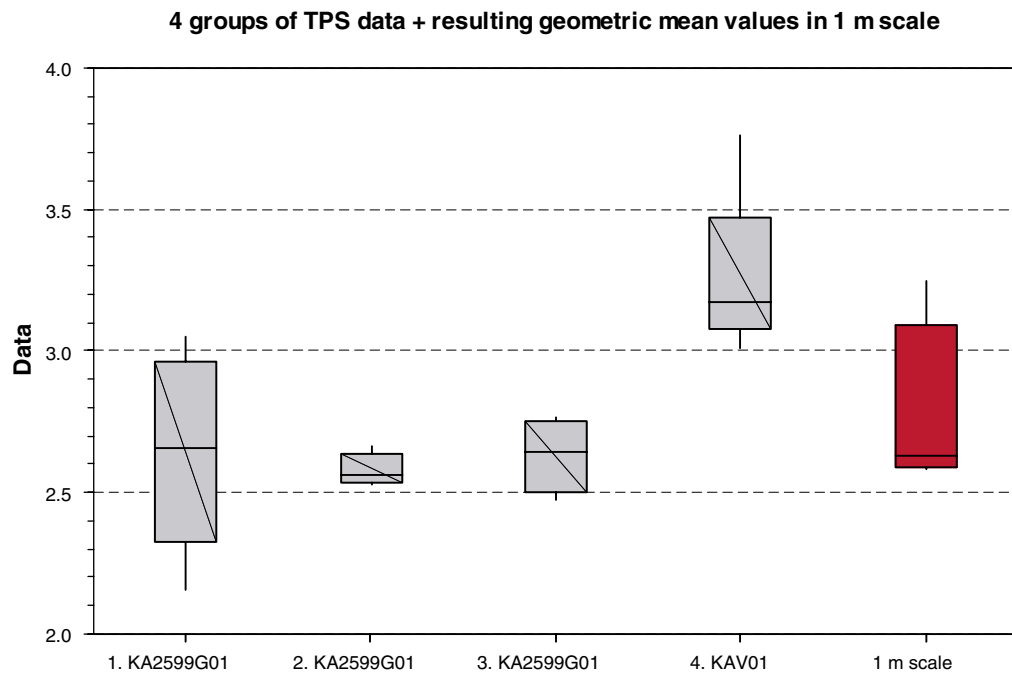


Figure 4-23. Upscaling of TPS measurements from cm scale to 1 m scale for rock type Ävrö granite (501044). Four groups of TPS measurements (grey boxes), each representing approximately 1 m, are used to estimate thermal conductivity at the 1 m scale (red box).

4.7.2 Spatial variability in thermal conductivity from density loggings

There are three main causes for the spatial variability of thermal conductivity at the domain level; (1) small scale variability between minerals, (2) spatial variability within each rock type, and (3) variability between the different rock types making up the domain. The first type entails variability in small samples (TPS measurements and modal analysis). At this scale, the small scale variability can be substantial. However, the variability is rapidly reduced when the scale increases.

The second type of variability causes variability in sample data from a rock type and cannot be explained by small scale variations. This is believed to be especially important for the rock type Ävrö granite, where this (spatial) variability is large. The reason for the variability within a rock type is the process of rock formation but also the system of classifying the rock types. This variability cannot be reduced but the uncertainty of the variability may be reduced. This is achieved by collecting a large number of samples at varying distances from each other, so that reliable variograms can be created.

Spatial variability of thermal conductivity within rock types has only been studied for rock type Ävrö granite (501044), where density loggings could be used. For other rock types it was not possible to study the spatial variability because of few measurements and lack of reliable relationship between density and thermal conductivity.

Variograms of thermal conductivity for Ävrö granite (501044) in KAV01 is illustrated in Figure 4-24 to Figure 4-26 in five different scales 0–700 m, 0–200 m, 0–80 m, 0–20 m and 0–5 m. For the variogram in scale 0–5 m an exponential model has been fitted to data. Variograms of Ävrö granite (501044) in KSH01A is illustrated in Figure 4-27 to Figure 4-28 in the four scales 0–350 m, 0–100 m, 0–20 m and 0–5 m. An exponential model has been fitted to data in the scale 0–5 m. Variograms of Ävrö granite (501044) in KLX02 is illustrated in Figure 4-29 in the two scales 0–5 m and 0–300 m. Exponential models have been fitted to data in both scales. Variograms are based on the same data as the plot of thermal conductivity along the borehole.

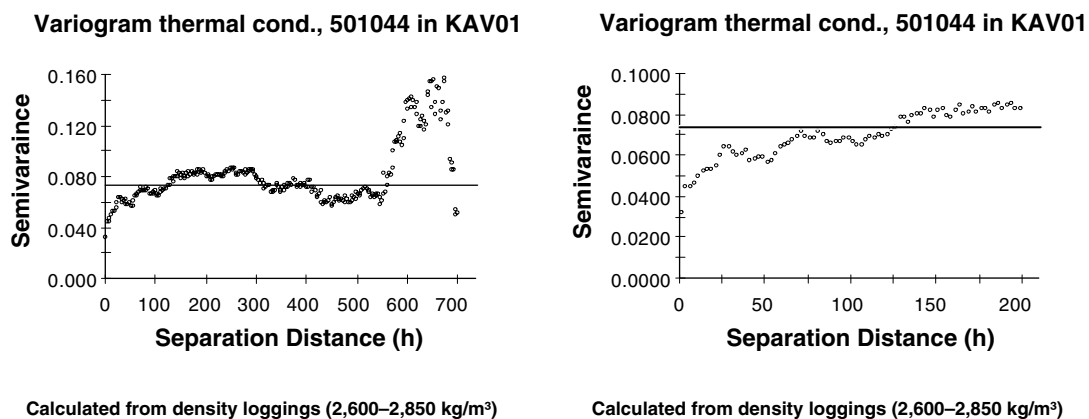
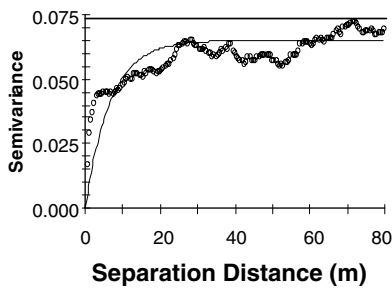


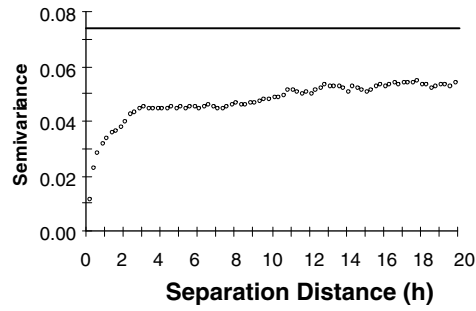
Figure 4-24. Variogram of thermal conductivity for Ävrö granite (501044) in KAV01, estimated from density logging; 0–700 m and 0–200 m separation distance. The straight line indicates the total variance in data.

Therm. cond. 501044 in KAV01



Exponential model ($C_0 = 0.00000$; $C_0 + C = 0.06500$; $A_0 = 6.67$; $r^2 = 0.697$
 RSS = 7.557E-03)

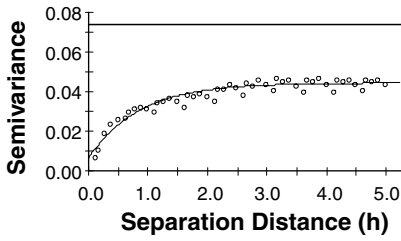
Variogram thermal cond., 501044 in KAV01



Calculated from density loggings (2,600–2,850 kg/m³)

Figure 4-25. Variogram of thermal conductivity for Ävrö granite (501044) in KAV01, estimated from density logging; 0–80 m and 0–20 m separation distance. The straight line indicates the total variance in data.

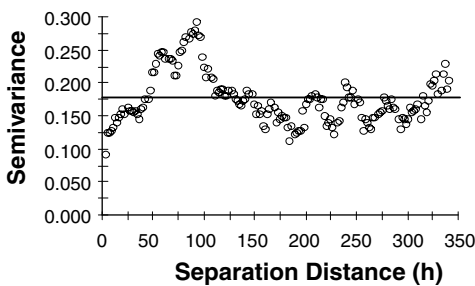
Therm. cond.: Isotropic Variogram



Exponential model ($C_0 = 0.00640$; $C_0 + C = 0.04440$; $A_0 = 0.85$; $r^2 = 0.918$
 RSS = 3.340E-04)

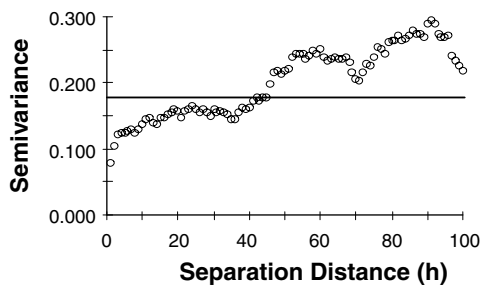
Figure 4-26. Variogram of thermal conductivity for Ävrö granite (501044) in KAV01, estimated from density logging; 0–5 m separation distance. The straight line indicates the total variance in data. An exponential model has been fitted to the data.

Variogram thermal cond., 501044 in KSH01A



Calculated from density loggings (2,600–2,850 kg/m³)

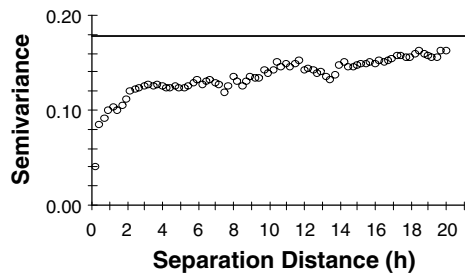
Variogram thermal cond., 501044 in KSH01A



Calculated from density loggings (2,600–2,850 kg/m³)

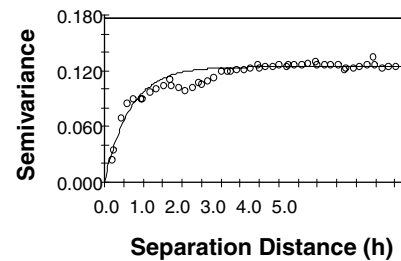
Figure 4-27. Variogram of thermal conductivity for Ävrö granite (501044) in KSH01A, estimated from density logging; 0–350 m and 0–100 m separation distance. The straight line indicates the total variance in data.

Variogram thermal cond., 501044 in KSH01A



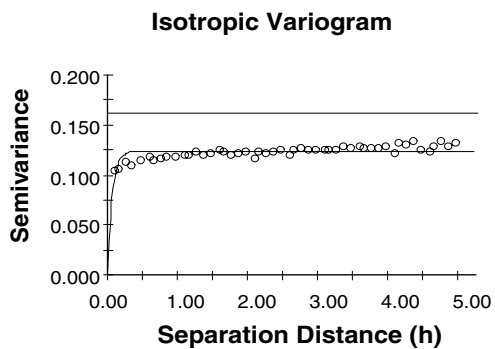
Calculated from density loggings (2,600-2,850 kg/m³)

Thermal cond., 501044 in KSH01A with variogram model.

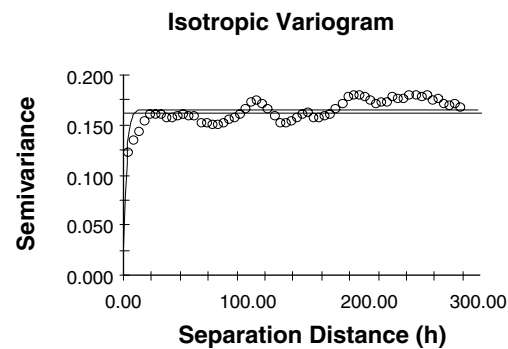


Exponential model ($C_0 = 0.00010$; $C_0 + C = 0.12420$; $A_0 = 0.44$; $r_2 = 0.899$
RSS = 2.580E-03)

Figure 4-28. Variogram of thermal conductivity for Åvrö granite (501044) in KSH01A, estimated from density logging; 0–20 m and 0–5 m separation distance. The straight line indicates the total variance in data. An exponential model has been fitted to the data in the figure on the right hand side.



Exponential model ($C_0 = 0.00010$; $C_0 + C = 0.12420$; $A_0 = 0.07$; $r_2 = 0.348$;
RSS = 1.313E-03)



Exponential model ($C_0 = 0.02790$; $C_0 + C = 0.16580$; $A_0 = 2.70$; $r_2 = 0.262$;
RSS = 6.276E-03)

Figure 4-29. Variogram of thermal conductivity for Åvrö granite (501044) in KLX02, estimated from density logging; 0–5 m and 0–300 m separation distance. The straight line indicates the total variance in data. An exponential model has been fitted to the data in both figures.

Exponential variogram models fits the experimental variograms best, see Figure 4-26, Figure 4-28 and Figure 4-29. Several different correlation lengths (ranges) can be identified depending on scale. Each scale will have its own variogram model. Three different scales are illustrated in Figure 4-24 to Figure 4-26. At least the following scales can be identified:

- Strong correlation up to about 3 m. About 60% of the total variance in data can be explained by variability within this range. About 50% of the total variance can be explained by variability up to distances of 1–1.5 m. The correlation up to 0.5 m is to some extent affected by the filtering of logging data, and possibly also by overlapping measurement volumes due to the density logging technique.
- Correlation up to about 25 m and similar pattern at about 75 m.
- Weak correlation up to 150–200 m. The variability at this scale is larger (> 10%) than the total variability in data. At even larger distances the variance decreases slightly.

One interpretation of the variogram in Figure 4-24 is that there is a more or less cyclic trend overlaying a more linear trend up to distances of about 200 m.

Variograms for the three different boreholes (KAV01, KSH01A and KLX02) show similar trends:

- Several rapid changes in correlation occurs.
- Cyclic trend overlaying a linear trend up to 100 m or more.

This means that it is not a one time exceptional phenomenon in borehole KAV01.

The third variability is due to the presence of different rock types in the lithological domain, see Table 5-1. This variability is more pronounced where the difference in thermal conductivity is large between the most common rock types of the domain. Large such variability can also be expected in a domain of many different rock types. It is believed that the variability between rock types is important for all domains. It is only reduced significantly when the scale becomes large compared to the spatial occurrence of the rock.

4.7.3 Spatial variability of rock types

To examine the spatial variability of different rock types several indicator variograms have been made and are presented in Appendix C. Data has been worked through for separate boreholes but not summarised regarding domain belonging. The evaluation of spatial variability of rock types is not complete and do not include all boreholes for which data is available. In this model version the indicator variograms have not been used.

4.8 Anisotropy

Anisotropic measurements of the thermal conductivity and heat capacity for samples within the Simpevarp subarea have not been carried out. The effect from anisotropy for the thermal properties has been assumed as small, although this ought to be verified in further investigations.

Anisotropic effects may result due to occurrence of subordinate rock types in forms of dykes with significant extension, consisting of a rock type with different thermal characteristics.

4.9 Heat capacity from determinations

4.9.1 Method

Heat capacity has been determined through measurements with the TPS (Transient Plane Source) method. No direct laboratory measurements of the heat capacity have been carried out but the heat capacity has been calculated from conductivity and diffusivity measurements performed with the TPS method. For method description see Section 4.3.1.

4.9.2 Result

In Table 4-22 the results from all heat capacity determinations are summarised. Determination of heat capacity has been performed on the same samples as used for measurement of thermal conductivity, cf Section 4.3. Therefore the same problem concerning representativeness of the rock mass exists. Observe that samples from rock type

Ävrö granite (501044) are collected from both the Simpevarp subarea /Adl-Zarrabi, 2004a,b,c/ and the Äspö HRL /Sundberg and Gabriëlsson, 1999; Sundberg, 2002; Sundberg et al. 2005/. Samples from rock type Fine-grained dioritoid (501030) and Quartz monzodiorite (501036) all comes from the Simpevarp subarea /Adl-Zarrabi, 2004a,b,c/. Some of the samples are spatially located in groups with approximately 2–5 samples in each group.

Table 4-22. Determined heat capacity (MJ/(m³·K)) of samples from different rock types, using the TPS method. Samples are from boreholes KAV01, KSH01A and KSH02 (Simpevarp subarea) together with borehole KA2599G01 (Äspö HRL) and boreholes from the prototype repository tunnel (Äspö HRL).

Rock name (sample location)	Mean	St. dev	Number of samples
Fine-grained dioritoid (borehole KSH01A and KSH02)	2.23	0.10	26
Quartz monzodiorite (borehole KSH01A)	2.25	0.06	10
Ävrö granite (borehole KAV01, KA2599G01 and Äspö HRL prototype tunnel)	2.18	0.21	37

4.9.3 Temperature dependence

The temperature dependence of heat capacity has been investigated by measurements, for the two rock types Fine-grained dioritoid (501030) and Quartz monzodiorite (501036), at three different temperatures (20, 50 and 80°C) /Adl-Zarrabi, 2004a,b/. Eleven samples from rock type Fine-grained dioritoid (501030) and five from Quartz monzodiorite (501036) have been measured. For rock type Ävrö granite (501044), thermal conductivity has been measured on four samples at four different temperatures (25, 40, 60 and 80°C) /Sundberg, 2002/. The temperature dependence of each sample is illustrated in Figure 4-30 to Figure 4-32 and summarised per rock type in Table 4-23.

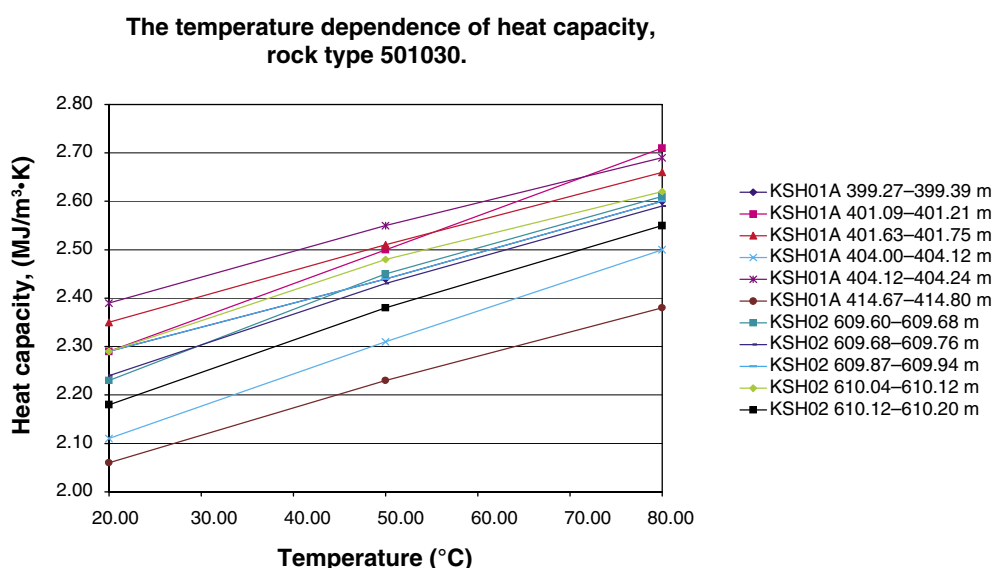


Figure 4-30. Temperature dependence of heat capacity, rock type Fine-grained dioritoid (501030).

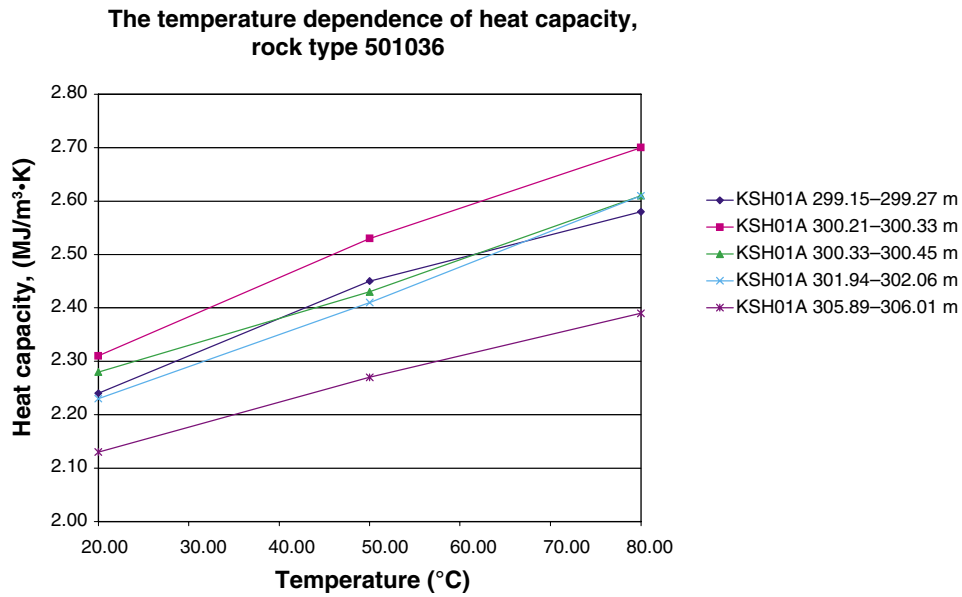


Figure 4-31. Temperature dependence of heat capacity, rock type Quartz monzodiorite (501036).

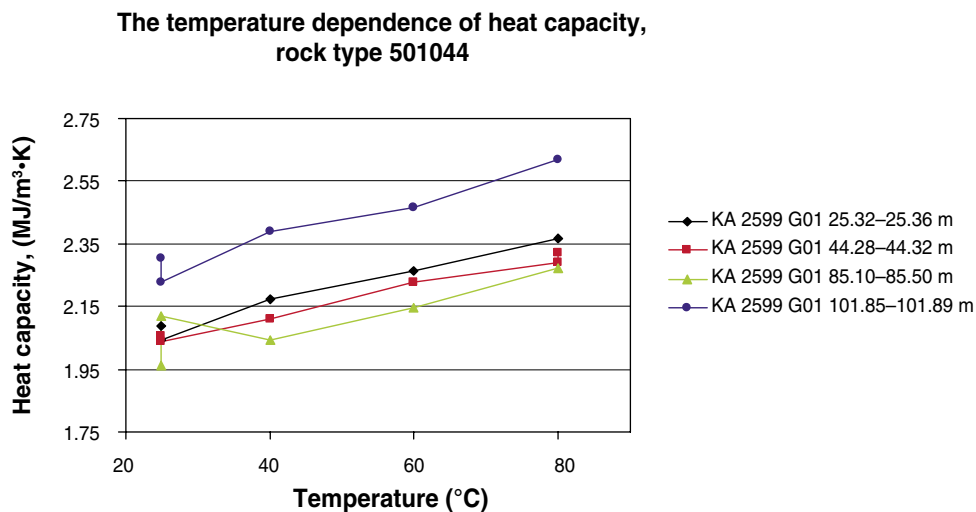


Figure 4-32. Temperature dependence of heat capacity, rock type Ävrö granite (501044).

Table 4-23. Determined temperature increase of heat capacity (per 100°C temperature increase) on samples from different rock types in borehole KAV01, KSH01A, and KSH02 in the Simpevarp subarea. The mean of the temperature dependence is estimated by linear regression.

Rock name (rock type) (sample location)	Mean	St. dev	Number of samples
Fine-grained dioritoid (501030) (boreholes KSH01A and KSH02)	25.6%	3.5%	11
Quartz monzodiorite (501036) (borehole KSH01A)	25.3%	3.3%	5
Ävrö granite (501044) (borehole KA2599G01)	32.0%	5.6%	4

4.9.4 Modelling of heat capacity (rock type level)

Rock type models of heat capacity have been produced from the results of the determinations in Table 4-2. For heat capacity the normal distribution of data is presented in Figure 4-33. Three TPS measurements for 501044 are excluded when modelling the heat capacity, see Figure 4-33 where the samples are excluded in 501044*. The reason for exclusion is a large deviation in values compared to repeated measurements with a larger sensor.

Models of heat capacity for different rock types are presented in Table 4-24. Data is approximately normal distributed, if outliers are removed, which is illustrated in Figure 4-33.

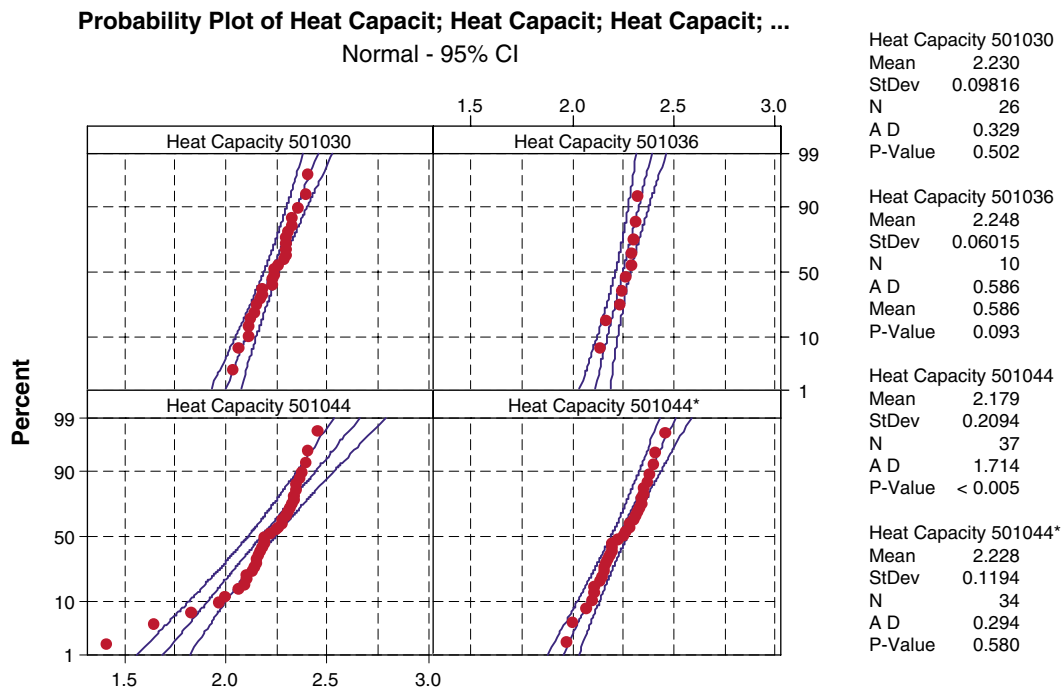


Figure 4-33. Probability plots (normal distributions) of heat capacity divided on rock types. In 501044* three measured values of heat capacity have been excluded (outliers).

Table 4-24. Rock type models of heat capacity for rock type Fine-grained dioritoid (501030), Quartz monzodiorite (501036) and Ävrö granite (501044).

Rock name (rock type)	Mean	St. dev	Number of samples	Distribution
Fine-grained dioritoid (501030)	2.23	0.098	26	normal
Quartz monzodiorite (501036)	2.25	0.060	10	normal
Ävrö granite (501044)	2.23	0.119	34	normal

4.10 Coefficient of thermal expansion

The coefficient of thermal expansion have been measured on samples from three different boreholes; KAV01, KSH01A, and KSH02 in the Simpevarp subarea /Åkesson, 2004a,b,c/. Results as obtained for three rock types, are presented in Table 4-25.

At the Äspö HRL, measurements regarding the coefficient of thermal expansion have been performed at two occasions. Three samples from the Ävrö granite (501044) have been measured from borehole KQ0064G01 and KQ0064G05 with results between $6.7\text{--}8.1 \cdot 10^{-6}$ m/(m·K) within the measuring interval 20–40°C /Staub et al. 2004/. Further, nine samples have been measured from borehole KA2599G01 within the temperature interval 5–95°C with results between $7.24\text{--}8.98 \cdot 10^{-6}$ m/(m·K) /Sundberg and Ländell, 2002/. The mean value of the samples were $7.86 \cdot 10^{-6}$ m/(m·K) and the standard deviation $0.63 \cdot 10^{-6}$ m/(m·K). The original rock classifications of the samples were done according to Äspö nomenclature as Äspö diorite. The exact same samples have not been reclassified but samples very close by have been reclassified as Ävrö granite (501044) /Sundberg et al. 2005/.

Table 4-25. Measured thermal expansion (m/(m·K)) between 20°C and 80°C on samples of different rock types from boreholes KAV01, KSH01A, and KSH02 in the Simpevarp subarea.

Rock name (sample location)	Mean	St. dev	Number of samples
Fine-grained dioritoid (boreholes KSH01A and KSH02)	6.9 E–6	1.5 E–6	17
Quartz monzodiorite (borehole KSH01A)	8.0 E–6	1.4 E–6	10
Ävrö granite (borehole KAV01)	6.0 E–6	0.5 E–6	5

4.11 In situ temperature

4.11.1 Method

Temperature and gradient profiles has been investigated for borehole KSH01A, KSH02, KSH03A, KAV01, KLX01, and KLX02. The temperature was measured by fluid temperature loggings. Measured temperature delivered from Sicada was not filtered. These data have been plotted versus elevation in the diagrams below, Figure 4-34 to Figure 4-40.

To all series with temperature measurements, an equation was also fitted, to be used for other applications. In cases were two or three temperature loggings had been made in the same borehole, one equation was evaluated for each of the series. For KLX02 year 2002, there were too many temperature values for the calculation program to handle. For this series, every second value was excluded when calculating an equation. Both linear, second degree and third degree equations where evaluated. The linear equations where estimated to be good enough, and higher degree equations did not give a larger correspondence.

The thermal gradients were calculated for the midpoint of a 9 m interval and for the midpoint of a 50 m interval. For most of the loggings, this means that 91 and 501 temperature values, respectively, were used for each gradient value. The gradients were calculated according to Equation 4-3.

$$\text{Gradient} = \frac{1000(n\sum zT - \sum z\sum T) \sin \phi}{n\sum z^2 - (\sum z)^2} \quad \text{Equation 4-3}$$

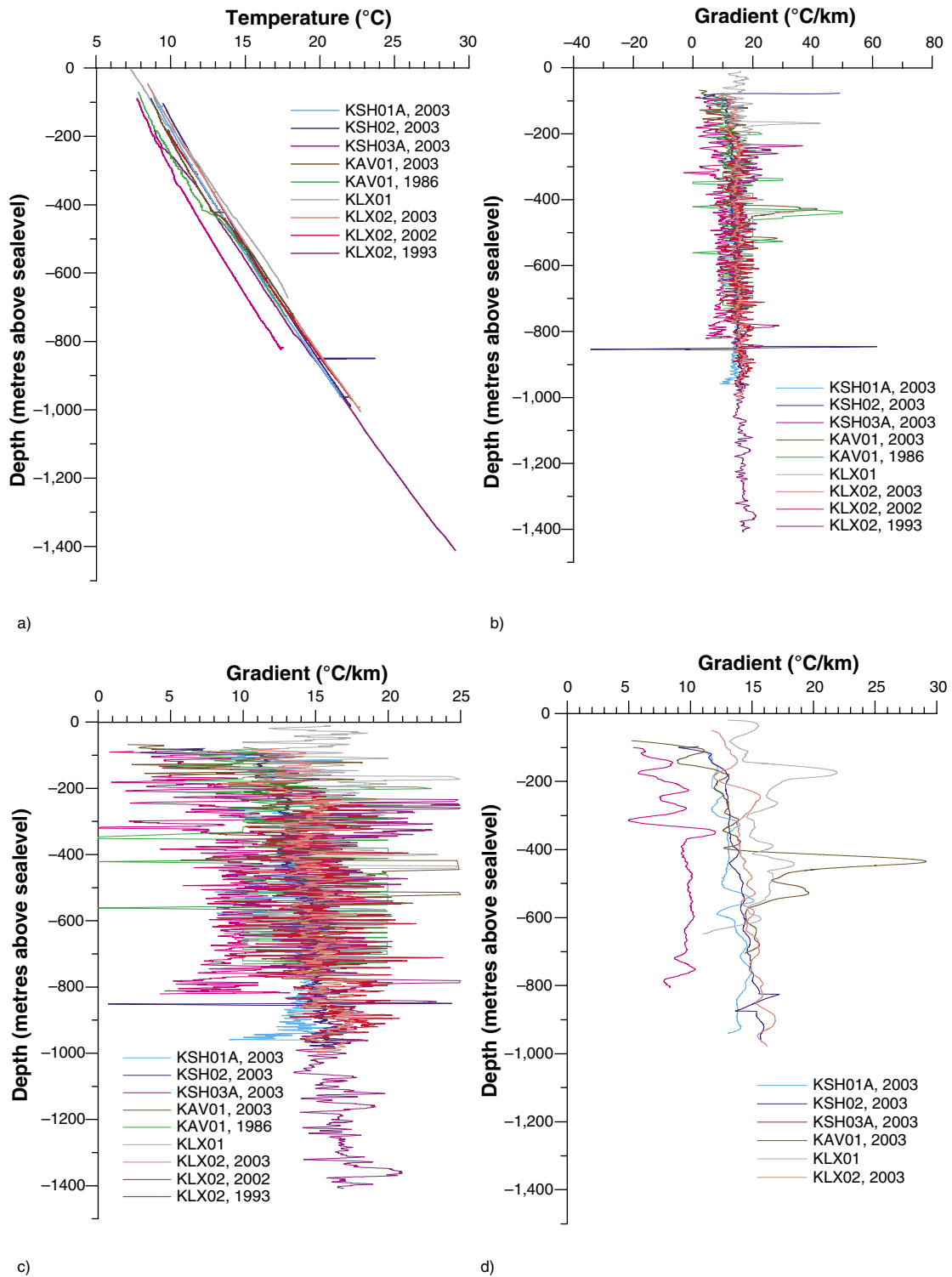
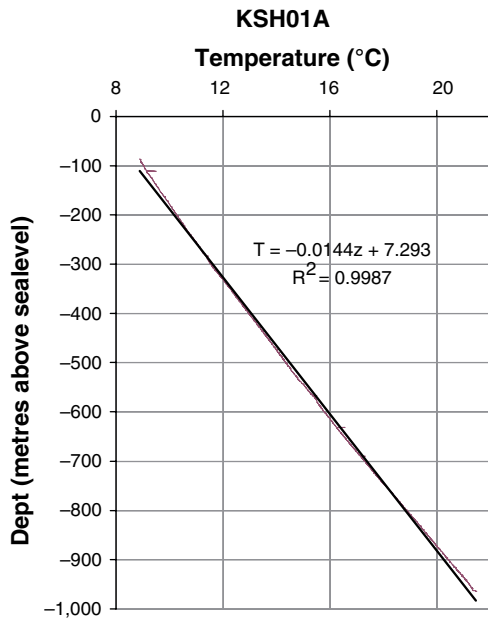
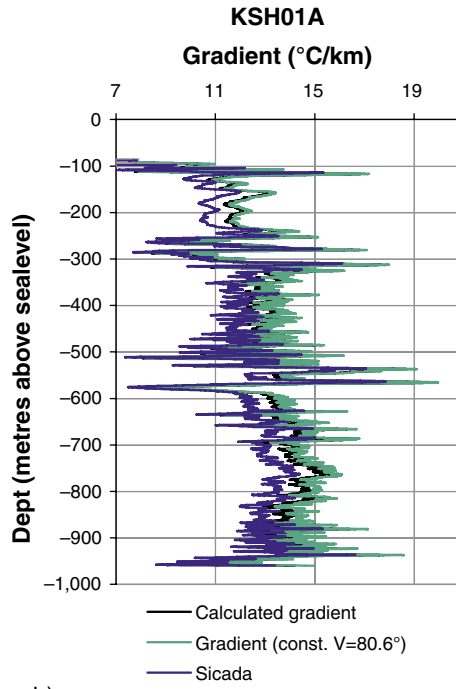


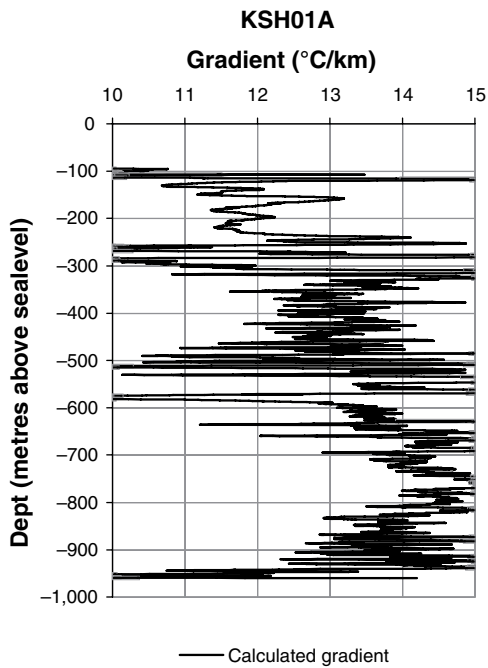
Figure 4-34. Temperature (a) and temperature gradients in boreholes (b–d) for three boreholes at Simpevarp, one at Ävrö and two at Laxemar. Figure b and c shows the temperature gradient calculated for nine-meter intervals, while figure d shows the gradient calculated for 50 m intervals. In figure d, gradients from old loggings are not presented.



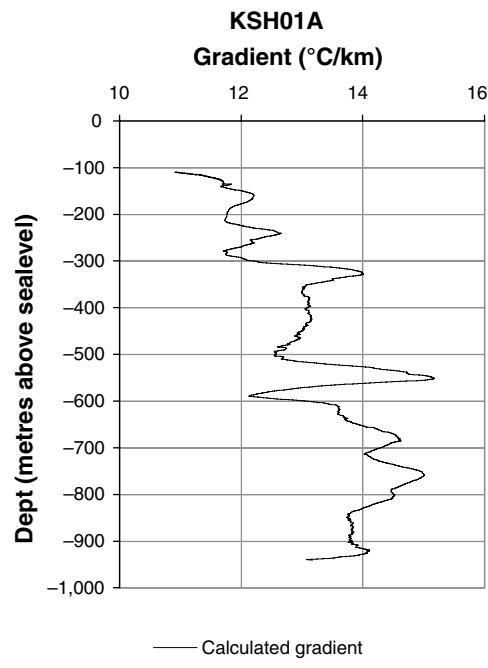
a)



b)

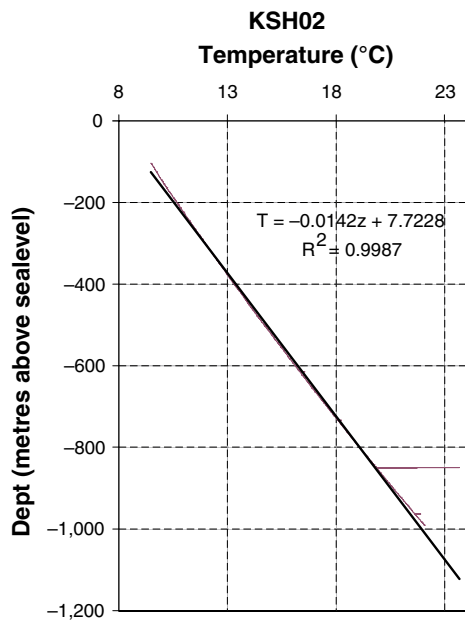


c)

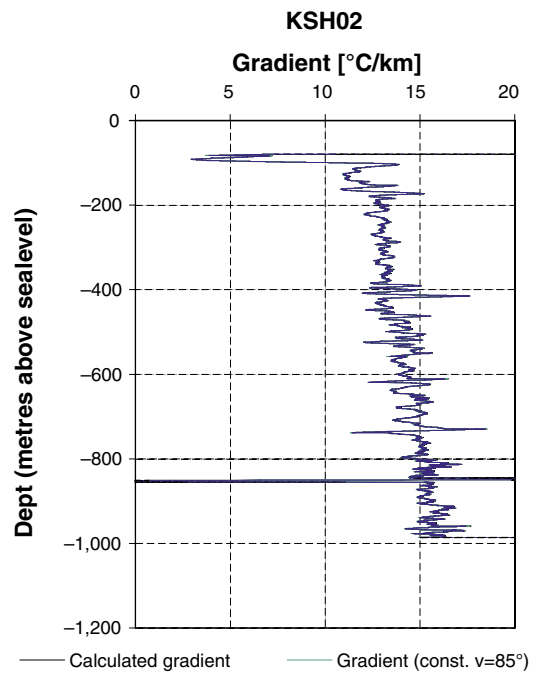


d)

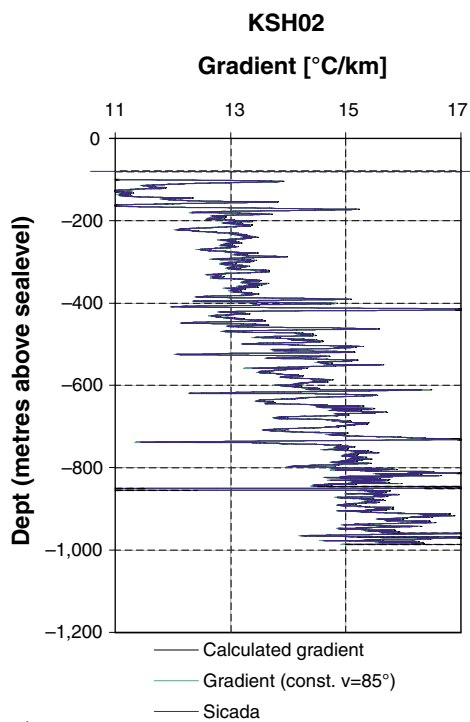
Figure 4-35. Temperature (a) and gradient (b–d) for KSH01A, Simpevarp subarea. Figure b and c shows the gradient calculated for nine meter intervals, while figure d shows the gradient calculated for 50 m intervals.



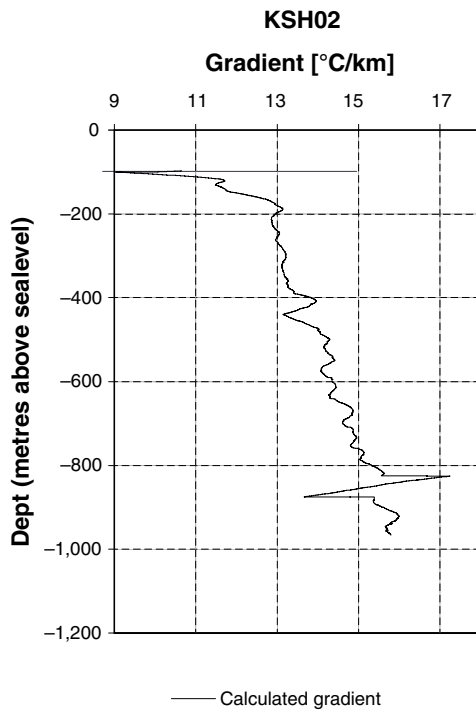
a)



b)

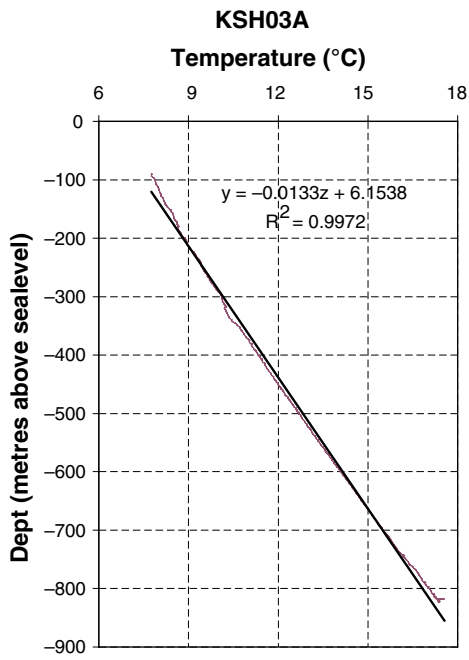


c)

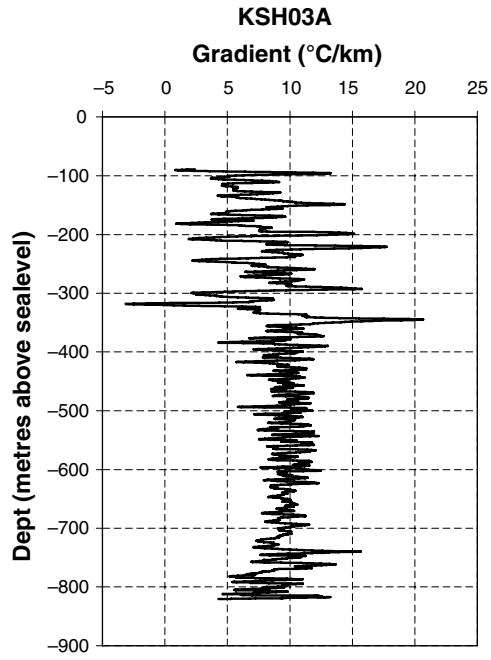


d)

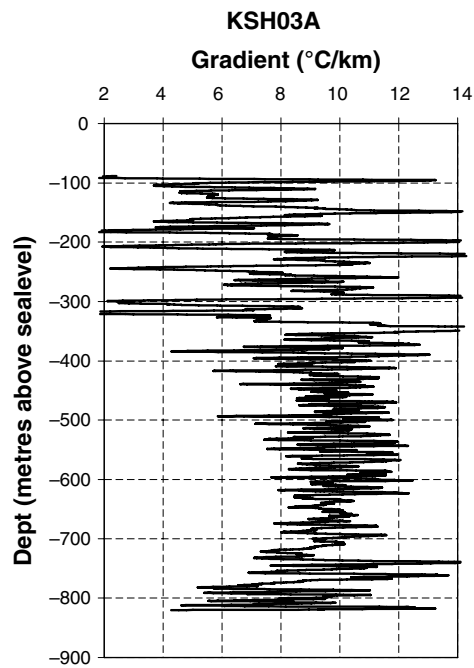
Figure 4-36. Temperature (a) and gradient (b–d) for KSH02, Simpevarp subarea. Figure b and c shows the gradient calculated for nine meter intervals, while figure d shows the gradient calculated for 50 m intervals.



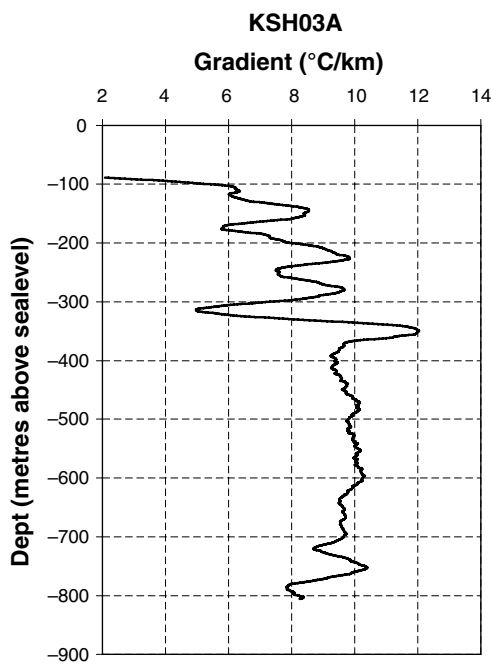
a)



b)

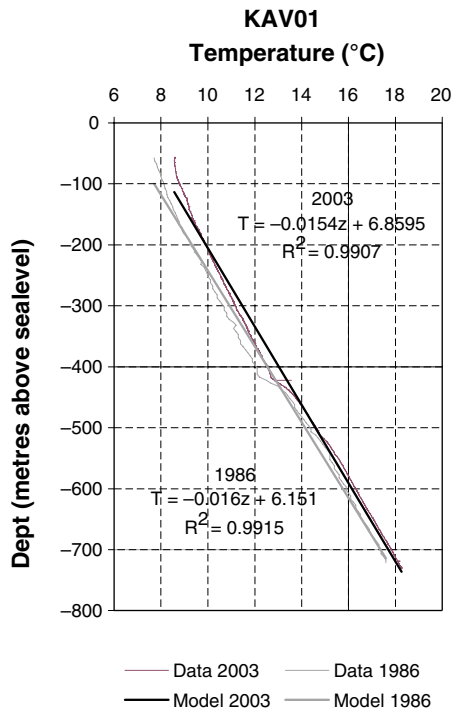


c)

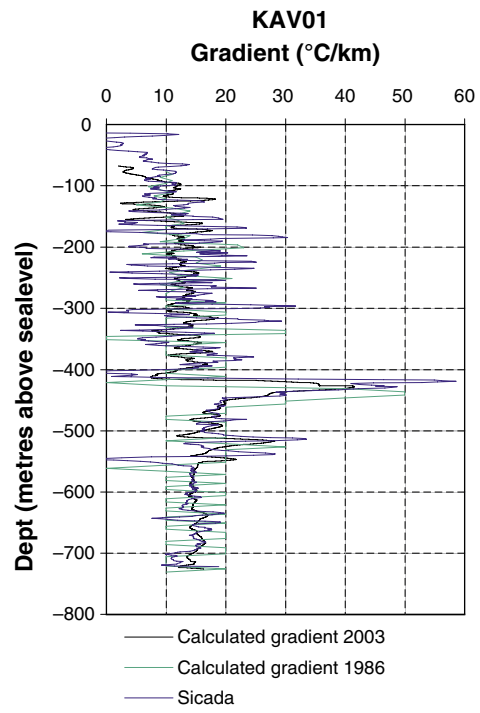


d)

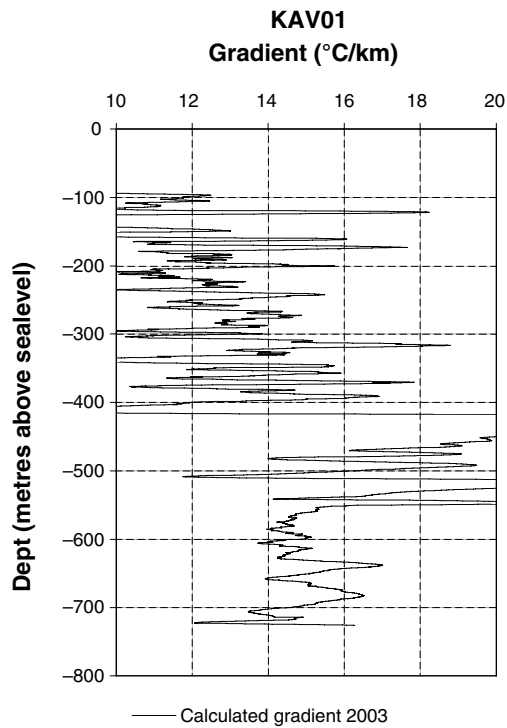
Figure 4-37. Temperature (a) and gradient (b–d) for KSH03A, Simpevarp subarea. Figure b and c shows the gradient calculated for nine meter intervals, while figure d shows the gradient calculated for 50 m intervals.



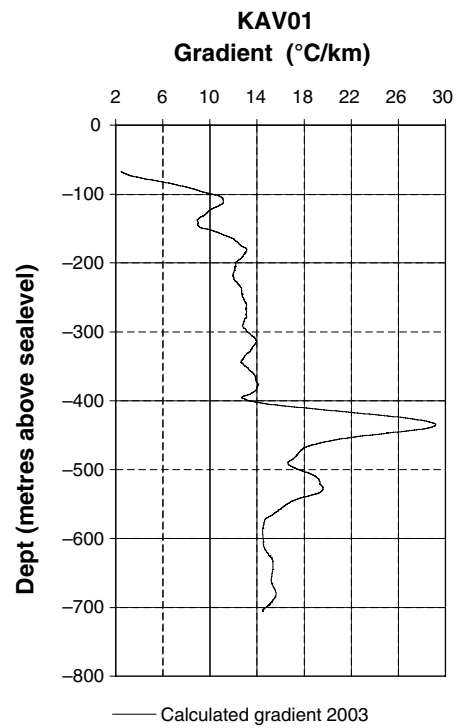
a)



b)

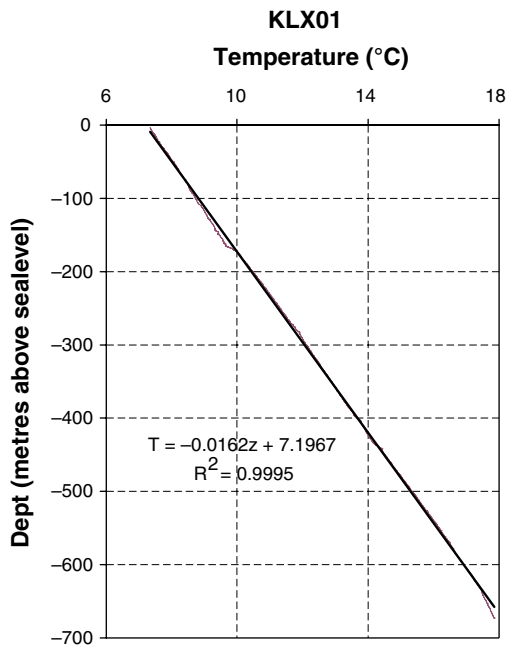


c)

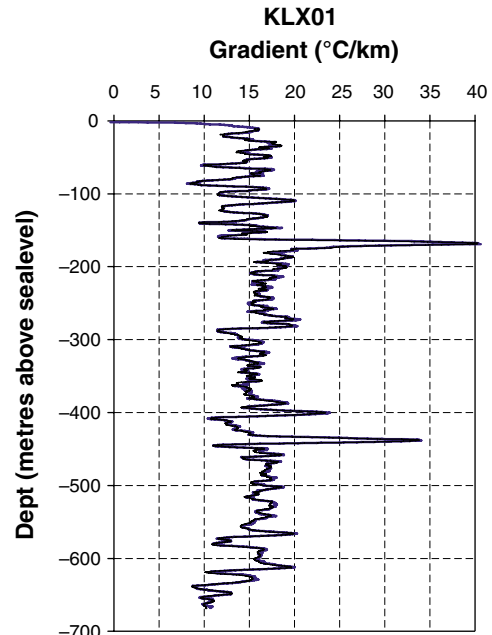


d)

Figure 4-38. Temperature (a) and gradient (b–d) for KAV01, Ävrö subarea. Figure b and c shows the gradient calculated for nine meter intervals, while figure d shows the gradient calculated for 50 m intervals.

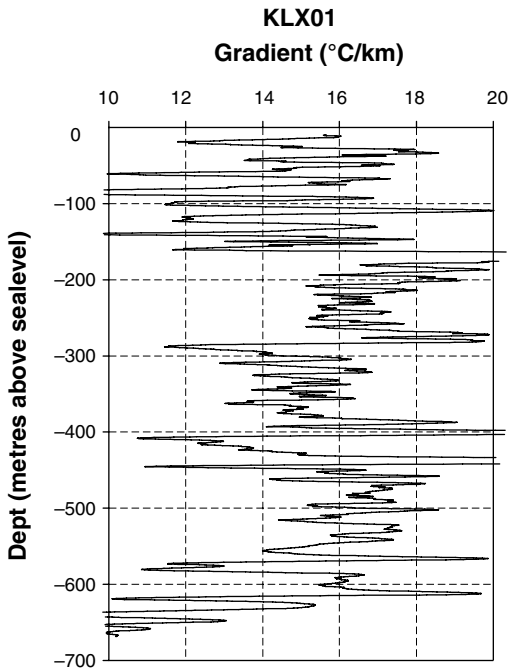


a)



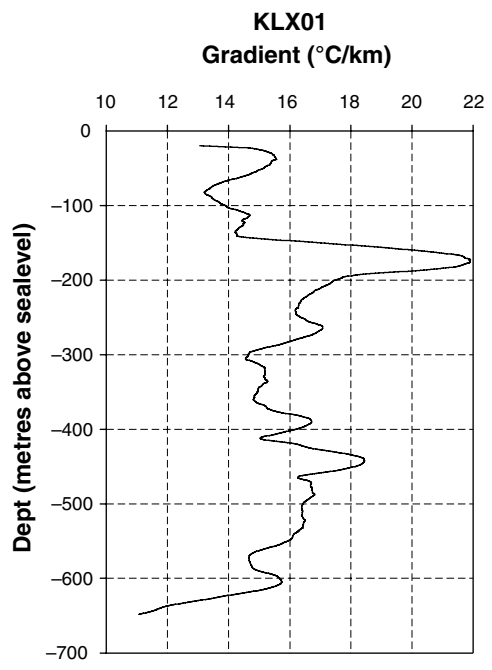
— Sicada — Calculated gradient

b)



— Calculated gradient

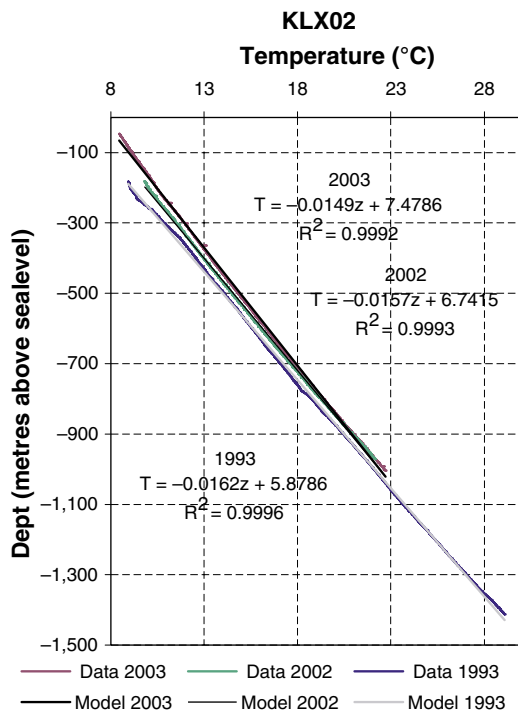
c)



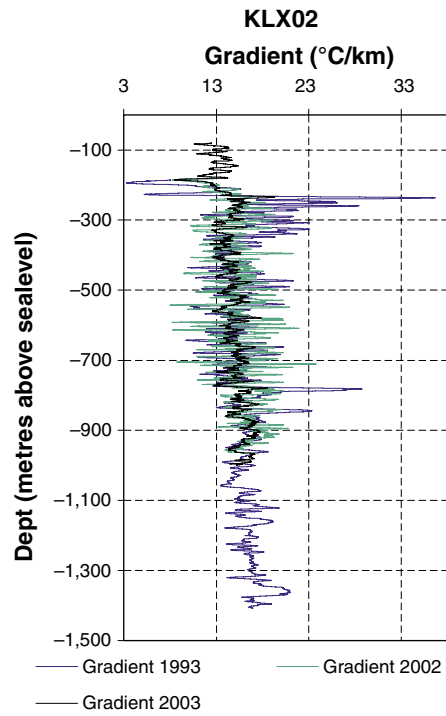
— Calculated gradient

d)

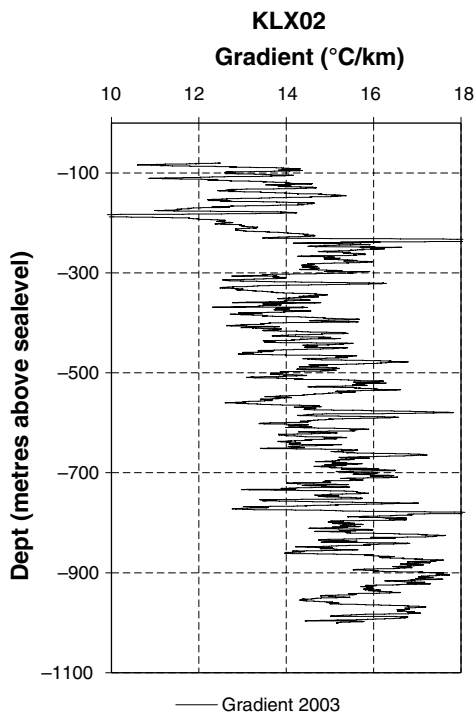
Figure 4-39. Temperature (a) and gradient (b–d) for KLX01, Laxemar subarea. Figure b and c shows the gradient calculated for nine meter intervals, while figure d shows the gradient calculated for 50 m intervals.



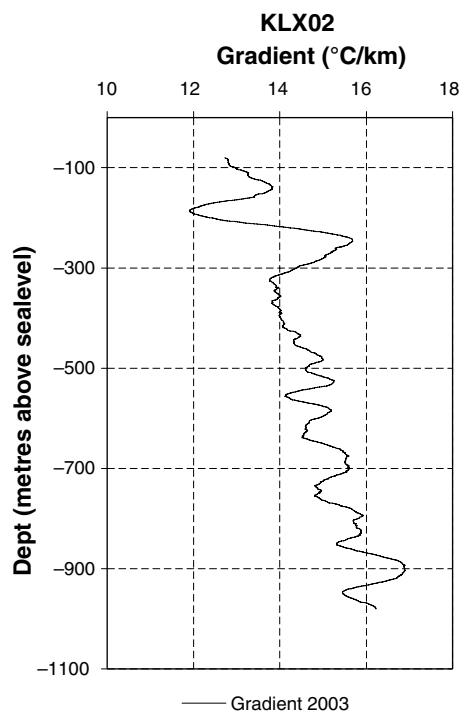
a)



b)



c)



d)

Figure 4-40. Temperature (a) and gradient (b–d) for KLX02, Laxemar subarea. Figure b and c shows the gradient calculated for nine meter intervals, while figure d shows the gradient calculated for 50 m intervals.

Parameter z is the depth co-ordinate (m), T is the measured temperature (K), ϕ is the angle between the borehole and a horizontal line, and n is the number of temperature measurements in an interval of 9 m or 50 m, respectively.

Data from some of the boreholes have earlier been investigated and reported to the Sicada database /Mattsson and Thunehed, 2004a,b/. The purpose of these investigations were to visualize the results from the geophysical loggings, the material is being used as basis for further investigations. Gradients, calculated within these investigations, have been used for comparison in this work. When calculating the gradient, /Mattsson and Thunehed, 2004a,b/ have used filtered data for the temperature and the inclination for the borehole has been set to a mean value for the borehole.

4.11.2 Result

The results from the temperature loggings, the equations for the temperature and the calculated gradients are presented in Figure 4-34 to Figure 4-40. Figure 4-34 illustrates a summary of all investigated boreholes and Figure 4-35 to Figure 4-40 the boreholes separately. If several measurements from different occasions exist, this is illustrated in the figures. The gradient for a 50 m interval is only calculated for the latest temperature logging. The y-axis in the figures illustrates depth below sea level (not the borehole length). In Table 4-26 the elevation (metres above sea level) for the start points for the boreholes are presented. The differences depend mainly on the ground level above sea level.

Close to the surface (ca 0 to –100 m) there are large variations in the temperature and these data have been excluded. Deeper, the temperature seems to be almost linear with depth. A few temperature measurements have failed, the value of –999° is then given in the temperature logging and these values have also been excluded. In Table 4-27 the temperature at different depths are presented for the investigated boreholes at different measurements. In the same table, also the approximate inclinations for the boreholes are presented. The difference for the same borehole at different times, might depend on the fact that the measurements are made to different depths. As seen in Table 4-27 and Figure 4-34 the temperature of borehole KSH03A is deviant and the reason is unknown. The borehole is not included in the calculation of mean temperature in Table 4-27.

Table 4-26. Ground level for the start points of boreholes within the Simpevarp, Ävrö and Laxemar subarea.

Borehole	Elevation (metres above sea level)
KSH01A	5.3
KSH02	5.5
KSH03A	4.1
KAV01	14.1
KLX01	16.8
KLX02	18.4

Times for core drillings and fluid temperature loggings for three of the boreholes are given in Table 4-28. The times between core drilling and temperature logging are about 8 weeks for KSH01A, 3 weeks for KSH02 and almost 4 weeks for KSH03A. The relatively short period between the drilling activity and temperature logging might result in a disturbance of the logging results due to the borehole not being stabilised. The drilling activity increases the temperature in the borehole but a temperature decrease probably occurs due to the added drilling fluid. Also a temperature equalisation occurs in the borehole when the drilling fluid is transported in the borehole. Thus, there is a potential error in the loggings and this is indicated by the noted difference in temperature for the same borehole logged at different occasions. However, this difference in temperature is relatively small for a specified depth but the influence on the design of a repository may be significant.

For the borehole KAV01 two loggings of the temperature have been made. One was made in year 1986 and one in 2003. For KLX02 there are values from three different loggings, made in year 1993, 2002 and 2003. The loggings gives temperatures every 10 cm, except for KLX02 in year 2002 and KAV01 in 1986, were measurements where made every 2 cm and every 1 m respectively.

The calculated angle between the borehole and a horizontal line for KSH01A varies between 75° and 76° to a depth of 650 m, and then it decreases to 69°. The gradient has been calculated by /Mattsson and Thunehed, 2004a/, who has used the constant angle 80.6°. The gradient calculated with varying angle and the one calculated with constant angle differs about 10%, see Figure 4-35. Calculations of the gradient with constant angle (80.6°) do not give better correspondence with the gradient from Sicada. Yet, in spite of the differences between the gradients, they follow each other well. In the two intervals –250 to –320 and –530 to –600 m, there are greater oscillations than in the rest of the borehole. This might be a result of water bearing fractures at these levels /Mattsson and Thunehed, 2004a/. At –800 m the gradient is about 14–15°C/km.

Table 4-27. Measured temperature (°C) at different depths; 400, 500, and 600 m below sea level. Approximate inclination of the boreholes is also indicated.

Borehole	400 m	500 m	600 m	Approximate inclination (°)
KSH01A, 2003	12.97	14.34	15.80	74
KSH02, 2003	13.31	14.69	16.12	87
KSH03A, 2003	11.34	12.69	14.09	56
KAV01, 2003	12.55	14.62	16.31	88
KAV01, 1986	12.10	14.40	15.90	87
KLX01	13.67	15.35	16.92	86
KLX02, 2003	13.36	14.82	16.32	84
KLX02, 2002	12.98	14.46	16.06	84
KLX02, 1993	12.57	14.07	15.58	83
Mean	12.8	14.4	15.9	(KSH03A excluded in calculation of mean temperatures)

Table 4-28. Occasions for core drilling and fluid temperature and resistivity loggings for the boreholes KSH01A, KSH02 and KSH03A.

Borehole	Core drilling Start time	Core drilling Stop time	Fluid temperature and resistivity logging
KSH01A	2002-10-07	2002-12-18	2003-02-14
KSH02	2003-01-28	2003-06-11	2003-07-01
KSH03A	2003-09-11	2003-11-07	2003-12-02

For KSH02 the angle varies between 86° and 87°. The gradient has been calculated by /Mattsson and Thunehed, 2004b/, who has used the constant angle 85°. Calculated with varying angle, the gradient is slightly smaller than with constant angle. Even when calculated with a constant angle (85°) there is a small difference between the calculated gradient here and the gradient from Sicada. Yet, the differences between the gradients are small, see Figure 4-36. The gradient grows by depth, at –600 m it is approximately 14°C/km and at –800 m it is approximately 15°C/km. Two anomalies can be seen, one at about –100 m and one at about –855 m. The first probably depends on a large zone with low resistivity and the other on an increase in the water salinity /Mattsson and Thunehed, 2004b/.

The angle for KSH03A varies between 56° and 58° to –550 m and then it starts to decrease down to 46° at –820 m. No gradient for comparison has been found in the Sicada database. There are oscillations for the calculated gradient, especially from the top down to –350 m and below –750 m. At –600 m the gradient is about 10°C/km.

For KAV01 the angle between the borehole and a horizontal line varies between 86° and 90°. Gradients have been calculated for both series of data (from 1986 and from 2003). There are also values for the gradient calculated by /Mattsson and Thunehed, 2004b/, which originate in the temperature values from 1986 and the constant angle 88° for the borehole. Oscillation of the gradients is rather large. The oscillation is larger for the gradients calculated for year 1986 than for 2003. This might be due to the fact that in the series from 1986, there are only measurements for every 5 m borehole interval. According to data from 2003, the gradient is 14–15°C/km at the depth –600 m. The gradient increases slightly by depth. Two anomalies can be seen, one at 420–465 m and one at 520–545 m. This is probably because of areas with more fractures than in other parts /Mattsson and Thunehed, 2004b/.

The angle for borehole KLX01 varies between 85° and 87°. From the Sicada database, a calculated gradient has been received. The difference between these two gradients is small. There are great variations and anomalies in the gradients, which makes it hard to decide if the gradients change by depth. At –600 m the gradient is about 15°C/km.

The angle for borehole KLX02 decreases from 85° close to the ground, to 83° at –1,000 m and to 82° at –1,400 m. No calculated gradient has been found for comparison. Gradients for the three different loggings (1993, 2002 and 2003) have been calculated and are shown in Figure 4-40. For the logging made in 2002, measurements were done every second centimetre. The equation (Equation 4-3) has been modified for this, and the gradient is still calculated for a 9 m interval. There are great oscillations for all three of the gradients and they do not follow each other. For the gradient, calculated for data from 2003, the oscillations are smaller than for the other two. The gradient is increasing with depth. Data from 2003 gives the gradient 14–15°C/km at –600 and 15–16°C/km at –800 m.

The differences between the gradients calculated here and the ones received from Sicada, are generally small and may have different reasons. The data used by /Mattsson and Thunehed, 2004a,b/ are filtered, while the data used here are not. /Mattsson and Thunehed, 2004a,b/ have used a constant angle for the borehole, while the calculations here are made with an angle calculated for every point of measurement along the borehole. Here, temperature data received from Sicada are used. They are rounded, which causes a small error in the results.

The difference between the temperature at different occasions and in different boreholes is sometimes rather large, see Figure 4-34. This is further discussed in Section 6.3.

4.11.3 Modelling from temperature loggings

In this site descriptive model version 1.2 of the Simpevarp subarea no modelling from temperature loggings has been done. Ideally, the temperature loggings reflect a spatial variability in thermal properties for the investigated borehole. However, historical climate and temperature data for the area have not been available but are possible to produce for a later model version. Another problem is that available temperature loggings are disturbed.

5 Thermal modelling of lithological domains

5.1 Modelling assumptions and input from other disciplines

5.1.1 Geological model

The lithological model from the Simpevarp site descriptive model version 1.2 is the geometrical base for the thermal model and is described in Section 4.2 and /SKB, 2005/. The geological Boremap log of the boreholes, showing the distribution of dominant and subordinate rock types, has been used as input to the thermal modelling jointly with a lithological domain classification of borehole intervals (Table 5-2).

The geological model with rock type distributions of the four lithological rock domains RSMA01 (Ävrö granite), RSMB01 (Fine-grained dioritoid), RSMC01 (mixture of Ävrö granite and Quartz monzodiorite) and RSMD01 (Quartz monzodiorite) is illustrated in Table 5-1 where the dominating rock types are marked in red (Preliminary version of geological model, September 2004). Domain RSMD01 is assumed to consist of Quartz monzodiorite (501036) only.

When performing the thermal modelling of the lithological domains, a calculation of the rock type compositions for each domain is conducted and this is described in Table 5-1. For rock type compositions divided on each borehole which constitute the lithological domain (calculated in the thermal domain modelling), see Section 5.4.1. The two different distributions of the lithological domains differ slightly since the thermal domain modelling includes rock type sections with an occurrence less than 1m from the Boremap logging. There is also a small difference in the basic data since a less amount of boreholes have been used in the thermal domain modelling than in the geological model. The reason for this is described further in section 0 below.

Table 5-1. Comparison between rock type percentages (%) used in the thermal domain modelling and in the geological model. Dominating rock types are marked in red.

Rock type	Domain RSMA01 (Ävrö granite)		Domain RSMB01 (Fine-grained dioritoid)		Domain RSMC01 (Mixture of Ävrö granite and Quartz monzodiorite)	
	Modelling	Geological model	Modelling	Geological model	Modelling	Geological model
501044	78.92	75.8–84.7			31.58	22.9–34.1
501030	12.95	9.0–17.0	89.33	90.6–94.2	7.59	6.5
501036			0.93	0–3.5	47.82	51.5–73.9
511058	2.40	0.8–21.5	6.59	0.9–6.7	7.28	1.8–4.2
501061	0.31		1.73	0.8–1	2.04	0.3–1.4
501033		0–1.7			0.28	0.2
505102	4.27	3.0–4.9	0.90	0.6–0.8	1.74	1.2
501058	1.16		0.52		1.67	2.0

Table 5-2. Boreholes classified by domain /Wahlgren, 2004/.

Domain	Borehole
RSMA01	KAV01 KLX01 KLX02 0–1,450 m KSH03A 270–1,000 m
RSMB01	KSH02 KSH01A 320–620 m
RSMC01	KSH01A 100–320 m and 620–1,000 m KSH01B KSH03A 100–270 m and KSH03B 0–100 m

5.1.2 Borehole data

It was not possible to use all of the boreholes mentioned in Table 5-2 for the modelling of thermal properties on domain level due to lack of accurate density loggings and lithological data. In boreholes where the Ävrö granite is present (domain RSMA01 and RSMC01) two criteria have to be fulfilled for the borehole, otherwise it may not be used in the modelling. Primary a complete rock classification of the borehole and secondly the density logging has to be of good quality. In boreholes without the presens of Ävrö granite (domain RSMB01) only the first criteria with an up to date rock classification of the borehole has to be fulfilled.

The rock type classifications need to be up to date with both dominant and subordinate rock types. In cases were rock types with only four digit were available they were assumed possible to be upgraded by adding 50 in front of the four-digit code.

This is the status of available input data from other disciplines regarding rock type classifications (lithology) and density loggings.

- KAV01, KSH01A, KSH02: The input data of these boreholes is complete to use for the lithological domain modelling, meaning both density loggings and rock type classifications are available.
- KLX02: The input data of this borehole in complete although the density logging (190–1,000 m) have not been compared to measured samples and it has not been filtered.
- KSH01B: density logging 0–100 m available but no rock type classification.
- KSH03A: density logging 0–1,000 m available but of bad quality (not used). Rock type classification 100–1,000 m available.
- KSH03B: density logging 0–100 m available but no rock type classification.
- KLX01: no up to date density logging and no rock type classification.

5.2 Conceptual model

There are three main causes for the spatial variability of thermal conductivity at the domain level; (1) small scale variability between minerals, (2) spatial variability within each rock type, and (3) variability between the different rock types making up the domain. The first type entails variability in small samples (based on TPS measurements and modal analysis). At this scale, the small scale variability can be substantial. However, the variability is rapidly reduced when the scale increases.

The second type of variability is associated with variability in sample data from a rock type and cannot be explained by small scale variations. This is believed to be especially important for the rock type Ävrö granite, where this (spatial) variability is large. The reason for the variability within a rock type is associated with the process of rock formation, but also the system of classifying the rock types. This variability cannot be reduced, but the uncertainty in the variability may be reduced. This is achieved by collecting large number of samples at varying distances from each other, so that reliable variograms can be created.

Spatial variability of thermal conductivity within rock types has only been studied for rock type Ävrö granite (501044), where density loggings could be used. For other rock types, it was not possible to study the spatial variability because of few measurements and the lack of a reliable relationship between density and thermal conductivity. Variograms of thermal conductivity for different boreholes and separation distances are presented in /Sundberg et al. 2005b/. As an example, variograms for Ävrö granite in borehole KAV01 are illustrated in Figure 5-1. About 50% of the variability occurs at scales of less than about 2 m. However, there are relatively large differences of spatial variability within the rock type Ävrö granite between the different boreholes in the Ävrö granite domain (RSMA01).

The third type of variability is due to the presence of different rock types in the lithological domain. This variability is more pronounced where the difference in thermal conductivity is large between the most common rock types of the domain. Large variability of this type can also be expected in a domain of many different rock types. It is believed that the variability between rock types is important for all defined domains. It is only reduced significantly when the scale becomes large compared to that of the spatial occurrence of the rock type.

Of importance at the domain level is the scale representative for the canister, i.e. at which the thermal conductivity is important for the heat transfer from the canister. At present knowledge, this scale is not known in detail, but it is believed to be in the order of 1 to 10 m. Therefore, the approach in the domain modelling is to use different scales to study the scale effect, and to draw conclusions of representative thermal conductivity values from that. However, there are large uncertainties and relatively small scales are used in modelling and analysis.

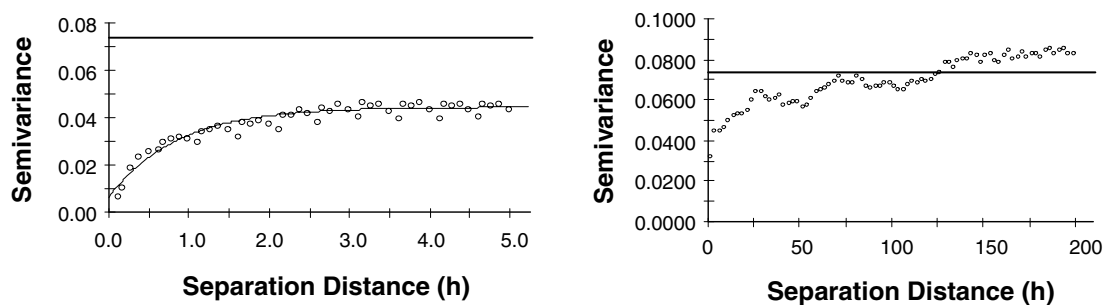


Figure 5-1. Variogram of thermal conductivity of Ävrö granite (501044) in KAV01, estimated from density logging; 0–5 m and 0–200 m separation distance. The straight line indicates the total variance in data. Increasing semivariance indicates correlation between data at the actual separation distance due to the occurrence and composition of the Ävrö granite in the borehole. Therefore, the correlation structure is borehole dependant.. The variograms indicate correlation at different scales.

5.3 Modelling approach for domain properties

5.3.1 Introduction

The methodology for thermal conductivity domain modelling and the modelling of scale dependency were developed for the Prototype Repository at the Äspö HRL /Sundberg et al. 2005/. Different approaches are used in the modelling. Modelling of the mean for the thermal conductivity at domain level is performed according to the main approach in Figure 5-2 and Figure 5-3. This approach is applied to the lithological domains RSMA01 (Ävrö granite), RSMB01 (Fine-grained dioritoid), and RSMC01 (mixture of Ävrö granite and Quartz monzodiorite). Rock domain RSMD01 (Quartz monzodiorite) is not represented by any boreholes and is therefore handled differently, see approach below. In order to evaluate the spatial variability at domain level, three alternative/complementary approaches were applied (Approach 2–4). Mean value results on a domain level and concluding standard deviations are presented in Table 5-14.

It would be useful to develop a spatial model of thermal conductivity and its variability for the domains. However, in this version of the site descriptive modelling the spatial variability has only been modelled for Ävrö granite in specific boreholes.

For a heat capacity a much more simplified approach has been used based on Monte Carlo simulation. The heat capacity modelling approach is described after the four different approaches for thermal conductivity.

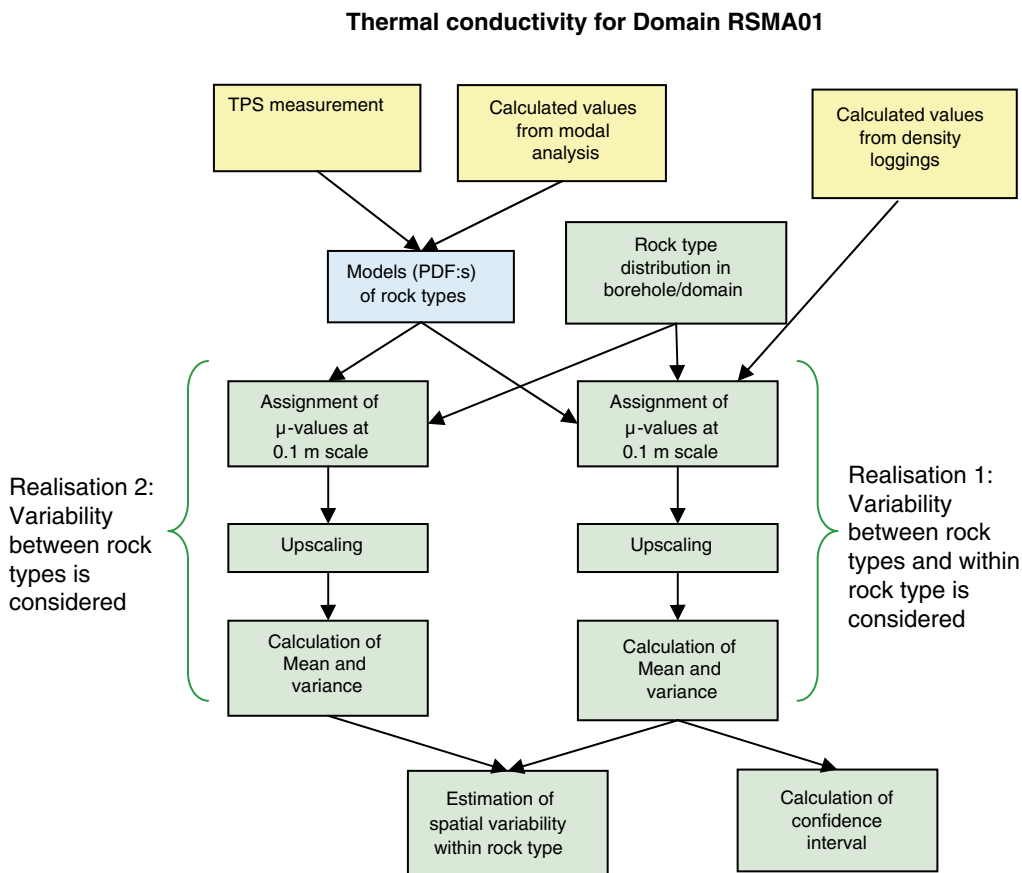


Figure 5-2. Main approach for estimation of thermal conductivity for domain RSMA01 (Ävrö granite). Yellow colour indicates the data level, blue the rock type level, and green the domain level. The parameter λ refers to thermal conductivity.

Thermal conductivity for Domain RSMB01 and RSMC01

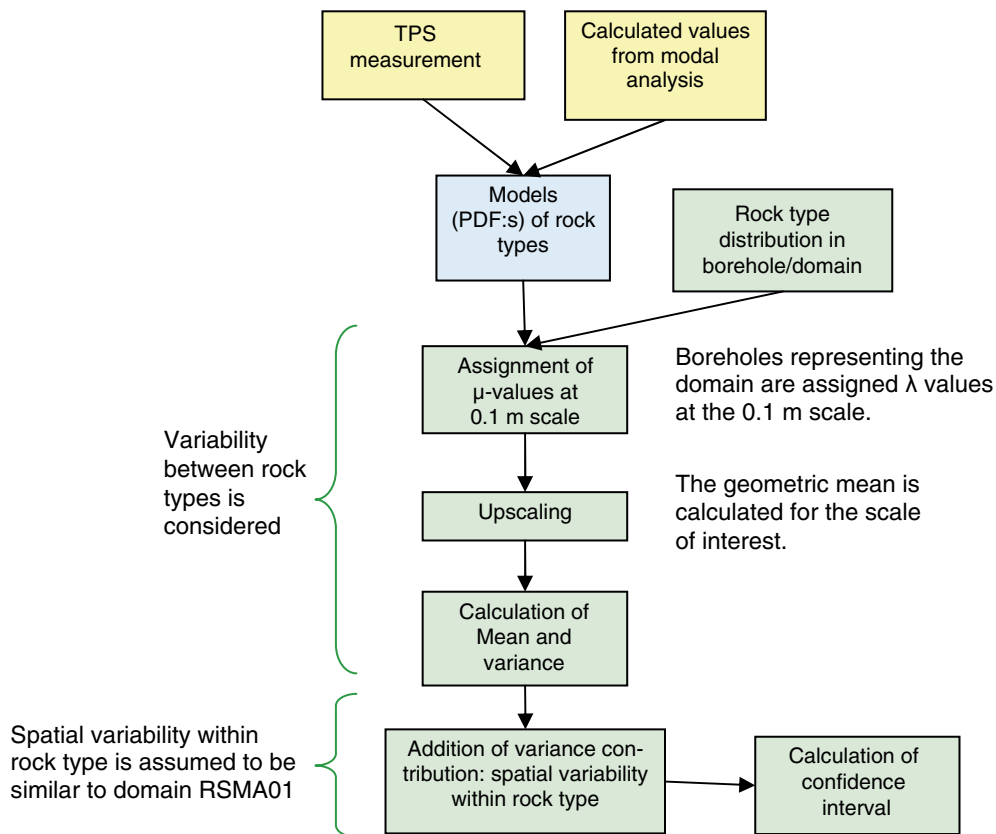


Figure 5-3. Main approach for estimation of thermal conductivity for domain RSMB01 (Fine-grained dioritoid) and RSMC01 (mixture of Ävrö granite and Quartz monzodiorite). Yellow colour indicates the data level, blue the rock type level, and green the domain level. The parameter λ refers to thermal conductivity.

5.3.2 Approach 1: Main approach

The main approach for domain RSMA01 (Ävrö granite), RSMB01 (Fine-grained dioritoid), and RSMC01 (mixture of Ävrö granite and Quartz monzodiorite) is as follows:

Thermal conductivity values, both measured and calculated from modal analysis, are used to produce a PDF (Probability Density Function) model for rock types present in the domains, according to Table 4-20. Density loggings are transformed into thermal conductivity estimates according to the model described in Section 4.5.

The summed up length of boreholes, or parts of boreholes, belonging to a domain is assumed to be a representative realisation of the domain. Each borehole belonging to a domain is divided into 0.1 m long sections and each section is assigned a thermal conductivity value according to the lithological classification of that section. Both dominating and subordinate rock types are considered in this context, including rock occurrence less than 1 m. However, only dykes and veins with an apparent thickness of at least 5 cm are considered. The principles for the assignment of thermal properties are as follows for rock type 501044 (Ävrö granite):

- Primary, the thermal conductivity values calculated from density loggings are used. This implies that the spatial variability within rock type Ävrö granite is considered.

- If the density value is outside the valid range as stipulated by the correlation between density and thermal conductivity, a value of the thermal conductivity is randomly selected from the rock type model (PDF).

Other dominating and subordinate rock types are assigned thermal properties according to:

- A value of thermal conductivity is randomly selected according to the rock type model (PDF), see Table 4-20. An example showing the principle for assigning thermal conductivity for the rock types is shown in Figure 5-4.
- For rock types where no rock type model (PDF) is available (due to lack of data), no value is assigned to that 0.1 m section (section ignored in the calculations). Such rock types, primarily pegmatite, have a low degree of occurrence in the domains and are therefore assumed not to influence the result significantly.

The next step is the upscaling from 0.1 m scale to the appropriate scale of the canister. The significant scale for the canister has not yet been determined in detail and therefore upscaling is performed on scales ranging from 0.1 m to 60 m. The upscaling is performed in the following way:

1. The boreholes representing the domain are divided into a number of sections with a length according to the desired scale (0.1–60 m).
2. Thermal conductivity is calculated for each section by geometric mean calculations of the values at the 0.1 m scale.
3. The mean and the variance for all sections of the domain are calculated. For each scale, the calculations are repeated at least 10 times with different assignments of thermal conductivity values at the 0.1 m scale, according to principle in Figure 5-2 and Figure 5-3. This produces representative values of the mean and the standard deviation for the desired scale.
4. The calculations are repeated for the next scale.

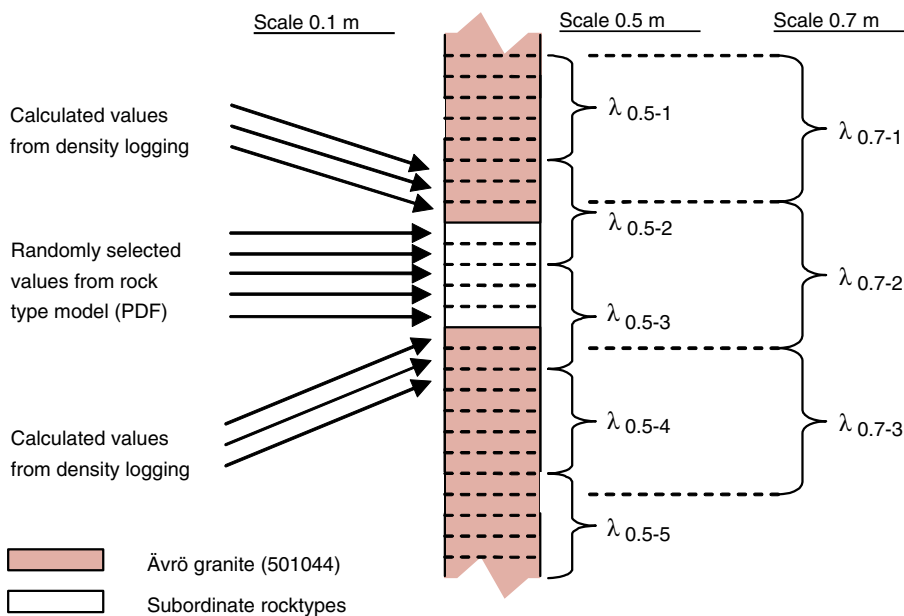


Figure 5-4. Thermal conductivity is assigned to 0.1 m sections by calculation from density loggings or randomly selected from the rock type models. Upscaling is done by calculating geometric means for different scales, for example 0.5 and 0.7 m.

The principle for upscaling of data for different rock types is illustrated both in Figure 5-4 and in Figure 5-5. In Figure 5-4, 25 sections are indicated, each with a length of 0.1 m. For the scale 0.5 m, the thermal conductivity $\lambda_{0.5-1}$ is estimated as the geometric mean of the five 0.1 m sections, $\lambda_{0.5-2}$ as the geometric mean for the next five 0.1 m sections, and so on. The mean and variance is then easily computed for the 0.5 m scale. This sequence is repeated for the other scales of interest. In Figure 5-5 the effects of upscaling are illustrated. The geometric mean equation is often applied for mean estimation of transport properties /Dagan, 1981; Sundberg, 1988/.

As illustrated in Figure 5-2 and Figure 5-3, the approach is slightly different between domain RSMA01 (dominated by Ävrö granite) and the other domains. The reason is that density loggings can be used for domain RSMA01 to take into account spatial correlation within the dominating rock type. This is not possible for domain RSMB01 (Fine-grained dioritoid) and only to a limited degree for domain RSMC01 (mixture of Ävrö granite and Quartz monzodiorite) because the two latter rock domains are dominated by other rock types, for which no reliable relationship between density and thermal conductivity is presently available. Therefore, the variance for domain RSMB01 and RSMC01 is underestimated in the approach described above. The spatial variability within the dominating rock types needs to be added. This is solved in the following way, as illustrated in Figure 5-2 and Figure 5-3:

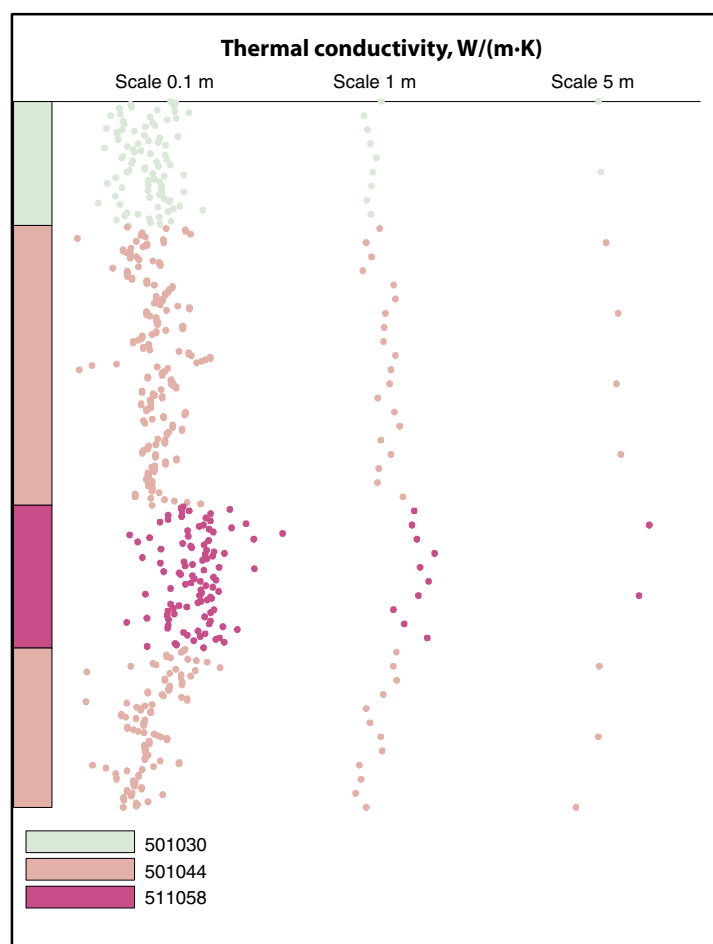


Figure 5-5. Effects of applying the principle for upscaling of thermal conductivity, as given in Figure 5-4, where mean values, standard deviations, and lower and upper confidence intervals for the domains are calculated for different scales. The figure is conceptual.

1. Variance caused by spatial variability within rock type Ävrö granite (501044) is estimated for domain RSMA01 (Ävrö granite). This is performed in the following way: A second realisation is performed where all thermal conductivity values are randomly selected from the rock type PDF models and no data from density loggings are used. The variance contributed by spatial correlation within rock types is assumed to be the difference between realisation 1 and 2, see Figure 5-2 and Figure 5-6.
2. For domain RSMB01 (Fine-grained dioritoid) and RSMC01 (mixture of Ävrö granite and Quartz monzodiorite), no density loggings are used, see Figure 5-3. Instead it is assumed that the variance caused by spatial variability within the rock types is identical to that of domain RSMA01. Therefore, the spatial contribution of variance in Figure 5-6 is added to the variance for domain RSMB01 and RSMC01.

The addition of variances is assumed valid because:

- The processes behind spatial variability within and between rock types can be regarded as the effects of stochastic processes resulting in stochastic variables. It is reasonable to assume that these variables are fairly independent, at least for the purpose of the modelling.
- Addition of variances of stochastic variables is possible if they are independent.

Domain RSMD01 (Quartz monzodiorite) is handled differently because no borehole data from this lithological domain were available. An assumption is made that the domain solely consists of Quartz monzodiorite (501036). The PDF model for this rock type (Figure 4-18) is used to estimate the variability at the 0.1 m scale. No direct upscaling is possible due to lack of borehole data (lithology etc).

Confidence intervals are calculated for each scale under the assumption of normally distributed data at the scale of interest.

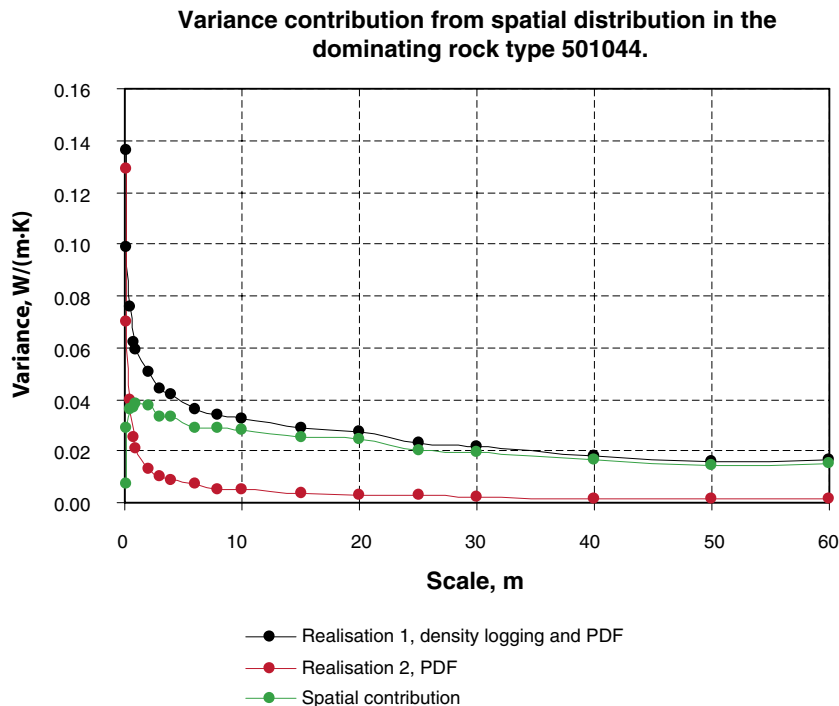


Figure 5-6. Variance contribution from spatial distribution in the dominating rock type Ävrö granite (501044) of domain RSMA01.

5.3.3 Approach 2: Extrapolation – spatial variation in all rock types

When modelling domain RSMA01 (dominated by Ävrö granite) according to the main approach, spatial distribution was only considered for 71.3% of the borehole length since not all 0.1 m sections of the domain contained density logging data within the range of validity. For the remainder of the borehole, 28.7%, thermal conductivity values were randomly assigned from the rock type models. Therefore, an approach was made to correct for this (it is assumed that all rock types have the same spatial variation as Ävrö granite, 501044). By randomly replacing thermal conductivity values estimated from density logging with random PDF values it is possible to study the effect of ignoring the spatial variability for 28.7% of the borehole.

5.3.4 Approach 3: Reduction of small scale variability

In the third approach, variograms are used to estimate the small scale variance of Ävrö granite (501044) in RSMA01 (dominated by Ävrö granite). The variograms are based on data from boreholes KAV01 and KLX02, both of which belong to domain RSMA01.

In this approach, the small-scale variability for the scale of interest within Ävrö granite (501044) is subtracted from the total variability of the same rock type (from PDF's). This residual variability is assumed to be the variance after averaging to the desired scale. The basis for the approach is that variability in scales smaller than the desired is evened out.

5.3.5 Approach 4: Addition of “between rock type” and “within rock type” variance

The approach of randomly selecting thermal conductivity values from rock type models (PDF's) without consideration of spatial variability was described in the main approach. Modelling according to main approach estimates the thermal conductivity at different scales. This variance includes variability due to rock type changes in the boreholes (“between rock type” variability) but the variability within each rock type is effectively and rapidly reduced when the scale is increased because of the random assignment of thermal conductivity values. The resulting variance is therefore mainly a result of the presence of different rock types in the boreholes. Below, this variance is denoted as V_1 .

One way of compensating for the variance reduction caused by ignoring spatial variability is to add the spatial variability within the dominating rock type in the domain. This is a similar, although not identical, approach to the main approach for domain RSMB01 (Fine-grained dioritoid) and RSMC01 (mixture of Ävrö granite and Quartz monzodiorite). The spatial variability within the dominating rock type can be estimated in different ways, from density loggings (Ävrö granite) or TPS measurements. The variances as a function of scale were calculated in these ways (geometric mean for the actual scale). This type of variance is denoted V_2 below.

The total variance for the domain can be estimated as the sum of variance due to different rock types and the variance due to spatial variability within the dominating rock type:
 $V_{\text{tot}} = V_1 + V_2$.

5.3.6 Modelling approach: Heat capacity

Distribution models of heat capacity based on TPS measurements for rock type Ävrö granite (501044), Quartz monzodiorite (501036) and Fine-grained dioritoid (501030) are calculated. A Monte Carlo simulation is performed by weighting the occurrence of different rock types in the domain (Table 4-3) together with the distribution models. The simulation calculates a mean value together with a standard deviation in data values which gives the possibility to calculate a confidence interval for the heat capacity on domain level.

5.4 Domain modelling results

5.4.1 Approach 1: Main approach

Figure 5-7 illustrates the modelled (according to the main approach) thermal conductivity plotted towards depth for the different boreholes which constitutes the three domains RSMA01 (Ävrö granite), RSMB01 (Fine-grained dioritoid) and RSMC01 (mixture of Ävrö granite and Quartz monzodiorite). The results for domain RSMA01 and RSMC01 relates to realisation 1 whereas the results of domain RSMB01 relates to realisation 2. The plotted thermal conductivity values are calculated geometrical mean values over 50 m long sections (moving average).

In Figure 5-9, Figure 5-12 and Figure 5-14 the mean value of the thermal conductivity calculated according to the main approach and based on different modelling assumptions is presented. In Figure 5-10, Figure 5-13 and Figure 5-15 the mean value of thermal conductivity together with a two-sided 95% confidence interval regarding spatial distribution in data values for the present scale is presented under assumption of normal distribution. Probability plots of domain modelling results in different scales are presented in Appendix B. Table 5-7 illustrates the variance and standard deviation of the thermal conductivity for different scales on domain level.

It must be stressed that the confidence intervals in Figure 5-9 to Figure 5-15 mainly includes uncertainty due to natural variability in the rock mass. Uncertainties resulting from lack of knowledge of representativeness etc have not been included in the domain modelling. An approach for including lack-of-knowledge uncertainty is presented in /Sundberg et al. 2005/.

Domain RSMA01, Ävrö granite (501044)

Domain RSMA01 is dominated by the rock type Ävrö granite (501044) which constitutes approximately 78.9% of the domain (75.8–84.7% according to a preliminary version of the geological model, September 2004). For the rock type distribution of the domain and for the boreholes which constitutes the domain see Table 5-3. The modelling of domain RSMA01 is based on data from the two boreholes KAV01 and KLX02. A 741 m long section of borehole KAV01 is included where 80.6% of the thermal conductivities are calculated from the density logging together with a 799 m long section of borehole KLX02 where 66.0% of the thermal conductivities are calculated from the density logging. Generally, thermal conductivities from density loggings gives higher mean values than measured and calculated values from mineral compositions which is illustrated in Figure 4-15. This might depend on a systematic error (bias) in the mean value calculations based on density loggings or due to the fact that measured and calculated values not are representative for the same rock mass as the density logging has been conducted for. In the later case, the density logging ought to represent a more accurate value. Modelling results for the domain and per borehole with mean value and standard deviation in 0.7 m scale is presented in Table 5-3.

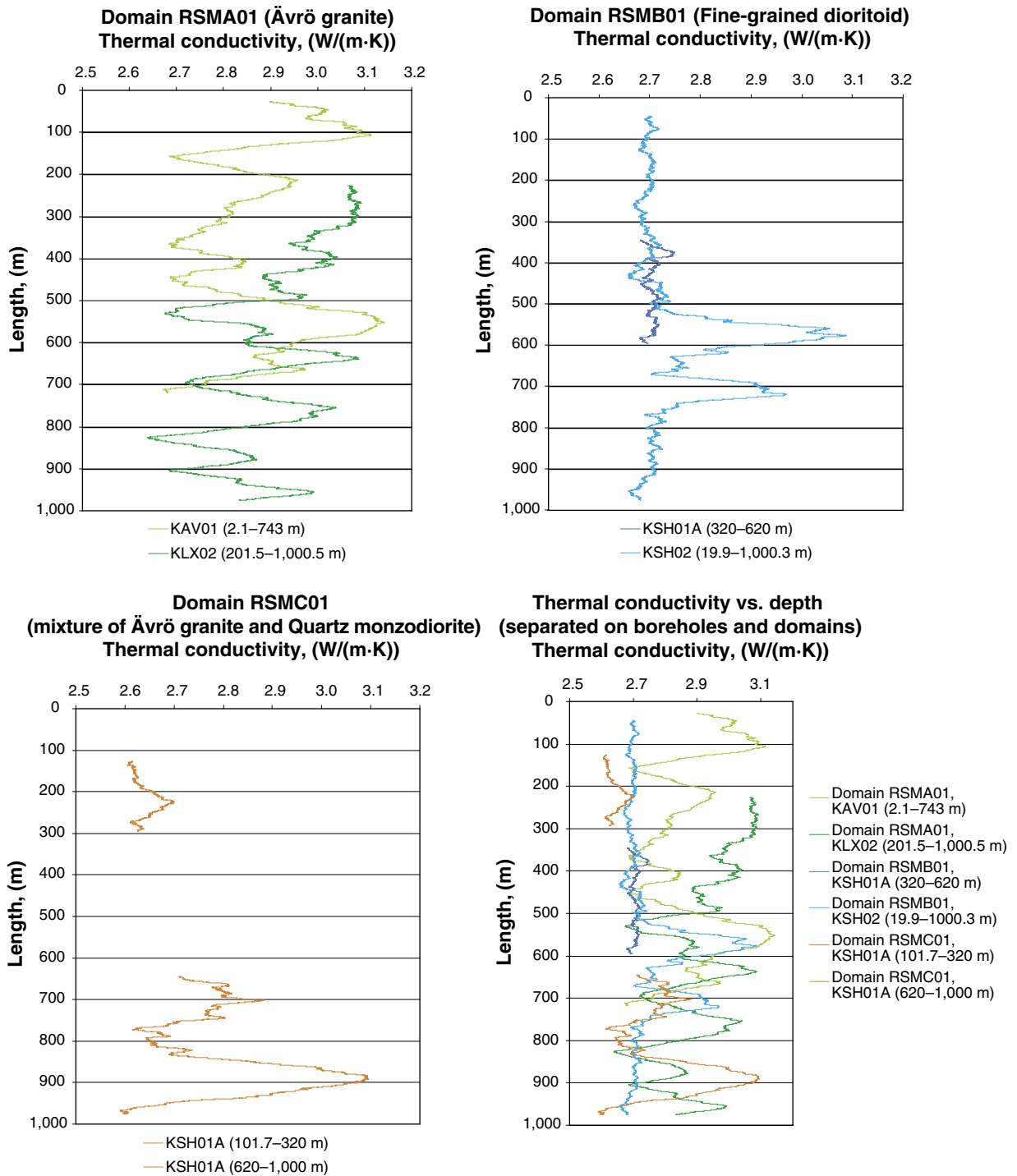


Figure 5-7. Modelling results of three domains (RSMA01, RSMB01 and RSMC01) separated on each borehole, which constitutes the domain. Thermal conductivity values are geometrical mean value calculations over 50 m long sections (moving average). For domain RSMB01 and RSMC01 the spatial variability within rock types is not considered. The results origin from only one realisation.

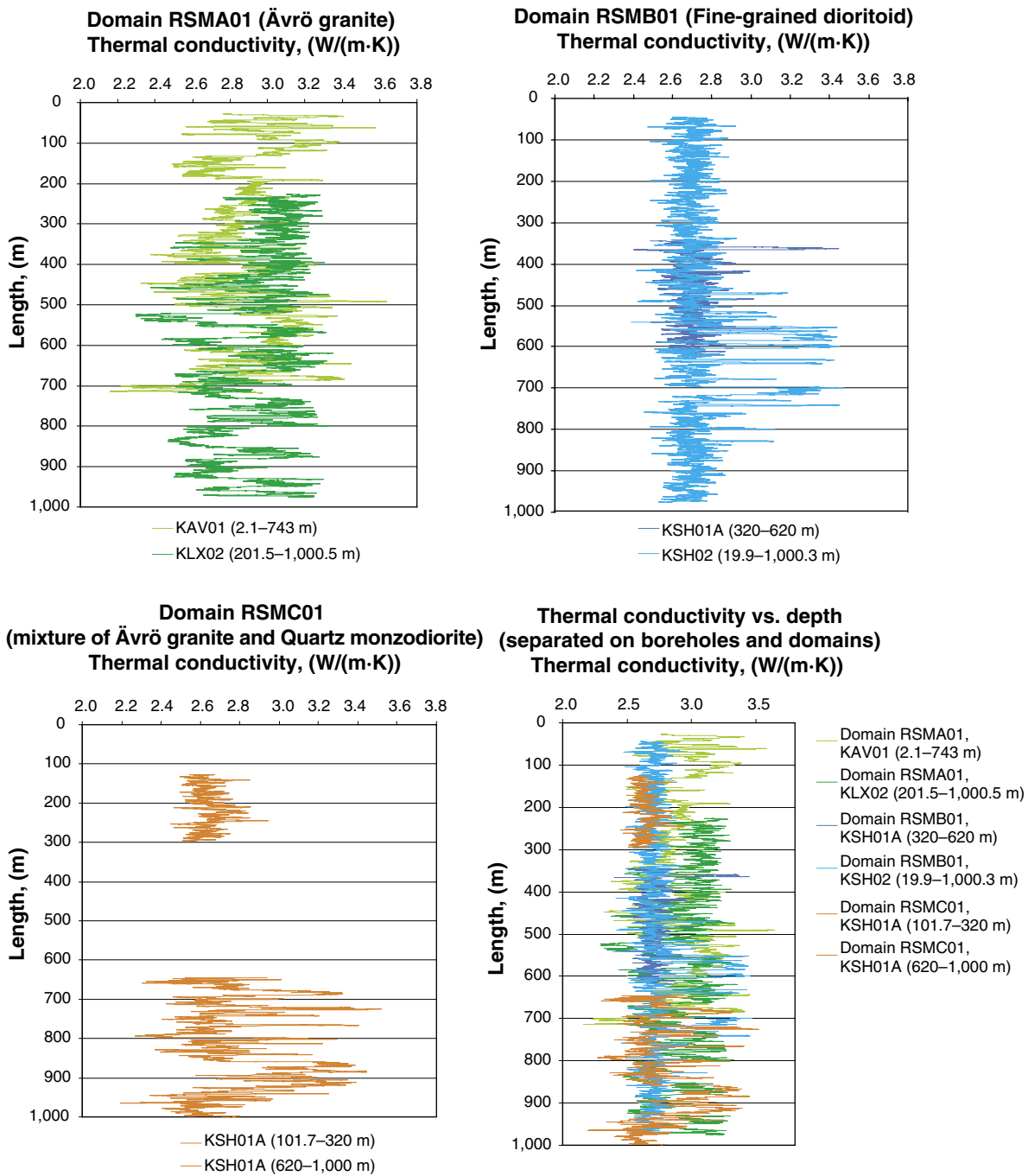


Figure 5-8. Modelling results of three domains (RSMA01, RSMB01 and RSMC01) separated on each borehole, which constitutes the domain. Thermal conductivity values are geometrical mean value calculations over 2 m long sections (moving average). For domain RSMB01 and RSMC01 the spatial variability within rock types is not considered. The results origin from only one realisation.

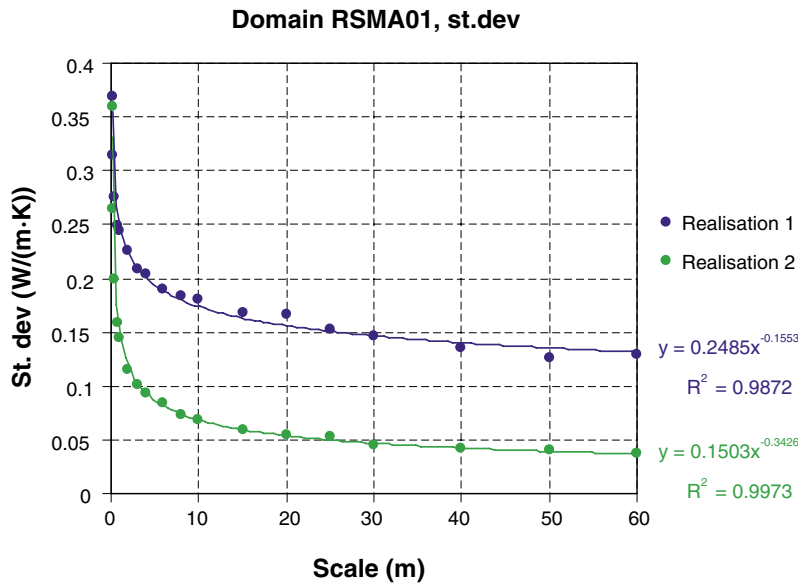


Figure 5-9. Modelling results of domain RSMA01 (Ävrö granite), standard deviation for thermal conductivity based on different modelling assumptions.

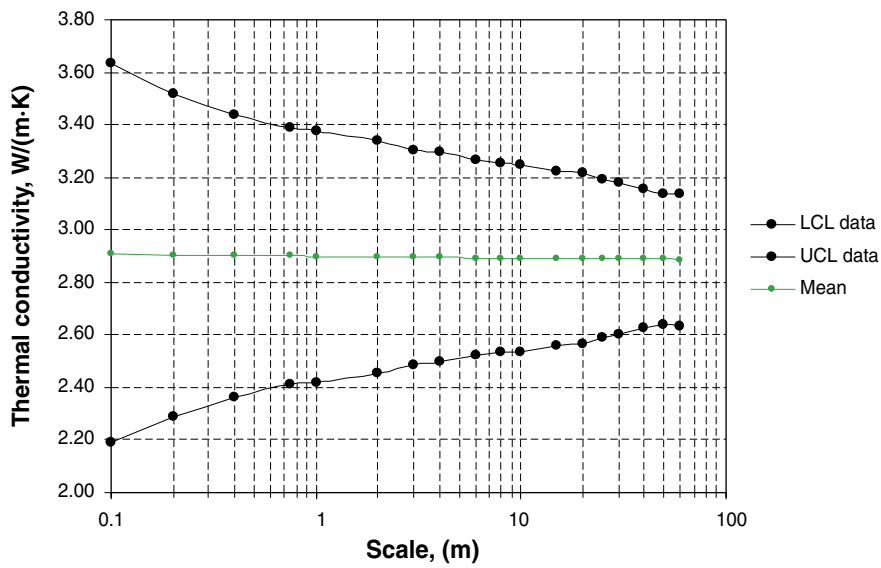


Figure 5-10. Mean value of thermal conductivity for domain RSMA01 (Ävrö granite) and two-sided 95% confidence interval. Observe the logarithmic scale on the x-axis.

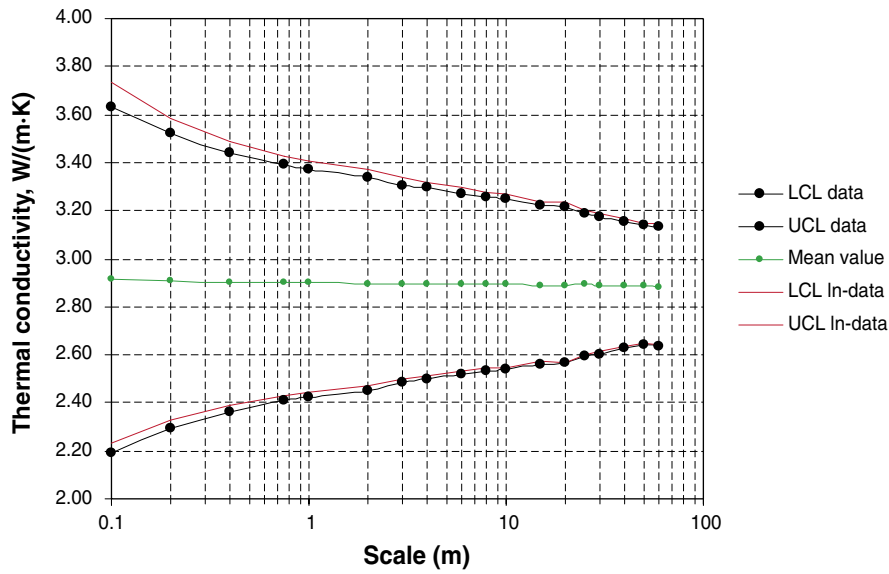


Figure 5-11. Two-sided 95% confidence intervals assuming both normally and lognormally distributed data for domain RSMA01 (Ävrö granite). Observe the logarithmic scale on the x-axis.

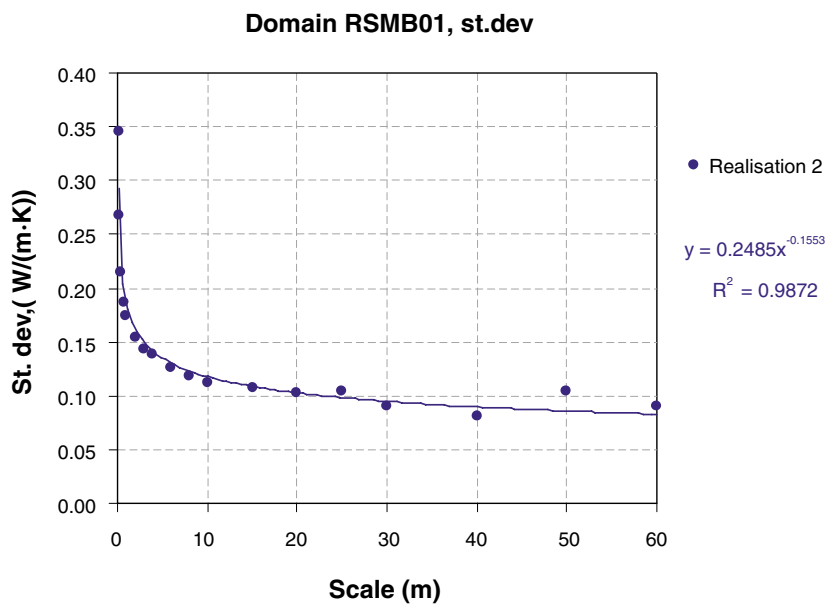


Figure 5-12. Modelling results of domain RSMB01 (Fine-grained dioritoid), standard deviation for thermal conductivity based on modelling assumption realisation 2.

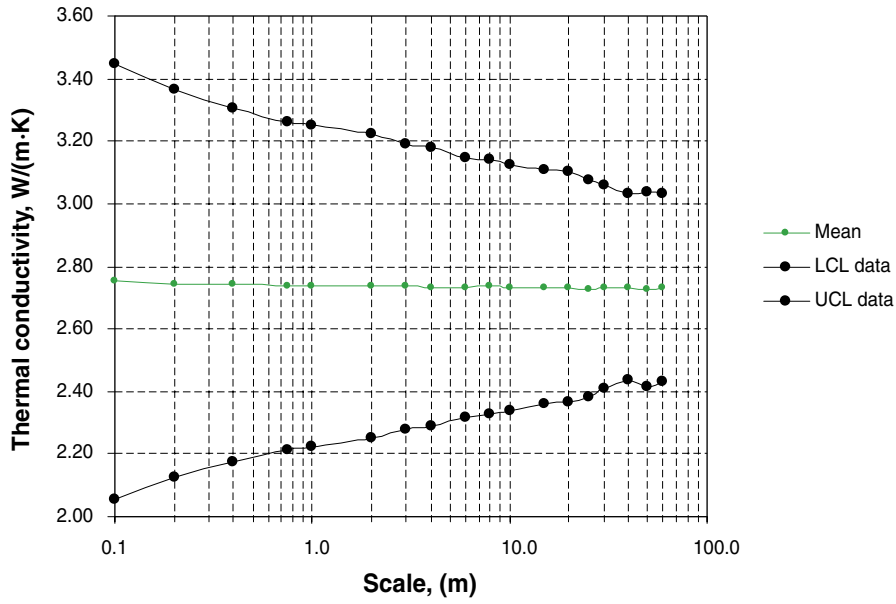


Figure 5-13. Mean value of thermal conductivity for domain RSMB01 (Fine-grained dioritoid) and two-sided 95% confidence interval. Observe the logarithmic scale on the x-axis. Spatial variability within dominating rock type has been applied.

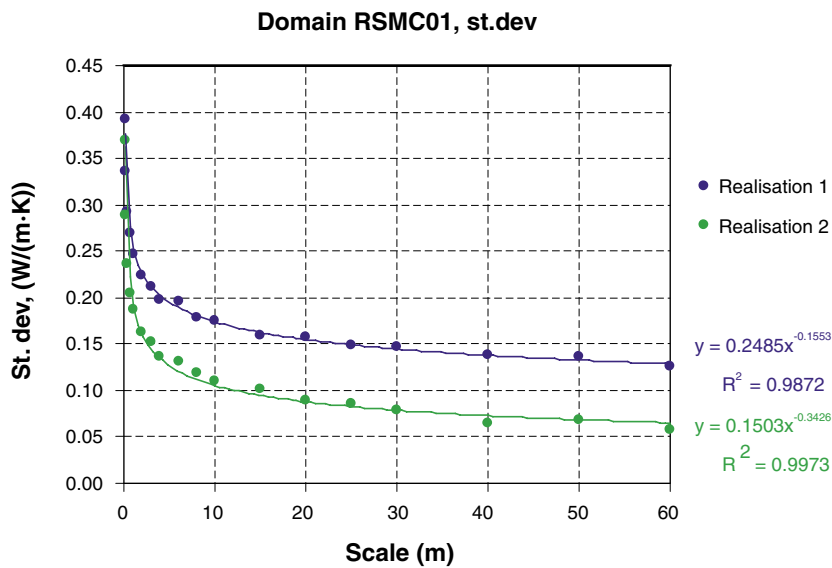


Figure 5-14. Modelling results of domain RSMC01 (mixture of Ävrö granite and Quartz monzodiorite), standard deviation for thermal conductivity based on different modelling assumptions.

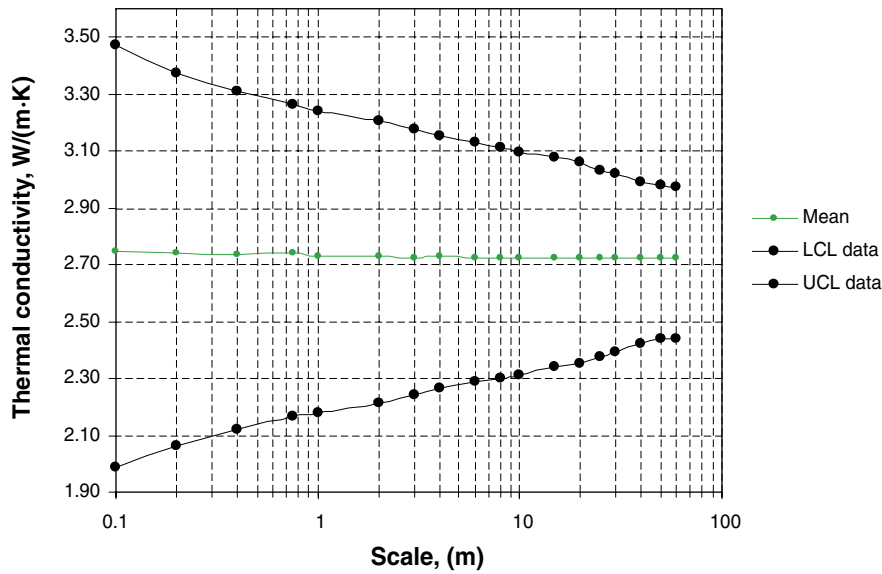


Figure 5-15. Mean value of thermal conductivity for domain RSMC01 (mixture of Ävrö granite and Quartz monzodiorite) and two-sided 95% confidence interval. Observe the logarithmic scale on the x-axis. Spatial variability within dominating rock type has been applied.

Table 5-3. Modelling results for the domain and per borehole with mean and standard deviation of the thermal conductivity (W/(m·K)) in 0.7 m scale and rock type distributions in percent.

Borehole interval		Domain RSMA01	KAV01 2.1–743 m	KLX02 201.5–1,000.5 m
Thermal conductivity in 0.7 m scale	Mean	2.90	2.89	2.91
	St. dev	0.25	0.24	0.25
Fine-grained dioritoid	501030	13.0	8.6	17.0
Quartz monzodiorite	501036	0	0	0
Diorite/Gabbro	501033	0	0	0
Ävrö granite	501044	79.0	82.0	76.0
Granite	501058	1.2	1.3	1.1
Pegmatite	501061	0.3	0.5	0.1
Fine-grained diorite-gabbro	505102	4.3	3.1	5.4
Fine-grained granite	511058	2.4	4.5	0.4

Tests performed for domain RSMA01 (Ävrö granite) indicate that data deviates more from a normal distribution when the scale increases. Thus, the estimated confidence limits are more uncertain for larger scales than for small ones. For domain RSMA01, the deviation of the lower confidence limit (two-sided 95% confidence) was less than 2 % at the 10 m scale. No such tests can be performed on domain RSMB01 and RSMC01 because of the modelling approach for these domains.

For domain RSMA01, calculations of confidence intervals have been performed while assuming data to be normally and lognormally distributed (two cases). As illustrated in Figure 5-11, the difference between the confidence intervals based on the different distributions is small. This shows the data to be weakly lognormal distributed. When the data is assumed to be normally distributed, as in the thermal modelling of the Simpevarp subarea, the lower confidence limit is on the safe side (lower) compared to an assumed lognormal distribution. Similar results may be expected for the other lithological domains.

Domain RSMB01, Fine-grained dioritoid (501030)

Domain RSMB01 is dominated by the rock type Fine-grained dioritoid (501030) which constitutes approximately 89.3% of the domain (90.6–94.2% according to a preliminary version of the geological model, September 2004). For the rock type distribution of the domain and for the boreholes which constitutes the domain see Table 5-4. For domain RSMB01 the modelling is based on 300 m of borehole KSH01A and 980.4 m of borehole KSH02. Since no Ävrö granite is present in these boreholes all thermal conductivities comes from the distributions models (PDF). Modelling results for the domain and per borehole with mean value and standard deviation in 0.7 m scale is presented in Table 5-4.

Table 5-4. Modelling results for the domain and per borehole with mean and standard deviation of the thermal conductivity (W/(m·K)) in 0.7 m scale and rock type distributions in percent.

Borehole interval		Domain RSMB01	KSH01A 320–620 m	KSH02 19.9–1,000.3 m
Thermal conductivity in 0.7 m scale	Mean	2.74	2.70	2.75
	St. dev	0.19	0.14	0.19
Fine-grained dioritoid	501030	89.3	90.4	89.0
Quartz monzodiorite	501036	0.9	4.0	0
Diorite/Gabbro	501033	0	0	0
Ävrö granite	501044	0	0	0
Granite	501058	0.5	0	0.7
Pegmatite	501061	1.7	1.2	1.9
Fine-grained diorite-gabbro	505102	0.9	1.3	0.8
Fine-grained granite	511058	6.6	3.1	7.7

Domain RSMC01, Ävrö granite and Quartz monzodiorite (501044 and 501036)

Dominating rock types in domain RSMC01 are Quartz monzodiorite (501036) and Ävrö granite (501044) which constitute 47.8% respectively 31.6% (51.5–73.9% respectively 22.9–34.1% according to a preliminary version of the geological model, September 2004). For the rock type distribution of the domain which coincides with a part of a borehole see Table 5-5. Modelling of domain RSMC01 is based on 598.5 m of KSH01A where 30.0% of the thermal conductivities may be calculated from the density logging. Modelling results for the domain and the borehole with mean value and standard deviation in 0.7 m scale is presented in Table 5-5.

Table 5-5. Modelling results for the domain and per borehole with mean and standard deviation of the thermal conductivity (W/(m·K)) in 0.7 m scale and rock type distributions in percent.

Borehole interval		Domain RSMC01 KSH01A 101.7–320 m and 620–1,000 m	
Thermal conductivity in 0.7 m scale	Mean	2.74	
	St. dev	0.27	
Fine-grained dioritoid	501030	7.6	
Quartz monzodiorite	501036	47.8	
Diorite/Gabbro	501033	0.3	
Ävrö granite	501044	31.6	
Granite	501058	1.7	
Pegmatite	501061	2.0	
Fine-grained diorite-gabbro	505102	1.7	
Fine-grained granite	511058	7.3	

Domain RSMD01, Quartz monzodiorite (501036)

The dominating rock type in domain RSMD01 is Quartz monzodiorite (501036). There are no boreholes with lithology in this domain whereas domain RSMD01 has been approximated to be the same as rock type 501036 for which there are 10 measured thermal conductivities and 12 calculated from mineral composition. Distributions of these are showed in Figure 4-17. In Table 5-6 the results from the Monte Carlo simulation of domain RSMD01 are presented.

Table 5-6. Thermal conductivity (W/(m·K)) of domain RSMD01 (Quartz monzodiorite) with two-sided 95% confidence interval.

Domain	Mean	St. dev	Lower confidence limit	Upper confidence limit
RSMD01	2.62	0.28	2.04	3.20

Table 5-7. Standard deviation / variance for thermal conductivity (W/(m·K)) on domain level in different scales. Results are calculated according to Section 5.3.2. For each domain, the representative values are given in the left column.

Scale	RSMA01		RSMB01		RSMC01	
	From density logging + PDF	Randomly from PDF	Randomly from PDF and compensated for spatial variability	Randomly from PDF	Randomly from PDF and compensated for spatial variability	Randomly from PDF
0.1	0.369/0.136	0.359/0.129	0.356/0.126	0.345/0.119	0.379/0.144	0.369/0.136
0.2	0.314/0.098	0.264/0.070	0.316/0.100	0.268/0.072	0.335/0.112	0.290/0.084
0.4	0.275/0.076	0.199/0.039	0.287/0.083	0.215/0.046	0.304/0.092	0.237/0.056
0.7	0.249/0.062	0.159/0.025	0.267/0.071	0.186/0.035	0.281/0.079	0.205/0.042
1	0.244/0.059	0.145/0.021	0.262/0.069	0.174/0.030	0.271/0.073	0.187/0.035
2	0.225/0.051	0.115/0.013	0.247/0.061	0.154/0.024	0.253/0.064	0.163/0.026
3	0.209/0.044	0.101/0.010	0.232/0.054	0.143/0.020	0.239/0.057	0.153/0.023
4	0.204/0.042	0.093/0.009	0.228/0.052	0.138/0.019	0.227/0.051	0.137/0.019

Scale	RSMA01		RSMB01		RSMC01	
	From density logging + PDF	Randomly from PDF	Randomly from PDF and compensated for spatial variability	Randomly from PDF	Randomly from PDF and compensated for spatial variability	Randomly from PDF
6	0.191/0.036	0.085/0.007	0.212/0.045	0.126/0.016	0.215/0.046	0.131/0.017
8	0.184/0.034	0.073/0.005	0.207/0.043	0.119/0.014	0.207/0.043	0.120/0.014
10	0.181/0.033	0.069/0.005	0.201/0.041	0.112/0.013	0.200/0.040	0.110/0.012
15	0.169/0.029	0.059/0.003	0.191/0.037	0.108/0.012	0.188/0.035	0.102/0.010
20	0.166/0.028	0.054/0.003	0.188/0.035	0.103/0.011	0.181/0.033	0.090/0.008
25	0.153/0.023	0.053/0.003	0.177/0.031	0.104/0.011	0.167/0.028	0.086/0.007
30	0.146/0.021	0.045/0.002	0.166/0.028	0.091/0.008	0.160/0.026	0.079/0.006
40	0.135/0.018	0.041/0.002	0.151/0.023	0.081/0.007	0.144/0.021	0.065/0.004
50	0.126/0.016	0.040/0.002	0.159/0.025	0.104/0.011	0.138/0.019	0.068/0.005
60	0.129/0.017	0.038/0.001	0.153/0.023	0.091/0.008	0.136/0.018	0.058/0.003

Summary of modelling according to main approach

A summary of the thermal conductivity on domain level is presented in Table 5-12. The thermal conductivity in canister scale (1–10 m) is of special interest. In order not to underestimate the variance due to different uncertainties, it is assumed that the thermal conductivity which is representative of the domain in canister scale is equal to the thermal conductivity in the 0.7 m scale.

The mean thermal conductivity of domain RSMA01 (Ävrö granite) at the 0.7 m scale has been corrected by a subtraction of 0.1 W/(m·K), which is motivated by a potential bias in the relationship between density and thermal conductivity, used for the dominating rock type in this domain. A corresponding subtraction of 0.1 W/(m·K) has also been made for the confidence limits. For the other domains no such correction for potential bias has been performed.

Observe that the above table is valid at 20°C. The thermal conductivity decreases slightly at higher temperatures, 1–4°C per 100°C temperature increase.

According to this approach the standard deviation of domain RSMB01, RSMC01 and RSMD01 is larger than the one for domain RSMA01. This is most probably an overestimation of the variance since the Ävrö granite (which RSMA01 mainly consists of) has the largest variation in chemical composition and therefore also the largest distribution in thermal conductivity.

Table 5-8. Thermal conductivity (W/(m·K)) per domain in 0.7 m scale with two-sided 95% confidence interval regarding spatial distribution in data values under assumption of normal distribution.

Domain	Mean	St. dev	Lower confidence limit	Upper confidence limit	Comment
RSMA01	2.80	0.25	2.31	3.29	Mean and confidence limits subtracted by 0.1, see text.
RSMB01	2.74	0.27	2.21	3.26	
RSMC01	2.74	0.28	2.16	3.26	
RSMD01	2.62	0.28	2.04	3.20	Modelled with Monte Carlo simulation.

5.4.2 Approach 2: Extrapolation – spatial variation in all rock types

As described above, when modelling domain RSMA01 (dominated by Ävrö granite) according to the main approach, spatial distribution was not considered for the whole borehole length. By randomly replacing thermal conductivity values estimated from density logging with random PDF values it is possible to study the effect of ignoring the spatial variability for part of the borehole.

Figure 5-16 illustrates an extrapolation of the standard deviation for the scale 0.7 m as a function of the percentage of spatial data used in the modelling of domain RSMA01. If the whole spatial variation is considered the standard deviation of domain RSMA01 at 0.7 m scale is estimated to be 0.32 W/(m·K), which corresponds to a variance of 0.10 W/(m·K). The variance contribution due to spatial variability within rock types is then 0.073 W/(m·K), which differs from 0.037 W/(m·K) used in the main modelling approach, see Table 5-12.

However, it is reasonable to assume that this approach of correction overestimates the total variance since the spatial variation of other rock types than Ävrö granite (501044) probably is significantly smaller, which is not considered in the correction.

5.4.3 Approach 3: Reduction of small scale variability

In the third approach, the small-scale variability for the scale of interest within Ävrö granite in RSMA01 is subtracted from the total variability of the same rock type. The basis for the approach is that variability in scales smaller than the desired is evened out. Variograms presented in Figure 4-24, Figure 4-26 and Figure 4-29 are used to estimate the small scale variance of 501044 (dominated by Ävrö granite). The variograms are based on data from boreholes KAV01 and KLX02, both of which belong to domain RSMA01.

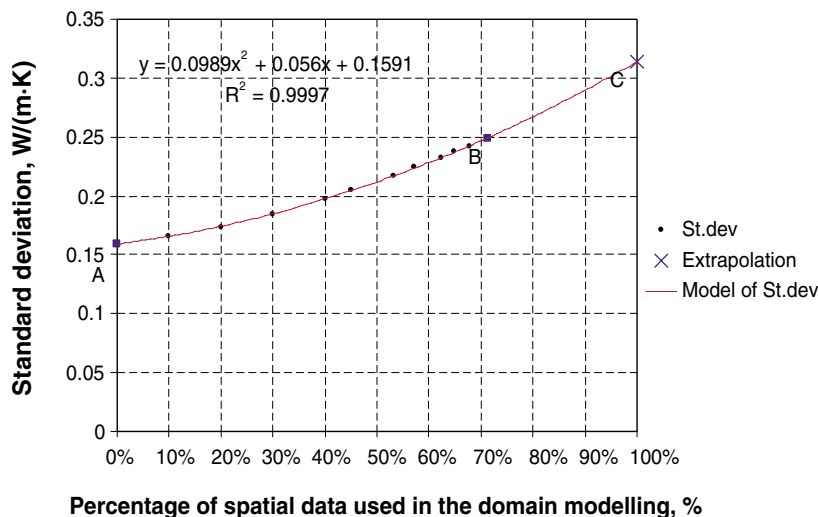


Figure 5-16. Extrapolation of standard deviation for thermal conductivity at scale 0.7 m for domain RSMA01. At point A, all data are randomly assigned without consideration of spatial variability within Ävrö granite. Point B corresponds to 71.3% of the values estimated from density loggings and thus considering spatial variability. Point C is extrapolated and corresponds to 100% spatial data values, assuming the same spatial variability as in Ävrö granite.

Table 5-9 illustrates rough estimations of the variance at different scales based on variograms and PDF's, and also the variance after averaging to the desired scale. The variograms of borehole KAV01 (Figure 4-26) and KLX02 (Figure 4-29), however do illustrate that there is a difference between the boreholes regarding spatial correlation. This means that there is uncertainty about the representativeness of the two boreholes for the domain.

For other lithological domains this approach was not applied since no variograms could be established. An attempt was made to calculate a variogram of Fine-grained dioritoid (501030) from TPS measurements but the variogram became very unstable due to sparse data.

There is a reason to believe that this approach may underestimate the variance because only the dominating rock type is considered and the others are ignored.

Table 5-9. Estimated variances (W/(m·K)) in different scales based on variograms of the Ävrö granite (501044) in domain RSMA01. Presented values are mean values of data from the two boreholes KAV01 (Figure 4-24 and Figure 4-26) and KLX02 (Figure 4-29).

	Scale 0.7 m		Scale 2 m	
	Variance	St. dev	Variance	St. dev
Total variability within the rock type	0.12		0.12	
Small scale variability	0.07		0.08	
Spatial variance left after equalization to desired scale.	0.05	0.22	0.04	0.20

5.4.4 Approach 4: Addition of “between rock type” and “within rock type” variance

The modelling according to the main approach resulted in estimates of thermal conductivity at different scales, see Table 5-7. This variance includes variability due to rock type changes in the boreholes (“between rock type” variability) but the variability within each rock type is effectively and rapidly reduced when the scale is increased. The resulting variance (V) is therefore mainly a result of the presence of different rock types in the boreholes. One way of compensating for the variance reduction caused by ignoring spatial variability is to add the spatial variability within the dominating rock type in the domain.

For Ävrö granite (501044) the calculated values from density loggings can be used and for Fine-grained dioritoid (501030) TPS measurements can provide a rough estimate of the spatial variability within the rock type. The variances (V_2) as a function of scale were calculated in these ways (geometric mean for the actual scale) and the results are presented in Figure 5-17 for Ävrö granite and Fine-grained dioritoid.

The total variance for the domain can be estimated as the sum of variance due to different rock types (Table 5-7) and the variance due to spatial variability within the dominating rock type (Figure 5-17): $V_{tot} = V_1 + V_2$

In calculating within rock type variability for domains RSMA01 and RSMB01, it is assumed that the within rock type variability for the dominating rock type represents the total within rock type variability for that domain. For domain RSMC01 there are two dominating rock types, Ävrö granite and Quartz monzodiorite. Here, it is assumed that the spatial variability of Quartz monzodiorite and other subordinate rock types is equivalent to that for Fine-grained dioritoid (501030). This is considered to be a reasonable assumption given the similarity in standard deviations of thermal conductivity data for the various rock types, see Table 4-20. The variance V_2 for the domain RSMC01 is estimated as a weighted sum of the spatial variance for Ävrö granite (30%) and Fine-grained dioritoid (70%), where the weighting factors are the fractions of Ävrö granite and other rock types respectively, see Table 5-1. Although this approach only provides a rough estimate of the total variability it encompasses all the major types of variability within the domain.

The total variance estimated for each domain is presented in Table 5-10.

For domain RSMB01 and RSMC01 the difference between Approach 1 and 4 is in the way the “variability within rock type” is estimated. For Approach 1 it is performed by looking at domain RSMA01 (Ävrö granite) but in Approach 4 it is achieved by studying at the dominating rock type in the domain.

It is not easy to assess whether this approach under- or overestimates the total variance for the domain. There are several factors that may influence this, such as the spatial variability in subordinate rock types compared to dominating rock type. In addition, the variance V_2 in Figure 5-17 is rather uncertain due to relatively few measurements and questions of representativeness. Still, it is believed that this approach gives a quite reasonable estimate of the variability compared to the other approaches.

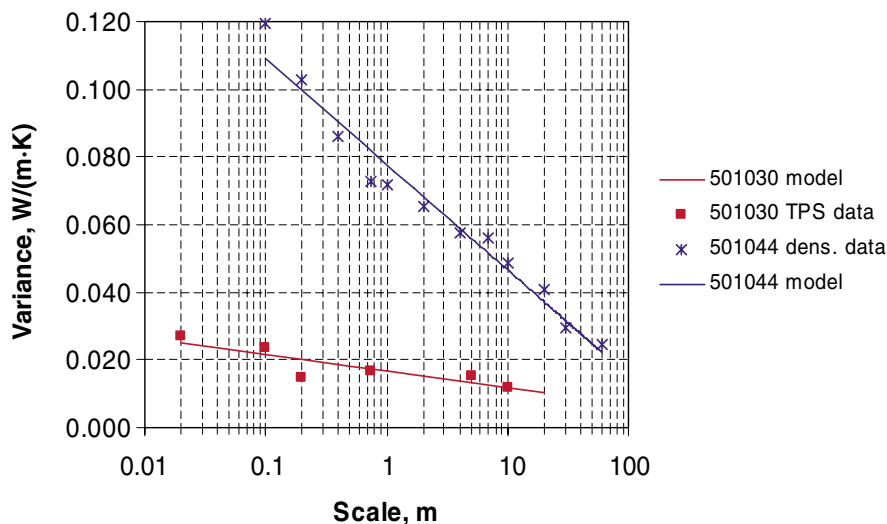


Figure 5-17. Comparison between variability within rock type 501030 and 501044 (V_2). Note that data for 501030 are sparse and based on 26 TPS measurement, while data for 501044 are based on calculated values determined from density loggings.

Table 5-10. Variances in two different scales for two different rock types – domains according to approach number four.

Rock type	Scale 0.7 m		Scale 2 m	
	501044 (RSMA01)	501030 (RSMB01)	501044 (RSMA01)	501030 (RSMB01)
Variance (V_1), Table 5-7	0.025	0.035	0.013	0.024
Variance (V_2), Figure 5-17	0.073	0.018	0.066	0.014
Variance (V_{tot})	0.098	0.053	0.079	0.038
St. dev _{tot}	0.313	0.230	0.281	0.195

5.4.5 Heat capacity

Results of thermal modelling on domain level for heat capacity is presented in Table 5-11. Observe that the table is valid at 20°C. With increasing temperature the heat capacity increases considerably. The increase is in the approximate size of 25% per 100°C temperature increase for rock type Quartz monzodiorite (501036) and Fine-grained dioritoid (501030). For the Ävrö granite (501044) there are no measurements from the Simpevarp subarea. Äspö samples of the Ävrö granite (501044) shows an increase in heat capacity of 25–35% per 100°C temperature increase.

Estimated change in heat capacity for domain RSMA01 is approximately 30% per 100°C temperature increase. The same for domain RSMB01 and RSMD01 is approximately 25% per 100°C temperature increase. For domain RSMC01 the result is approximately 25–30% per 100°C temperature increase.

Table 5-11. Heat capacity (MJ/(m³·K)) per domain with two-sided 95% confidence intervals under assumption of normal distribution.

Domain	Mean	St. dev	Lower confidence limit	Upper confidence limit
RSMA01	2.23	0.120	2.00	2.46
RSMB01	2.23	0.097	2.04	2.42
RSMC01	2.24	0.090	2.04	2.42
RSMD01	2.25	0.060	2.11	2.38

Observe that the above table is valid at 20°C. The heat capacity increases at higher temperatures.

5.5 Evaluation – Thermal conductivity

In the previous sections, modelling according to four different approaches has been performed on domain level for several different scales. Mean values for the domains are estimated according to the main approach. A summary of the mean thermal conductivity on domain level is presented in Table 5-12. The variation of the mean thermal conductivity according to scale is small.

Table 5-12. Mean thermal conductivity (W/(m·K)) by lithological domain.

Domain	Mean	Comment
RSMA01, Ävrö Granite	2.80	Mean subtracted by 0.1, see text.
RSMB01, Fine-grained dioritoid	2.74	
RSMC01, Mix of Ävrö granite and quartz monzodiorite	2.74	
RSMD01, Quartz monzodiorite	2.62	Modelled with Monte Carlo simulation.

The mean thermal conductivity of domain RSMA01 (Ävrö granite) at the 0.7 m scale has been corrected by a subtraction of 0.1 W/(m·K), which is motivated by a potential bias in the relationship between density and thermal conductivity, used for the dominating rock type in this domain. For the other domains no such correction for potential bias has been performed.

Observe that the above table is valid at 20°C. The thermal conductivity decreases slightly at higher temperatures, 1–4°C per 100°C temperature increase.

In order to be able to evaluate the spatial variability on domain level, four different approaches has been used as described above:

- Main approach.
- Extrapolation – spatial variation in all rock types.
- Reduction of small scale variability.
- Addition of “between rock type” and “within rock type” variance.

For Approach 1, mean values and standard deviations are calculated for each scale under the assumption of normally distributed data at the scale of interest /Sundberg et al. 2005b/. As described in the table, and also in previous sections, Approach 2 probably overestimates the standard deviation and Approach 3 underestimates it. Approach 1 is believed to underestimate the standard deviation for domain RSMA01, although it probably overestimates it for domain RSMB01 (Fine-grained dioritoid) and RSMC01 (mixture of Ävrö granite and quartz monzodiorite). Therefore, the standard deviation of domain RSMA01 is given the concluding value of 0.28 W/(m·K), which is the result from Approach 4 at the 2 m scale and is a value in between Approaches 1 and 2.

For domains RSMB01 and RSMC01 the standard deviation according to Approach 1 in Table 5-13 probably overestimates the variability. Therefore, the standard deviation is suggested to be identical to Approach 4 at the 2 m scale, in the same way as for RSMA01. For domain RSMD01 (Quartz monzodiorite) no changes have been made in the standard deviation compared with the realisation results.

Table 5-13. Summary of standard deviations (W/(m·K)) from modelling results at the domain level with the main approach (Approach 1) compared with the three alternative/complementary approaches (Approach 2–4). Numbers within brackets are calculated variances with the resulting standard deviation in bold.

Appr.	Scale (m)	RSMA01 (Ävrö granite)	RSMB01 (Fine-grained dioritoid)	RSMC01 (Mixture of Ävrö granite and Quartz monzodiorite)	RSMD01 (Quartz monzodiorite)	Comment
1	0.7	0.25 (0.025+0.037 = 0.062) (random+71.3% spatial variation)	0.27 (0.035+0.037 = 0.072) (random+spatial variation from RSMA01)	0.28 (0.042+0.037 = 0.079) (random+spatial variation from RSMA01)	0.28	Underestimation of RSMA01 and overestimation of RSMB01 and RSMC01. RSMD01 result of Monte Carlo simulation.
	2	–	–	–	–	
2	0.7	0.31 (0.025+0.073 = 0.098) (random+100% spatial variation)	–	–	–	Overestimation
	2	–	–	–	–	
3	0.7	0.22 (0.12–0.07 = 0.07) (total variance within rock type-small scale variance)	–	–	–	Underestimation
	2	0.20 (0.12–0.08 = 0.04)	–	–	–	
4	0.7	0.31 (0.025+0.073 = 0.098) (random+internal spatial)	0.23 (0.035+0.018 = 0.053) (random+internal spatial)	0.28 (0.042+0.035 ¹ = 0.077) (random+internal spatial)	–	
	2	0.28 (0.013+0.066 = 0.079)	0.20 (0.024+0.014 = 0.038)	0.24 (0.026+0.030 ² = 0.056)	–	

¹ Internal spatial variance within the rock types in this domain calculated with a composition of 30% Ävrö granite and 70% Fine-grained dioritoid (0.3·0.073+0.7·0.018 = 0.035), see Section 5.4.4 for explanation.

² Internal spatial variance in 2 m scale calculated as above (0.3·0.066+0.7·0.014 = 0.030).

5.6 Concluding domain modelling results

5.6.1 Thermal conductivity

Table 5-14 summarises the mean and suggested standard deviation of thermal conductivity per domain at the assumed canister scale.

A comparison of the results on domain level presented in the Simpevarp site descriptive model version 1.1 /SKB, 2004/ and the model version Simpevarp 1.2 is given in Table 5-15.

Table 5-14. Mean value and revised standard deviation of thermal conductivity (W/(m·K)) per domain in canister scale. Two-sided 95 % confidence intervals are indicated.

Domain	Mean	St. dev	Lower confidence limit	Upper confidence limit	Comment
RSMA01	2.80	0.28	2.25	3.35	Higher std comp. to Approach 1
RSMB01	2.74	0.20	2.35	3.13	Lower std comp. to Approach 1
RSMC01	2.74	0.24	2.27	3.21	Lower std comp. to Approach 1
RSMD01	2.62	0.28	2.04	3.20	No changes in std

Observe that the above table is valid at 20°C. The thermal conductivity decreases slightly at higher temperatures for the main rock types, 1–4°C per 100°C temperature increase.

Table 5-15. Comparison of modelling results (the mean and the standard deviation) from Simpevarp site descriptive model versions S1.1 and S1.2.

Domain	Mean (W/(m·K))			St. dev (W/(m·K))	
	Version S1.1	Version S1.2	Diff. (S1.2–S1.1)/S1.1	Version S1.1	Version S1.2
RSMA01	2.67	2.80	4.9%	0.25	0.28
RSMB01	2.23	2.74	22.9%	0.08	0.20
RSMC01	2.50	2.74	9.6%	0.09	0.24
RSMD01	2.38	2.62	10.1%	0.10	0.28

5.6.2 Heat capacity

Modelling of heat capacity on domain level is performed as a Monte Carlo simulation where the occurrence of different rock types in the domain is weighted together with the rock type models. Results are presented in Table 5-11.

5.6.3 Coefficient of thermal expansion

No domain modelling performed. For all domains a mean value for the coefficient of thermal expansion is suggested as $6\text{--}8 \cdot 10^{-6}$ m/(m·K), see Section 4.10.

5.6.4 In situ temperature

No domain modelling performed. For all domains, a mean of the in situ temperature at 400, 500 and 600 m depth is estimated at 12.8, 14.4 and 15.9°C, respectively, see Section 4.11.

6 Evaluation of uncertainties

A general description of uncertainties is provided in the strategy report for the thermal site descriptive modelling /Sundberg, 2003a/. In /Sundberg et al. 2005/ conceptual uncertainty model is presented. In the supporting document for thermal model version 1.2 /Sundberg et al. 2005b/, uncertainties are further described. To get an overview over in which stages uncertainties are introduced, the reader is referred to Figure 5-2 and Figure 5-3. Uncertainties are introduced at the following levels/stages:

- Data level.
- Rock type level.
- Domain level.

6.1 Thermal conductivity

6.1.1 Data level

Uncertainty at the data level results in data with a random or systematic deviation from the correct value for a sample. This applies to thermal conductivity data from TPS measurements, calculations with the SCA method, and calculations based on density measurements.

TPS data

The accuracy of TPS measurements is better than 5% and the repeatability is better than 2% according to the manufacturer of the measurement equipment /Sundberg, 2002/. Note that this uncertainty refers to the measurement volume (approx. 10 cm³) and not the volume of the sample, since only a subvolume of the sample is subject to measurement. If the TPS measurement is supposed to represent the sample scale (approx. 0.1 dm³) the uncertainty is larger and depends on the small-scale heterogeneity of the rock.

There is a potential bias (underestimation) in thermal conductivity data. The reason is that stress dependence has not been assessed. Measurements are made on stress released samples. However, the effect is assumed to be low since the samples are water saturated before measurement.

SCA data

The uncertainty associated with SCA data is significantly larger than for TPS data. For SCA data there are several sources of uncertainty and the three most important are; (1) alteration of minerals, (2) determination of the volume fraction of each mineral in the sample, and (3) representative values of thermal conductivity of the different minerals. An example of the first type of uncertainty is that parts of the plagioclase and biotite in Fine-grained dioritoid and Quartz monzodiorite are partly sericitised and chloritised, which is hard to detect and quantify.

The second type of uncertainty for SCA data results in a total mineral composition that does not add up to 100% for several samples. In addition, not all different types of minerals are easily distinguished from each other, resulting in slightly different estimates of fractions depending on the person performing the analyses. Another contributing factor is that modal analyses are performed on a 2D surface of the sample, which is assumed to represent 3D.

The third type of uncertainty results from using literature values for the thermal conductivity. These values are uncertain and may vary considerably depending on the composition of the mineral in the actual sample, especially for plagioclase, pyroxene, and olivine.

When comparing TPS and SCA data, there is also a fourth source of uncertainty since the modal analysis is not performed for the whole volume of the TPS sample, only a surface of the sample. In addition, the SCA calculation method presumes isotropic conditions. This can be a source of uncertainty but it is believed to be of minor importance /Sundberg, 1988/.

Density data

Thermal conductivities are calculated for Ävrö granite based on density loggings using the relationship in Figure 4-8. These values are more uncertain than both TPS and SCA data. The main sources of uncertainty are; (1) uncertainty in the density logging technique, (2) uncertainty in filtering and recalibration of density data, (3) high noise level in the density logging measurements and (4) uncertainty in the statistical relationship between density and thermal conductivity. The first type of uncertainty is reported to be 60 kg/m³ (accuracy) for borehole KSH02 /Mattsson and Thunehed, 2004b/. It is not clear which types of uncertainties are incorporated in this estimate (geological features, overlapping measurement volumes etc). Disturbances in the borehole, such as fractures and small dykes and veins, will of course affect the measurement.

The second type of uncertainty results from filtering of the data to remove spikes etc. The purpose of recalibration is to remove potential bias in the loggings by calibrating the data set against laboratory measurements of density performed on samples from the borehole. However, the limited number of samples is a source of uncertainty.

The third type of uncertainty might, for some of the boreholes, be as high as 50–60 kg/m³ /Mattsson and Thunehed, 2004b; Mattsson, 2004d/. To reduce the influence of the noise level, data have been filtered before further calculations. The noise level is still high and causes high noise level also for the calculated thermal conductivity.

The fourth type of uncertainty, statistical uncertainty, is believed to be the most important and result from; (a) TPS measurement on samples, (b) density measurements on samples at laboratory, (c) rock type classification, (d) natural variability within the rock type Ävrö granite, and (e) the selection of a regression relationship. TPS measurements are in this case assumed to be representative for the whole sample, not only the measurement volume (see TPS data above), while density logging data refer to a slightly larger scale. Uncertainty in laboratory measurement of density is believed to be insignificant compared to other uncertainties. Rock type classification affects which samples should be included in the regression analysis. Natural variability of mineral composition within Ävrö granite results in variability of both density and thermal conductivity, but the regression equation is only an approximation and is not capable of capturing all this variability. The subjective selection of the type of regression relationship is also a source of uncertainty. A linear model will result in slightly different thermal conductivity estimates compared to a parabolic relationship.

There is a potential bias in the calculated values from density measurement. One reason could be extrapolation slightly beyond the density range of the data for the statistical relationship. On the other hand, the difference in mean values between density loggings and calculated/measured data could be a natural result of the large scale heterogeneity of the Ävrö granite in relation to sample locations.

6.1.2 Rock type level

Uncertainty at the rock type level results in thermal conductivity estimates (PDF, mean and variance) that deviate from the true distribution for the rock type. Important causes are the issue of representativeness and the selection of rock type models.

Representativeness of data

The representativeness of samples selected for TPS measurements can be questioned. The samples are not taken with the purpose of statistically representing the rock mass, and consequently there is a potential for bias. As an example, TPS samples from the Simpevarp subarea are often grouped in groups up to 5 samples from a limited section of the borehole (1 or two meters). Similarly, the question of representativeness applies for the calculated values based on modal analyses (SCA method).

For both measured and calculated data, non-probabilistic selection of samples has resulted in bias of unknown magnitude. However, samples were taken in order to characterise the rock type – not to find odd varieties. The potential for bias, due to TPS and SCA data sets with low representativeness, is largest for rock types with high spatial variability, such as Ävrö granite.

Rock type models (PDF's) are based on all available TPS and SCA data. As mentioned, TPS and to a certain extent also SCA data are taken in groups and are not representative of the rock volume. At least for Ävrö granite, a more accurate distribution model could be achieved if some of the data (from both Simpevarp and Äspö HRL) was excluded or weighted using e.g. a declustering technique. This is achieved if the rock volume is divided into a number of grid cells, and if several samples occur in the same cell they are given a lower weight. By handling the samples in this way a more representative value could possibly be achieved for a rock type. However, this has not been done.

Rock type models

Some uncertainty results from the classification of rock samples, but this uncertainty is believed to be small compared to the other involved uncertainties.

For Fine-grained dioritoid and Ävrö granite the rock type models are based on TPS data and corrected SCA data. The correction is based on comparison of SCA data with TPS data. Because the comparison is based on only a few samples, there is uncertainty in the accuracy of this correction. For the other rock type models, no correction was performed due to lack of data, which of course leads to uncertain models.

The rock type models were chosen as normal distributions (PDF's). There is a slight deviation between data and model and one reason for this can be the question of representativeness of the samples. Generally, the rock type models slightly overestimate the occurrence of small thermal conductivity values and underestimate the number of large values. Rock type models are required in the domain modelling.

The data set is very small for several rock types, which implies that these rock type models are highly uncertain. This applies to Quartz monzodiorite (501036), Fine-grained diorite-gabbro (505102), Diorite/Gabbro (511033), Granite (501058), and Fine-grained granite (511058).

There are uncertainties in the rock type models due to temperature and pressure effects on the thermal conductivity measurements. Temperature effects are believed to be larger than pressure effects, but still smaller than other uncertainties. The temperature effect is only a few percent per 100°C temperature increase.

Spatial variability within rock type

A model of spatial variability within rock type has only been developed for Ävrö granite. It is primarily based on density logging data, see Section 4.7, with potential bias. For other rock types, spatial variability is only considered in the domain modelling.

6.1.3 Domain level

Uncertainty at the domain level results in thermal conductivity estimates (mean and variance) that deviate from the true distribution of values at the scale of interest. The most important sources of uncertainty are the geological model, the related issue of representativeness, the choice of significant scale for the canister, the upscaling methodology in the modelling, and spatial variability both within and between rock types. In addition, there are also a number of other uncertainties of less importance.

Geological model

Uncertainty in the geological model results from uncertainty in the Boremap logging, interpretations of spatial occurrence of different rock types, and the extension of lithological domains. It is not known how large these uncertainties are.

Influences from fractures and deformation zones on thermal properties have not been considered. No thermal data is available from the deformation zones.

Thermal influence of water movements has not been considered in the modelling.

Representativeness of boreholes

It is not known how representative the boreholes are for the different domains. Since the number of boreholes in a domain is low, it is reasonable to believe that there is a bias present. This is supported by borehole data showing large differences in e.g. spatial variability, especially for domain RSMA01 (Ävrö granite). This bias can only be reduced with additional boreholes, or a more complete understanding of the lithology. The random part of the uncertainty can be estimated by careful comparison of data from different boreholes. 3D geometry of most of the rock domains is also uncertain.

Spatial variability within the domain

Spatial variability within the domain is handled by modelling, see Section 5.3. This is a non-reducible uncertainty, only the uncertainty about the true state of variability can be reduced.

Anisotropy

Anisotropy has not been considered in the domain modelling. Anisotropic effects may result due to presence of subordinate rock types occurring as dykes of significant extension, consisting of a rock type with different thermal characteristics. At the present stage no evaluation of the extent of such anisotropic occurrence has been made. The effect of structure and foliation in dominating rock types is assumed to be small.

Upscaling methodology

For all rock types except Ävrö granite, thermal conductivity values are randomly assigned at the 0.1 m scale based on the rock type models. These rock type models probably overestimate the variance at the 0.1 m scale. The reason is that TPS and SCA data represent a smaller scale. At the 0.1 m scale, some reduction of variance should already have taken place. Therefore, this approach overestimates the likelihood of small values.

In the main modelling approach, spatial variability within other rock types than Ävrö granite is ignored. This results in too large a variance reduction when the scale increases. To compensate for this, the approach was modified such that the variance due to spatial variability within other rock types was assumed to be equal the spatial variability within Ävrö granite. This is probably an overestimation of the variance.

There is also a potential bias in the modelling approach for the same rock type (Ävrö granite). The assigned values based on density loggings are higher than predicted by the rock type model of Ävrö granite. The difference in mean value exceeds 0.1 W/(m·K). This might be due to a bias in values based on the density logging, or the fact that the rock type model is not representative for the same rock volume as the density logging has been conducted in. In the later case, the values based on the density logging are the more accurate ones. In the modelling the results have been corrected for this potential bias.

There are several other uncertainties in modelling Approaches 2–3. These include the procedure used in Approach 2 for adjustment of spatial variability, the addition and subtraction of variances in Approaches 1–4, and the estimation of spatial variability from variograms (Approach 3) and TPS data (Approach 4). These uncertainties all arises from lack of knowledge of spatial variability within the rock types and within the domains. The most straight-forward way of reducing this uncertainty is to collect considerable more data.

Significant scale for the canister

At present state of knowledge it is not known at which scale thermal conductivity is significant for the heat emitted from the canister. This implies a major source of uncertainty in the thermal modelling. It can be reduced by numerical simulation of heat flow. In this report, the uncertainty is handled by selecting a sufficiently small scale not to underestimate the variability. Therefore, modelling approaches have been applied at scales ranging from 0.7 m to 2 m. This is believed to be in the lower end of the uncertainty range for the significant scale (approximately 1–10 m) with the purpose not to underestimate the variability. However, no measurements of thermal properties have however been conducted for these scales to confirm the results.

Statistical assumptions

The confidence intervals calculated for each domain are based on the assumption that domain data at the significant scale are normally distributed. This is an uncertain assumption. As long as knowledge of spatial variability is insufficient, it is not possible to check the validity of this assumption.

The rock type models have been considered as normal distributions although the data are somewhat skewed. This results in a too small change of the mean value for the domain when the scale increases. The effect is however insignificant compared to the other uncertainties.

6.2 Heat capacity

There exists a problem with the representativeness for measured values (TPS data). The samples are few and focused on certain parts of the rock volume.

Subordinate rock types have not been considered when modelling the heat capacity.

The modelling is based on TPS data which means scale less than 0.1 m. Mean values and standard deviations only show a small variation, besides the data is normal distributed which means the properties in larger scales can be expected to be basically the same.

No direct laboratory measurements of heat capacity have been performed. Instead, heat capacity has been determined through conductivity and diffusivity measurements performed with the TPS method.

6.3 In situ temperature

Temperature loggings from different boreholes show a variation in temperature at specified depth. The difference implies an uncertainty in temperature loggings and even small uncertainties may influence the design. Possible sources of uncertainty are timing of the logging after drilling (drilling adds to temperature disturbance), water movements along the boreholes, calibration error, uncertainty in the temperature logging or in the measured inclination of the boreholes. The uncertainty imposed by water movements may be evaluated jointly with the hydrogeologists. However, the latter has not yet been done.

6.4 Thermal expansion

Problem with the representativeness for measured samples. The samples are few and focused to certain parts of the rock volume.

There are differences in the results of thermal expansion measurements since different methods and laboratories have been used.

There is a potential bias (underestimation) in thermal expansion data. The reason is that stress dependence has not been assessed. Measurements are made on stress released samples.

References

- Adl-Zarrabi B, 2004a.** Drill hole KSH01A Thermal properties: heat conductivity and heat capacity determined using the TPS method and mineralogical composition by modal analysis. SKB P-04-53, Svensk Kärnbränslehantering AB.
- Adl-Zarrabi B, 2004b.** Drill hole KSH02 Thermal properties: heat conductivity and heat capacity determined using the TPS method and mineralogical composition by modal analysis. SKB P-04-54, Svensk Kärnbränslehantering AB.
- Adl-Zarrabi B, 2004c.** Drill hole KAV01 Thermal properties: heat conductivity and heat capacity determined using the TPS method and mineralogical composition by modal analysis. SKB P-04-55, Svensk Kärnbränslehantering AB.
- Gustafsson S, 1991.** Transient plane source techniques for thermal conductivity and thermal diffusivity measurements of solid materials. *Rev. Sci. Instrum.* 62, p 797–804. American Institute of Physics, USA.
- Horai K, 1971.** Thermal conductivity of rock-forming minerals. *J. Geophys. Res.* 76, p 1278–1308.
- Horai K, Baldrige S, 1972.** Thermal conductivity of nineteen igneous rocks, Application of the needle probe method to the measurement of the thermal conductivity of rock. Estimation of the thermal conductivity of rock from the mineral and chemical compositions. *Phys. Earth Planet. Interiors* 5, p 151.
- HotDisk, 2004.** www.hotdisk.se, access 2004-09-22.
- Mattsson H, Thunehed H, 2004a.** Interpretation of geophysical borehole data from KSH01A, KSH01B, KSH02 (0–100 m), HSH01, HSH02 and HSH03 and compilation of petrophysical data from KSH01A and KSH01B. SKB P-04-28, Svensk Kärnbränslehantering AB.
- Mattsson H, Thunehed H, 2004b.** Interpretation of geophysical borehole data and compilation of petrophysical data from KSH02 (80–1,000 m) and KAV01. SKB P-04-77, Svensk Kärnbränslehantering AB.
- Mattsson H, 2004c.** GeoVista AB, Personal communication.
- Mattsson H, 2004d.** Interpretation of geophysical borehole data and compilation of petrophysical data from KSH03A (100–1,000 m), KSH03B, HAV09, HAV10 and KLX02 (200–1,000 m). SKB P-04-214, Svensk Kärnbränslehantering AB.
- Nielsen T, Ringgaard J, 2003.** Geophysical borehole logging in borehole KSH01A, KSH01B and part of KSH02. SKB P-03-16, Svensk Kärnbränslehantering AB.
- Nielsen T, Ringgaard J, Horn F, 2003.** Geophysical borehole logging in borehole KAV01. SKB P-04-232, Svensk Kärnbränslehantering AB.
- Nielsen T, Ringgaard J, 2004.** Geophysical borehole logging in borehole KSH03A, KSH03B, HAV09 and HAV10. SKB P-04-50, Svensk Kärnbränslehantering AB.

Nielsen T, Ringgaard J, Horn F, 2004. Geophysical borehole logging in boreholes KSH02 and KLX02. SKB P-03-111, Svensk Kärnbränslehantering AB.

SKB, 2004. Preliminary Site Description, Simpevarp area – version 1.1. SKB R-04-25, Svensk Kärnbränslehantering AB.

SKB, 2005. Preliminary Site Description Simpevarp subarea – version 1.2. SKB R-05-08, Svensk Kärnbränslehantering AB. Report in progress

Staub I, Andersson C, Magnor B, 2004. Äspö hard Rock Laboratory – Äspö Pillar Stability Experiment, Geology and mechanical properties of the rock mass in TASQ. SKB R-04-01, Svensk Kärnbränslehantering AB.

Sundberg J, 1988. Thermal properties of soils and rocks, Publ. A 57 Dissertation. Department of Geology, Chalmers University of Technology and University of Göteborg, Sweden.

Sundberg J, Gabrielsson A, 1999. Laboratory and field measurements of thermal properties of the rock in the prototype repository at Äspö HRL. SKB IPR-99-17, Svensk Kärnbränslehantering AB.

Sundberg J, 2002. Determination of thermal properties at Äspö HRL. Comparison and evaluation of methods and methodologies for borehole KA 2599 G01. SKB R-02-27, Svensk Kärnbränslehantering AB.

Sundberg J, Ländell M, 2002. Determination of linear thermal expansion. Samples from borehole KA 2599 G01. Äspö HRL. SKB IPR-02-63, Svensk Kärnbränslehantering AB.

Sundberg J, 2003a. A strategy for the model development during site investigations version 1.0. SKB R-03-10, Svensk Kärnbränslehantering AB.

Sundberg J, 2003b. Thermal properties at Äspö HRL. Analysis of distribution and scale factors. SKB R-03-17, Svensk Kärnbränslehantering AB.

Sundberg J, Back P-E, Bengtsson A, 2005. Uncertainty analysis of thermal properties at Äspö HRL prototype repository. Svensk Kärnbränslehantering AB. Report in progress.

Wahlgren C-H, 2004. SGU (Geological Survey of Sweden), Personal communication.

Wahlgren C-H, Ahl M, Sandahl K-A, Berglund J, Petersson J, Ekström M, Persson P-O, 2004. Bedrock mapping 2003 – Simpevarp subarea. Outcrop data, fracture data, modal and geochemical classification of rock types, bedrock map, radiometric dating. SKB P-04-102, Svensk Kärnbränslehantering AB.

Åkesson U, 2004a. Drill hole KSH01A Extensometer measurements of the coefficient of thermal expansion of rock. SKB P-04-59, Svensk Kärnbränslehantering AB.

Åkesson U, 2004b. Drill hole KSH02 Extensometer measurements of the coefficient of thermal expansion of rock. SKB P-04-60, Svensk Kärnbränslehantering AB.

Åkesson U, 2004c. Drill hole KAV01 Extensometer measurements of the coefficient of thermal expansion of rock. SKB P-04-61, Svensk Kärnbränslehantering AB.

Probability plots of thermal conductivity per rock type

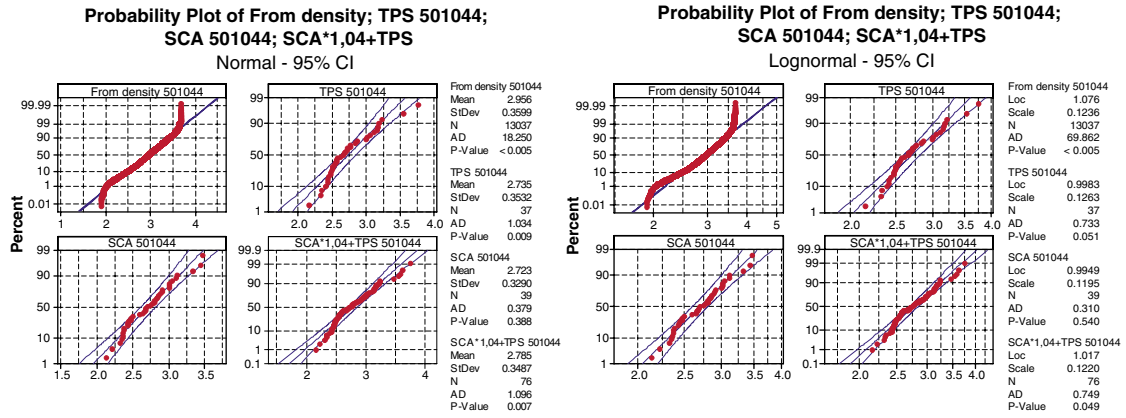


Figure A-1. Probability plots of rock type Ävrö granite (501044), normal and lognormal distributions.

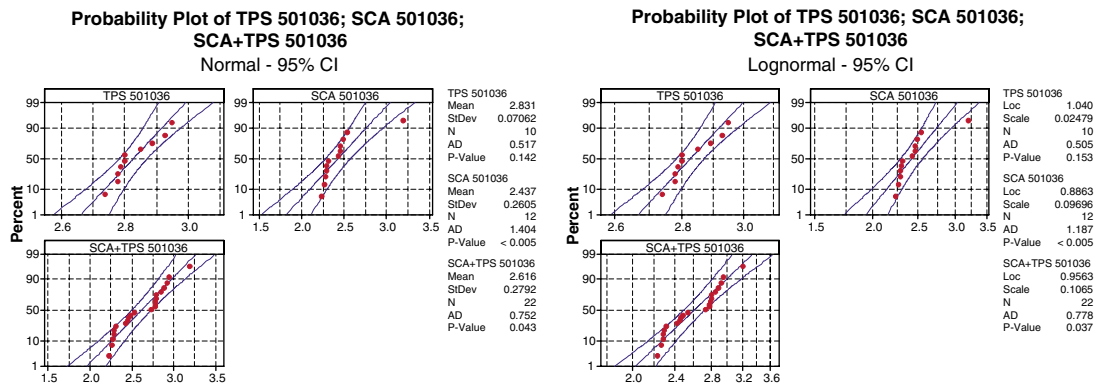


Figure A-2. Probability plots of rock type Quartz monzodiorite (501036), normal and lognormal distributions.

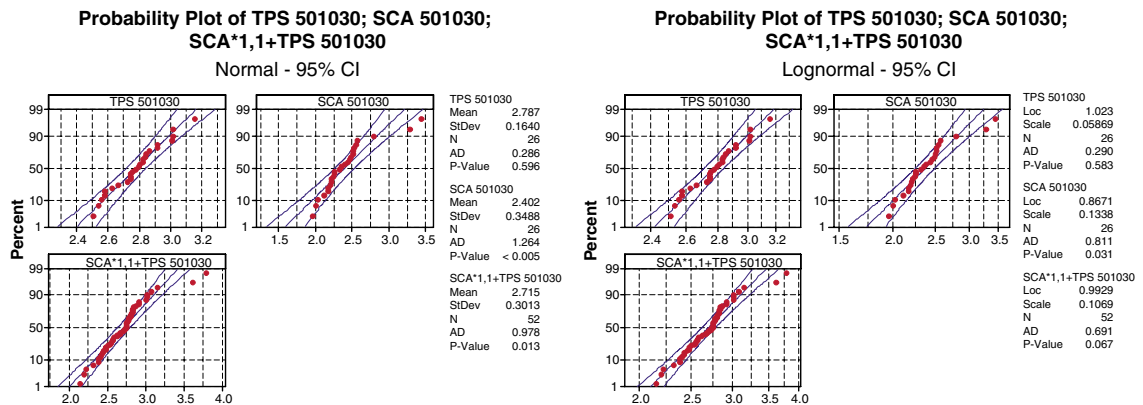


Figure A-3. Probability plots of rock type Fine-grained dioritoid (501030), normal and lognormal distributions.

Probability plots of domain modelling results

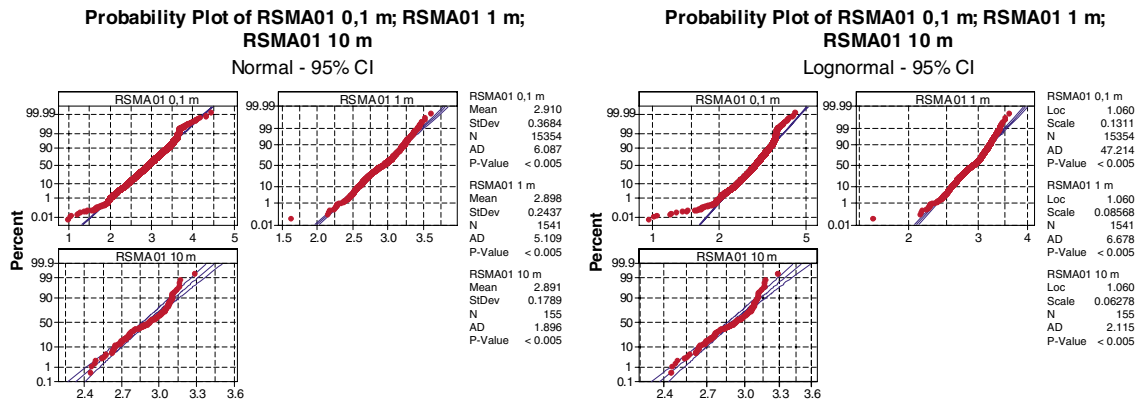


Figure B-1. Probability plots of modelling results for three scales of domain RSMA01 (dominated by Ävrö granite), normal and lognormal distributions.

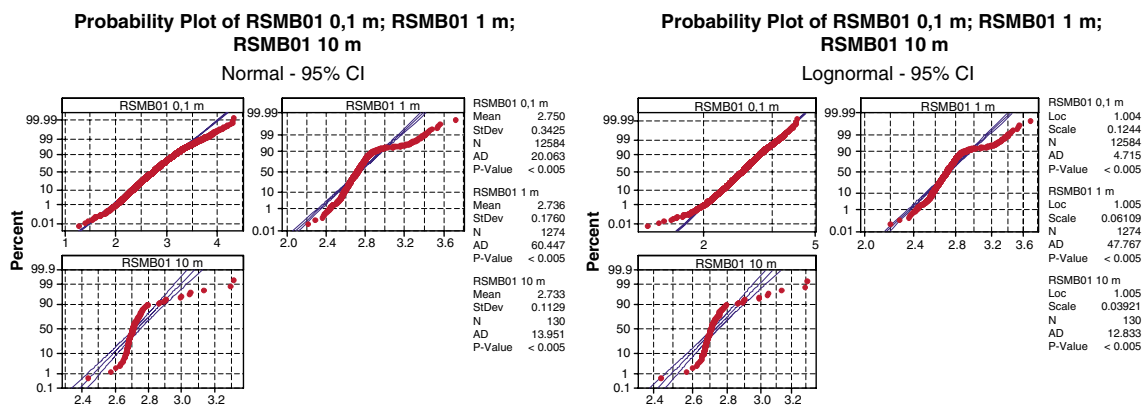


Figure B-2. Probability plots of modelling results for three scales of domain RSMB01 (dominated by Fine-grained dioritoid), normal and lognormal distributions.

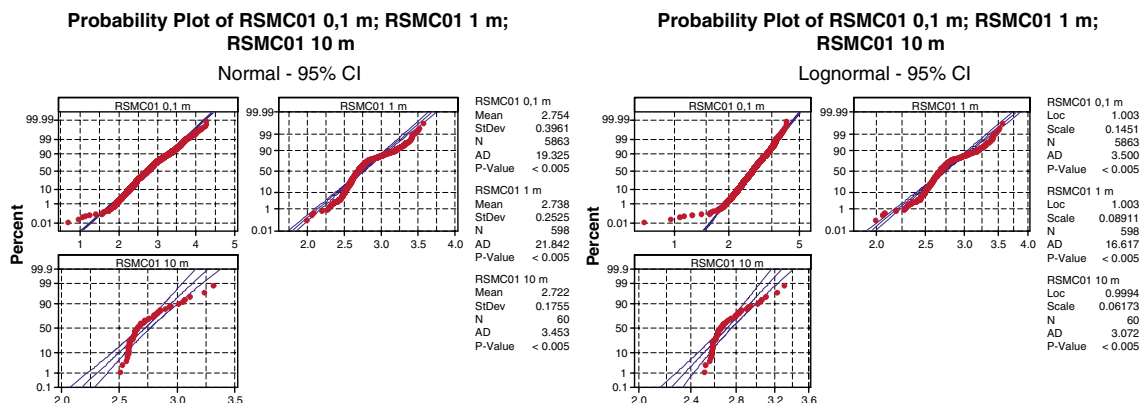


Figure B-3. Probability plots of modelling results for three scales of domain RSMC01 (mixture of Ävrö granite and Quartz monzodiorite), normal and lognormal distributions.

Spatial variation of rock types – indicator variograms

Indicator variograms showing the spatial correlation in borehole KAV01, KSH01A and KSH02 between different segments/sections of rock type 501044, 501036 and 501030 are presented in Figure C-1 to Figure C-6. A summary of illustrated variograms for the different boreholes together with lag/separation distances is presented in Table C-1. Segments / sections smaller than 1 m are included in the indicator variograms with a resolution of 5 cm.

For 501044 in KAV01 a strong spatial correlation is present up to about 10–15 m (magnified figure to the right) and variance stabilising on ca 0.11. On top of this a second type of variability appears temporarily from about 40 m to 150 m. The indicator variogram for rock type 501030 in KAV01 exhibit a similar pattern, which is logical since 501044 dominates and controls the spatial correlation in the borehole.

Table C-1. Summary of present indicator variograms with lag/separation distance.

Borehole	501044	501036	501030
KAV01	0–450 m		0–240 m
	0–80 m		0–50 m
KSH01A	0–450 m	0–450 m	0–450 m
	0–80 m	0–80 m	0–80 m
KSH02			0–500 m
			0–80 m

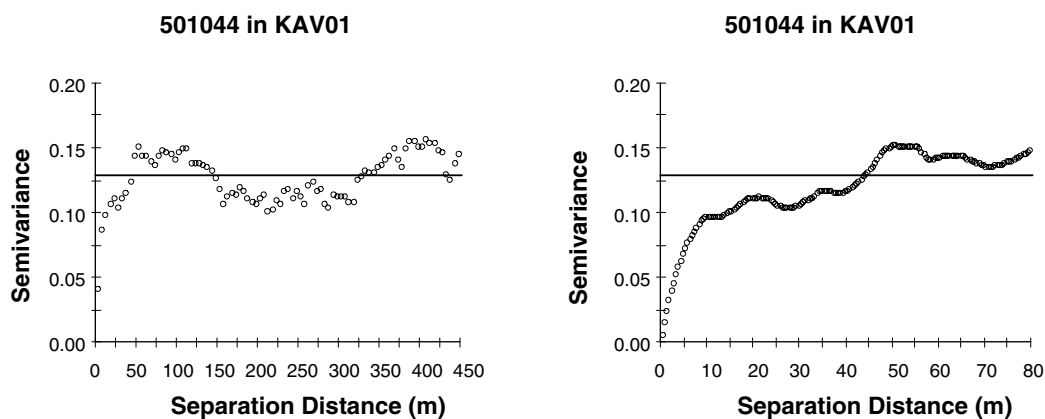


Figure C-1. Indicator variogram of Ävrö granite (501044) in KAV01, separation distance 0–450 m and 0–80 m.

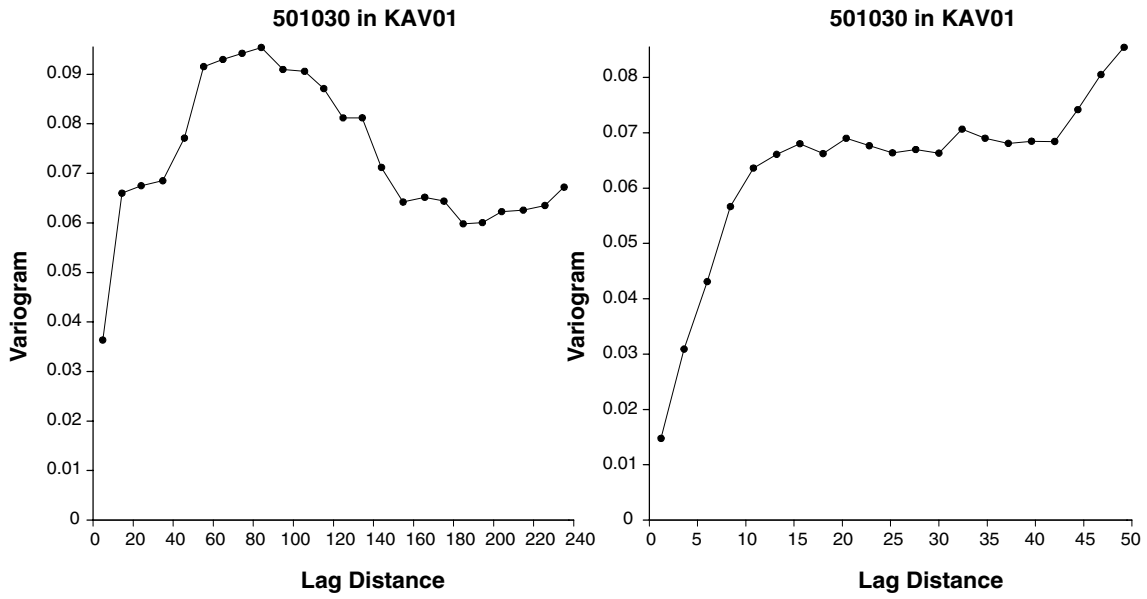


Figure C-2. Indicator variogram of Fine-grained dioritoid (501030) in KAV01, separation distance 0–240 m and 0–50 m.

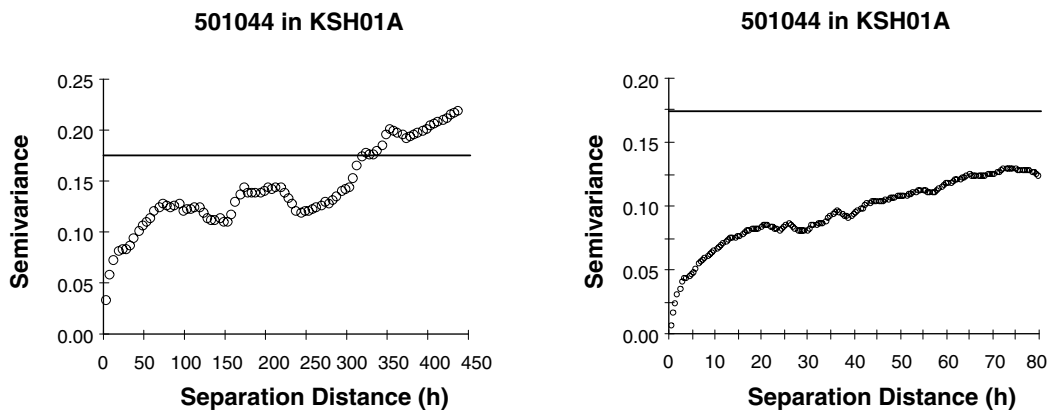


Figure C-3. Indicator variogram of Ävrö granite (501044) in KSH01A, separation distance 0–450 m and 0–80 m.

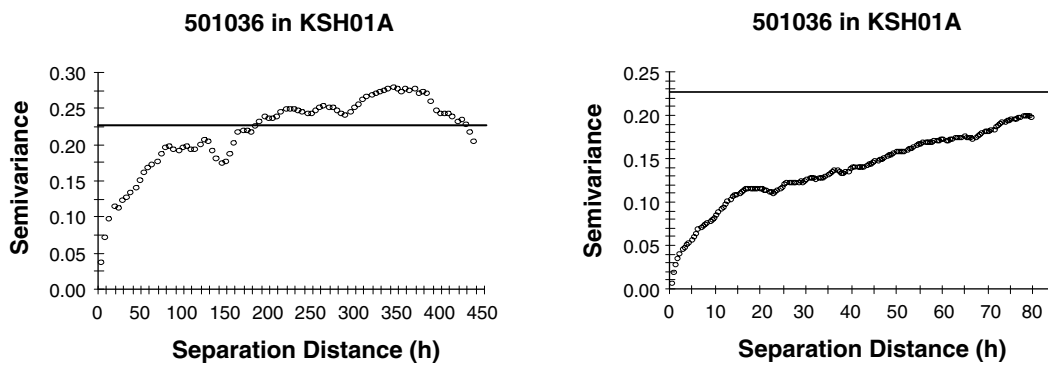


Figure C-4. Indicator variogram of Quartz monzodiorite (501036) in KSH01A, separation distance 0–450 m and 0–80 m.

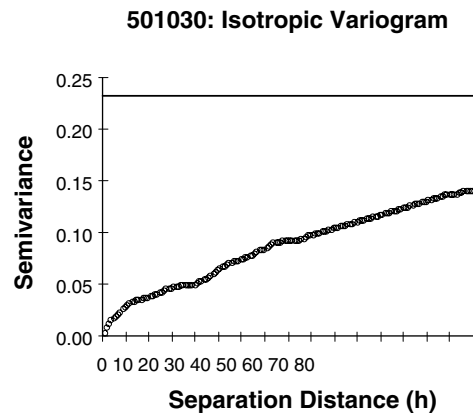
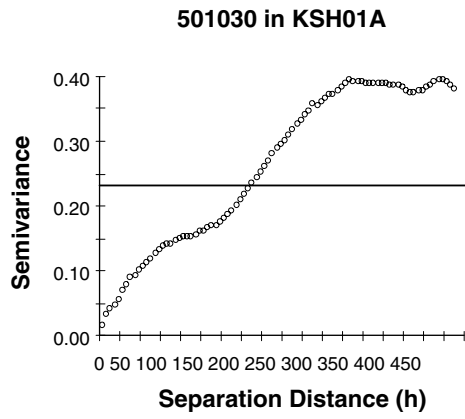


Figure C-5. Indicator variogram of Fine-grained dioritoid (501030) in KSH01A, separation distance 0–450 m and 0–80 m.

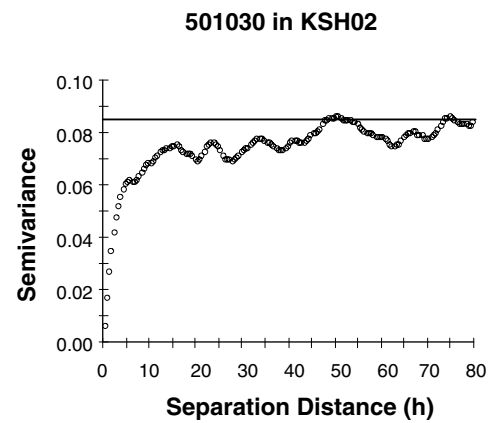
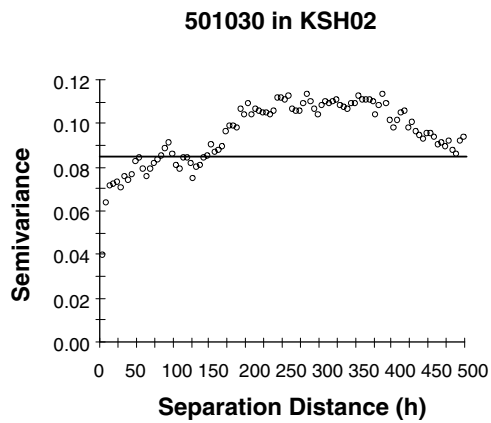


Figure C-6. Indicator variogram of Fine-grained dioritoid (501030) in KSH02, separation distance 0–500 m and 0–80 m.